

**Institut für Experimentelle Genetik
GSF-Forschungszentrum für Umwelt und Gesundheit
Neuherberg**



**Cellular requirements for cholesterol and
identification of genes involved in cholesterol
biosynthesis and homeostasis**

Zrinka Marijanovic

Vollständiger Abdruck der von der Fakultät Wissenschaftszentrum
Weihenstephan für Ernährung, Landnutzung und Umwelt der Technischen
Universität München zur Erlangung des akademischen Grades eines

Doktors der Naturwissenschaften

genehmigten Dissertation

Vorsitzender: Univ.-Prof. Dr. Erwin Grill

Prüfer der Dissertation: 1. Univ.-Prof. Dr. Johannes Buchner
2. Priv.-Doz. Dr. Jerzy Adamski
3. Univ.-Prof. Dr. Alfons Gierl

Die Dissertation wurde am 02.08.2002 bei der Technischen Universität München
eingereicht und durch die Fakultät Wissenschaftszentrum Weihenstephan für
Ernährung, Landnutzung und Umwelt am 14.10.2002 angenommen.

Table of contents

Abstract	5
Zusammenfassung	7
Abbreviations	9
1. INTRODUCTION	11
1.1. Cholesterol	11
1.1.1. Subcellular distribution and regulation of cholesterol biosynthetic enzymes	13
1.1.2. Regulation of cholesterol homeostasis in the cell	15
1.2. Ergosterol	18
1.2.1. Regulation of ergosterol biosynthetic enzymes	18
1.2.2. Regulation of ergosterol homeostasis	18
1.3. 17 β -hydroxysteroid dehydrogenase type 7 (17 β -HSD7)	19
1.4. C14orf1 and its yeast homologue ERG28 - connection between sterol biosynthesis and cellular proliferation	22
1.5. The aim of the study	22
2. RESULTS	25
2.1. Analysis of cholesterol auxotrophic U-937 cells in media containing different sterols	25
2.1.1. Cell survival and proliferation	25
2.1.2. Cholesterol and ergosterol levels	30
2.2. Identification of 17 β -HSD7 as a cholesterologenic enzyme	35
2.2.1. Expression of 17 β -HSD7 in cholesterol auxotrophic cell lines	35
2.2.2. Complementation assay	37
2.2.3. Cellular localization	40
2.3. Identification of C14orf1 as a possible 17 β -HSD7 interactor and its role in cholesterol biosynthesis	42
2.3.1. <i>In vitro</i> and <i>in vivo</i> interactions with C14orf1	42
2.3.2. Cellular localization of C14orf1 and yERG28	44
2.3.3. Cholesterol influenced changes in C14orf1 and yERG28 cellular localization	47

3. DISCUSSION	49
3.1. Cellular requirements for cholesterol	49
3.2. Role of 17 β -HSD7 in cholesterol biosynthesis	52
3.2.1. Ability of 17 β -HSD7 to restore ergosterol synthesis in yeast complementation assay	52
3.2.2. 17 β -HSD7 activity in yeast	53
3.2.3. Cellular localization of 17 β -HSD7	54
3.2.4. Expression of 17 β -HSD7 in cholesterol auxotrophic cell lines	54
3.3. Role of C14orf1 and ERG28 in sterol metabolism	55
3.3.1. C14orf1 and ERG28 as possible interaction partners of 17 β -HSD7 and ERG27	55
3.3.2. Cellular localization and potential involvement in sterol trafficking	56
3.4. Conclusions	61
4. MATERIALS AND METHODS	63
4.1. METHODS	63
4.1.1. Working with nucleic acids	63
4.1.2. Protein chemistry	70
4.1.3. Working with bacteria	72
4.1.4. Working with yeast	73
4.1.5. Working with mammalian cells	77
4.1.6. Analytical methods	80
4.2. MATERIALS	83
4.2.1. Buffers and media	83
4.2.2. Chemicals	87
4.2.3. Antibodies	88
4.2.4. Enzymes	89
4.2.5. Cells	89
4.2.6. Vectors	90
4.2.7. Kits	90
4.2.8. Other material	90
4.2.9. Devices	91
LITERATURE	93
5. APPENDIX	99
5.1. Primers and plasmid constructs	99
5.2. Figures of constructs used in the study	101
5.3. GC/MS spectra measured from media	104
5.4. GC/MS spectra measured from cell lysates	109

Abstract

Cholesterol is an essential sterol in vertebrates. It is involved in the regulation of membrane fluidity and permeability, steroid hormone and bile acid synthesis and in the posttranslational modification of proteins important for intercellular signaling and embryonic development. It can be synthesized by cells *de novo* or acquired by transfer between organs and receptor mediated endocytosis. Both processes are tightly regulated and any disturbance results in severe impairment during embryonic development, especially in the central nervous system. Recently, it was found that cholesterol influences cell cycle progression and it was suggested that it is not replacable by nonmammalian sterols in this particular role.

Recent phylogenetic and structural modeling studies implied that 17 β -HSD type 7 - previously identified as estrone converting enzyme - might have a physiological role in cholesterol biosynthesis, rather than in the steroid hormone metabolism. This conclusion was made on the basis of a high homology between 17 β -HSD7 and yERG27, a yeast protein involved in ergosterol biosynthesis. In addition, a new protein called C14orf1 was identified as a potential interactor of 17 β -HSD7. C14orf1 is highly expressed in testis and cancer cell lines and suggested to influence cellular proliferation. The yeast homologue of C14orf1, yERG28 was found to be involved in ergosterol biosynthesis, possibly enabling complex formation between yERG26 and yERG27. Therefore, the role of 17 β -HSD7 in cholesterol biosynthesis was investigated by yeast complementation experiments with and without co-transfected C14orf1. The physical interactions of the two mammalian proteins and of their yeast homologues yERG27 and yERG28 was also examined in a yeast two-hybrid assay.

The results presented here show that ergosterol could support growth of a cholesterol auxotrophic cell line U-937, but it was not kept in the free form inside the cells. Apparently ergosterol caused mobilization of internal cholesterol supplies, which enabled cells to survive and proliferate to certain extent. Cholesterol surprisingly did not cause the same effect most likely because of its perturbed distribution in the cell. It was also observed that free cholesterol was normally kept at a very low level inside the cell and that a nine-fold elevation in its level led to cell death.

17 β -HSD7 was able to restore ergosterol biosynthesis in the yERG27 deficient SDG110 yeast strain and was therefore confirmed to be involved in the conversion of zymosteron to zymosterol, an intermediate step in the cholesterol and ergosterol biosynthesis. It was found to be localized in the endoplasmatic reticulum, and for its proper localization as well as activity the C-terminus was required.

The proposed interaction between 17 β -HSD7 and C14orf1 was found to be unlikely. The same result was obtained for the yeast homologues. Since the subcellular localization of γ ERG28 was found to depend on external cholesterol supplies it is very likely that this protein, as well as its human counterpart, is involved in cholesterol trafficking and not in cholesterol biosynthesis as previously postulated.

Zusammenfassung

Cholesterin ist ein essentielles Sterol in Vertebraten. Es ist beteiligt an der Regulation von Membranfluidität und -durchlässigkeit, Steroidhormon- und Gallensäuresynthese und dient zur posttranslationalen Modifizierung einiger Proteine, die eine wichtige Rolle in Signalwegen und der Embryonalentwicklung spielen. Cholesterin kann in den meisten Zellen *de novo* synthetisiert oder durch Rezeptor-vermittelte Endozytose von außen aufgenommen werden. Beide Prozesse sind streng reguliert und jegliche Störung während der Embryogenese führt zu schweren Missbildungen und Fehlentwicklungen insbesondere des Zentralnervensystems. Vor kurzem wurde herausgefunden, dass Cholesterin den Zellzyklus beeinflusst und in dieser wichtigen Funktion nicht durch andere Sterole ersetzt werden kann.

17 β -HSD7 wurde ursprünglich als Östron-umsetzendes Enzym charakterisiert. Phylogenetische Untersuchungen und die Modellierung der Tertiärstruktur implizierten jedoch, dass das Protein nicht nur am Steroidhormonmetabolismus, sondern auch, bzw. vor allem, an der Cholesterinbiosynthese beteiligt sein könnte. Diese Schlussfolgerung basierte in erster Linie auf der großen Sequenz- und Strukturhomologie zwischen 17 β -HSD7 und yERG27, einem Ergosterolbiosyntheseenzym der Hefe. Darüber hinaus wurde ein neues Protein, C14orf1, identifiziert, das in Testes und Krebszelllinien hoch exprimiert ist und einen Einfluss auf die Zellproliferation zu haben scheint. Das Hefe-Homologe von C14orf1, yERG28, ist an der Ergosterolsynthese beteiligt. Wahrscheinlich ermöglicht es die Bildung eines Komplexes aus yERG26 und yERG27. Deshalb wurde die Rolle der 17 β -HSD7 in der Cholesterinbiosynthese nicht nur durch einen Hefe-Komplementierungs-Assay untersucht sondern auch eine mögliche Interaktion von 17 β -HSD7 mit C14orf1 bzw. zwischen deren Hefehomologen, yERG27 und yERG28, geprüft.

Die hier dargestellten Ergebnisse zeigen, dass Ergosterol das Wachstum der Cholesterin-auxotrophen Zelllinie U-937 unterstützen konnte und nicht in freier Form im Zellinneren vorlag. Ergosterol verursacht offensichtlich eine Mobilisierung der internen Cholesterinreserven, wodurch den Zellen ermöglicht wird, in bestimmtem Maße zu überleben und zu proliferieren. Unerwarteterweise zeigte Cholesterin nicht den gleichen Effekt, höchstwahrscheinlich wegen einer ungünstigen Verteilung in der Zelle. Es wurde auch beobachtet, dass Cholesterin unter Normalbedingungen in sehr niedriger Konzentration in der Zelle vorlag und dass eine neunfache Anhebung dieser Konzentration zum Zelltod führte.

17 β -HSD7 war in der Lage die Ergosterolbiosynthese im yERG27-defizienten Hefestamm SDG110 wiederherzustellen.

Dadurch wird bestätigt, dass das Enzym an der Umsetzung von Zymosteron zu Zymosterol und damit an der Ergosterol/Cholesterinbiosynthese beteiligt ist. Es wurde außerdem gezeigt, dass 17 β -HSD7 im Endoplasmatischen Retikulum lokalisiert ist und den C-Terminus sowohl für eine korrekte Lokalisierung als auch für die Enzymaktivität benötigt. Darüber hinaus wurde gezeigt, dass eine Interaktion zwischen 17 β -HSD7 und C14orf1 unwahrscheinlich ist. Das gleiche Ergebnis wurde für die Hefehomologen dieser Proteine erhalten. Da die zelluläre Lokalisation des Hefeproteins von der externen Cholesterinversorgung abhängig ist, ist es wahrscheinlich, dass yERG28 ebenso wie sein humanes Gegenstück am Transport von Cholesterin und nicht, wie bisher angenommen, an der Biosynthese beteiligt ist.

Abbreviations

ABCA1	ATP-binding cassette transporter 1
ACAT	acyl-CoA:cholesterol acyltransferase
APS	ammonium peroxydisulfate
BSA	bovine serum albumin
BSTFA	N,O-bis(trimethylsilyl)trifluoro-acetamid
cDNA	deoxyribonucleic acid complement of mRNA
CAS	carboxylic acid sterols
CFP	cyan fluorescent protein
CL	corpus luteum
CNS	central nervous system
DMSO	dimethyl sulfoxide
DNA	deoxyribonucleic acid
dNTP	deoxyribonucleotide 5'-triphosphate
E1	estrone
E2	estradiol
E.Coli	Escherichia coli
EDTA	ethylenediaminetetraacetic acid
EtOH	ethanol
ER	endoplasmic reticulum
FBS	fetal bovine serum
GC/MS	gas chromatography/mass spectrometry
GFP	green fluorescent protein
GST	glutathione S-transferase
HDL	high-density lipoproteins
hERG28	human C14orf1 protein (ERG28-like protein)
hHSD1	human 17 β -hydroxysteroid dehydrogenase type 1
hHSD5	human 17 β -hydroxysteroid dehydrogenase type 5
hHSD7	human 17 β -hydroxysteroid dehydrogenase type 7
hHSD7tr.	truncated form of 17 β -hydroxysteroid dehydrogenase type 7, missing the entire C-terminus
HPLC	high performance liquid chromatography
IPTG	isopropyl- β -D-thio-galactosid
kD	kilodalton
LCAT	lecithin:cholesterol acyltransferase
LDL	low-density lipoproteins
LDLR	low-density lipoprotein receptor
MeOH	methanol
NADPH	β -nicotinamide adenine dinucleotide 3'-phosphate, reduced form
NPC1	Niemann-Pick C1 protein
OD	optical density
PAGE	polyacrylamide gel electrophoresis
PBS	phosphate buffered saline
PCR	polymerase chain reaction
PEG	polyethylene glycol
PI	protease inhibitor
PRAP	prolactin receptor associated protein
PRL	prolactin
RNA	ribonucleic acid

mRNA	messenger ribonucleic acid
RT-PCR	reverse transcriptase polymerase chain reaction
SCAD	short-chain alcohol dehydrogenase
SCAP	SREBP cleavage activating protein
SDS	sodium dodecyl sulfate
SREBP	sterol regulatory element binding protein
SSD	sterol-sensing domain
TEMED	tetramethylethylenediamine
TMCS	trimethyl-chlorosilane
U	units
UV	ultraviolet radiation
V	volt
Vps	vacuolar sorting proteins
X-gal	5-bromo-4-chloro-3-indolyl- β -D-galactopyranosid
YFP	yellow fluorescent protein

1. INTRODUCTION

Sterols have long been known as ubiquitous components of eukaryotic cell membranes and precursors of steroid hormones and bile acids. Recently, sterols were also found to be important for embryonic development and cell functioning since an imbalance in sterol level was connected to pathological conditions in mammals (**Clayton P. 1998; Moebius F.F. et al. 2000**). In recent years numerous studies were performed to elucidate enzymes involved in sterol synthesis and to better understand the mechanisms underlying the regulation of this process. Although enormous progress was achieved in this field the exact connection between the sterols and complex cellular regulation mechanisms still remains to be elucidated.

1.1 Cholesterol

Cholesterol is a very important sterol in vertebrates. It plays many roles required for normal cell functioning. It is a component of the cellular plasma membrane and it is involved in regulation of membrane permeability and fluidity. Cholesterol was found to have an asymmetrical distribution in the membrane. It forms domains, which differ markedly between cell types. Such distribution may influence membrane receptors and modulate their activity (**Schroeder F. et al. 1995**). Furthermore, cholesterol serves as a precursor in steroid hormone and bile acid synthesis. It is also found to influence cell cycle and to modify proteins involved in signalling and embryonic development (**Roux C. et al. 2000; Martinez-Botas J. et al. 1999; Suarez Y. et al. 2002**).

Cells can acquire cholesterol from two principal sources: through *de novo* synthesis from acetyl-CoA (**Figure 1**) or from uptake via LDL receptor mediated pathway and further trafficking into different subcellular compartments (**Figure 3**). Both processes are tightly regulated and the disturbance in either of them influences cell functioning and leads to severe impairment during embryonic development, especially the development of the central nervous system (CNS). However, the exact mechanisms of cholesterol homeostasis and regulation are still not completely known.

INTRODUCTION

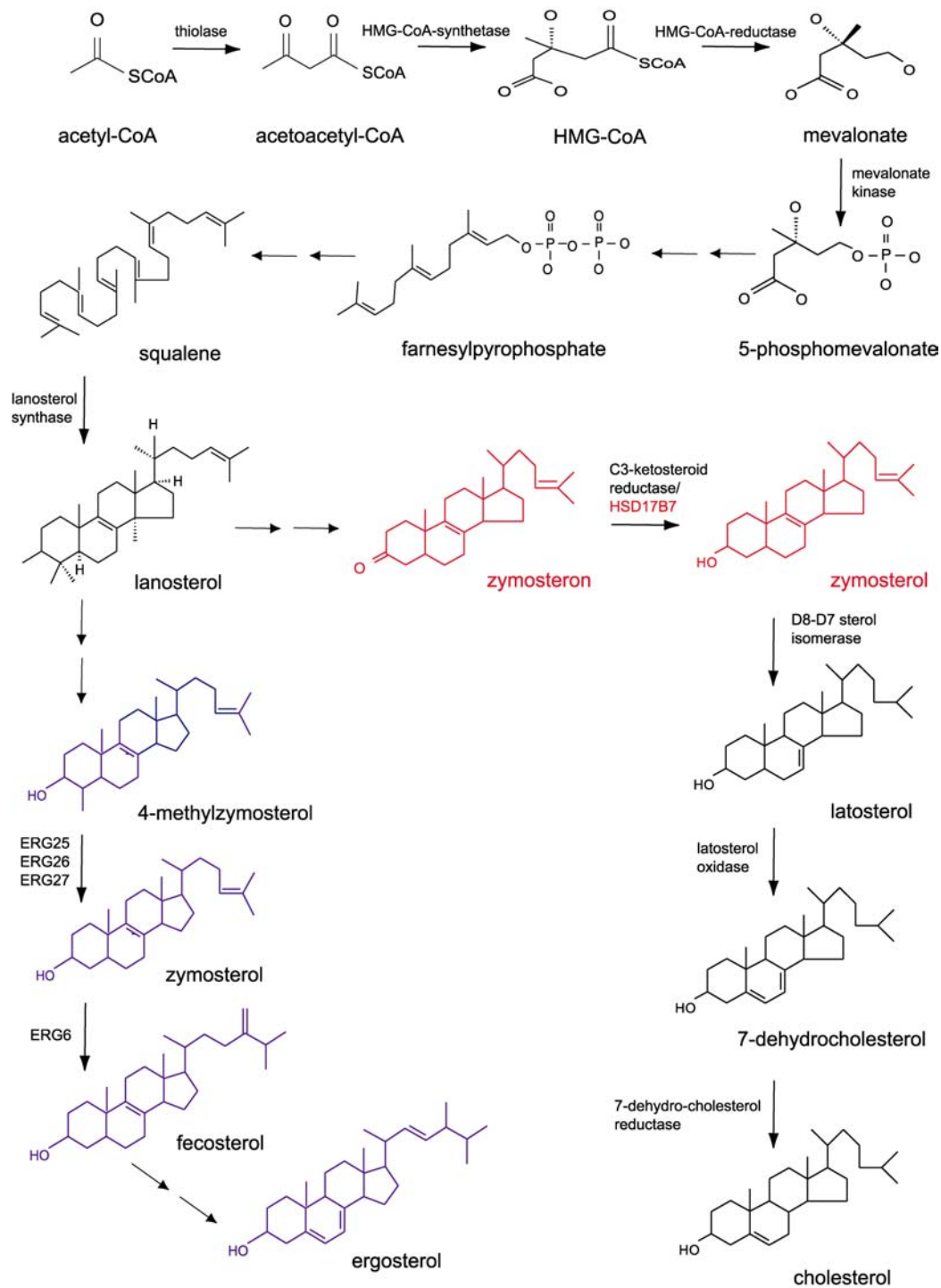


Figure 1. Cholesterol and ergosterol biosynthesis pathways. The first part of the pathway until lanosterol is the same for both sterols. The last steps of ergosterol biosynthesis in yeast are presented in blue on the left side. Cholesterol biosynthesis in mammalian cells is presented on the right side in black. Part of the step suggested to be catalysed by 17β -HSD7 is presented in red. Two arrows stand for more reactions between two intermediates.

1.1.1 Subcellular distribution and regulation of cholesterol biosynthetic enzymes

It was generally assumed that the enzymes of the cholesterol biosynthetic pathway are localized either in the endoplasmic reticulum (ER) or the cytosol. However, numerous studies have shown multiple localizations for some of them (**Figure 2**). The enzymes involved in the initial steps of cholesterol biosynthesis, acetoacetyl-CoA thiolase and HMG-CoA synthase are found in cytosol, peroxisomes and mitochondria. HMG-CoA reductase, the next enzyme in the pathway is localized in the ER and peroxisomes (**Olivier L.M. and Krisans S. 2000**). The current data indicate that the final steps of cholesterol biosynthesis can take place in both peroxisomes and ER, but how it is regulated or whether really both organelles are physiologically participating in cholesterol biosynthesis is not well understood.

It was already mentioned that tight regulation between cholesterol synthesis and uptake should be maintained for normal cell functioning. The cholesterol level is found to influence the transcription of cholesterologenic genes via sterol regulatory element binding proteins (SREBPs) (**Sakakura Y. et al. 2001; Osborne T. and LaMorte V.J. 1998**). The mechanism of this regulation involves multiple steps. When sterol levels in the cell are optimal SREBP is bound to SREBP cleavage activation protein (SCAP) in the ER membrane. Recently, an additional, so far unknown anchor protein is suggested to be involved in tethering this complex to the ER (**Yang T. et al. 2000**). In the sterol depletion condition when the ER cholesterol level is low, the complex is released from the ER anchor and transferred to the Golgi (**Figure 3**). SREBP is activated in the Golgi by releasing the amino-terminal part of the protein (bHLH-N) through a 2-step proteolytic cleavage. The released amino-terminus goes to the nucleus where it activates the gene for the LDL receptor. If this initial step satisfies the cholesterol needs SREBP is not further processed. Otherwise, further processing and accumulation of SREBPs in the nucleus will lead to the activation of genes for cholesterol biosynthetic enzymes.

INTRODUCTION

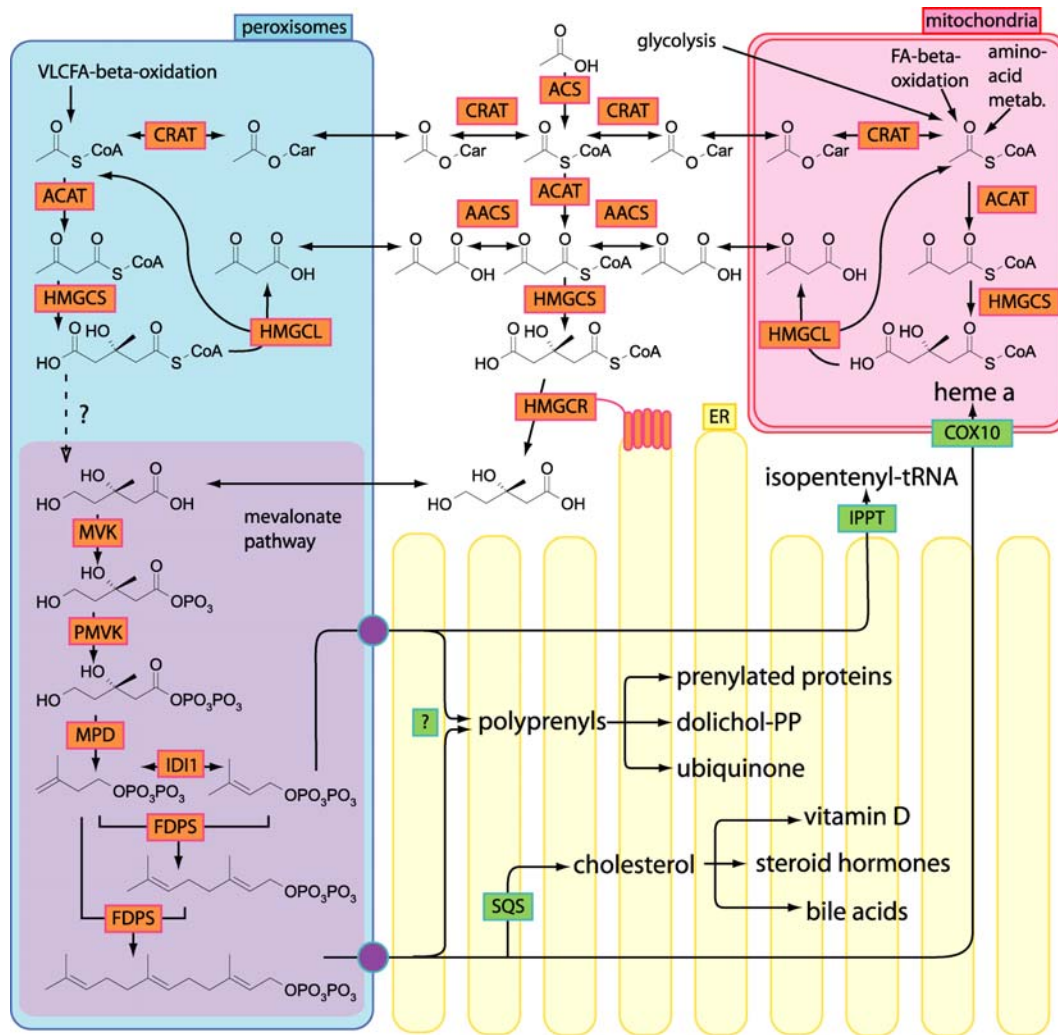


Figure 2. Current view of the subcellular localization of isoprenoid biosynthesis in mammalian cells. Reactions between mevalonate and farnesyl-pyrophosphate are assumed to be almost exclusively peroxisomal (purple shading). Several reactions downstream of farnesyl-diphosphate are omitted for clarity. Enzyme names are abbreviated as follows: AACS acetoacetyl-CoA synthase, ACAT acetoacetyl-CoA lyase, CRAT carnitine acetyltransferase, FDPS farnesyl diphosphate synthase, HMGCL HMG-CoA lyase, HMGCR HMG-CoA reductase, HMGCS HMG-CoA synthase, IDI1 isopentenyl diphosphate isomerase, IPPT isopentenyl tRNA transferase, MPD mevalonate diphosphate decarboxylase, MVK mevalonate kinase, PMVK phosphomevalonate kinase, SQS squalene synthase; VLCFA very long chain fatty acid; COX10 cytochrome c oxidase, subunit 10; ACS Acetyl-CoA synthase.

1.1.2. Regulation of cholesterol homeostasis in the cell

The cellular cholesterol homeostasis is preserved by regulation of the cholesterol import, synthesis de novo and export from the cell (**Figure 3**). It is still not completely known how exactly are those processes coregulated but the cholesterol sensors in the cell were reported to play a crucial role. Recently, a number of proteins having a sterol-sensing domain (SSD) were found to be responsible for proper cholesterol distribution in the cell and the regulation of cholesterol biosynthetic enzymes (**Kuwabara P.E. and Labouesse M. 2002**). Exogenous, low-density lipoprotein (LDL) derived cholesterol is transported via the endosomal pathway to the Golgi apparatus and then redistributed to the plasma membrane and the ER (**Figure 3**). Niemann-Pick C1 protein (NPC1) was described as a key player, which would direct cholesterol movement from late endosomes to the Golgi (**Higgins M.E. et al. 1999**). A mutation in this protein leads to cholesterol accumulation in an aberrant endosomal / lysosomal compartment and an overall increase of the free cholesterol level in the cell and a decrease in transcription of cholesterologenic genes (**Blanchette-Mackie E.J. 2000**).

Other proteins that are involved in cholesterol homeostasis are caveolins, which were first identified to be localized in plasma membrane caveolae, a specialized form of raft domain. It was shown that mutations in caveolins could inhibit ras signalling pathways in the cell by acting indirectly via an effect on cholesterol levels (**Roy S. et al. 1999**). Recently, several studies reported that caveolin-1 could influence cholesterol trafficking in a complex process involving caveolae, ER and the Golgi. Although a transmembrane protein, it can be localized in the cytosol, in excretory vesicles and mitochondria depending on the cell type. It was also found to form complexes with chaperon proteins in the cytosol and to transport newly synthesized cholesterol from ER to the plasma membrane (**Smart J.E. et al. 1996; Li W.P. et al. 2001**). Additionally, a connection between caveolin-1 expression and NPC1 was described in NPC1 knockout mice (**Garver W.S. et al. 1997**). It was also reported that a caveolin mutant that associates with lipid bodies derived from ER causes cholesterol accumulation in late endosomes similar to NPC1 mutants and a decrease in surface cholesterol, cholesterol efflux and synthesis (**Poi A. et al. 2001**).

The SCAP/SREBP complex as already described controls the regulation of the cholesterol synthesis in the cell. SCAP protein contains a SSD and can sense cholesterol level in the ER and therefore regulate the activation of SREBP and the transcription of cholesterologenic genes.

Since most mammalian cells except for liver and steroidogenic tissues are unable to catabolise cholesterol, additional mechanisms to prevent cholesterol accumulation are present.

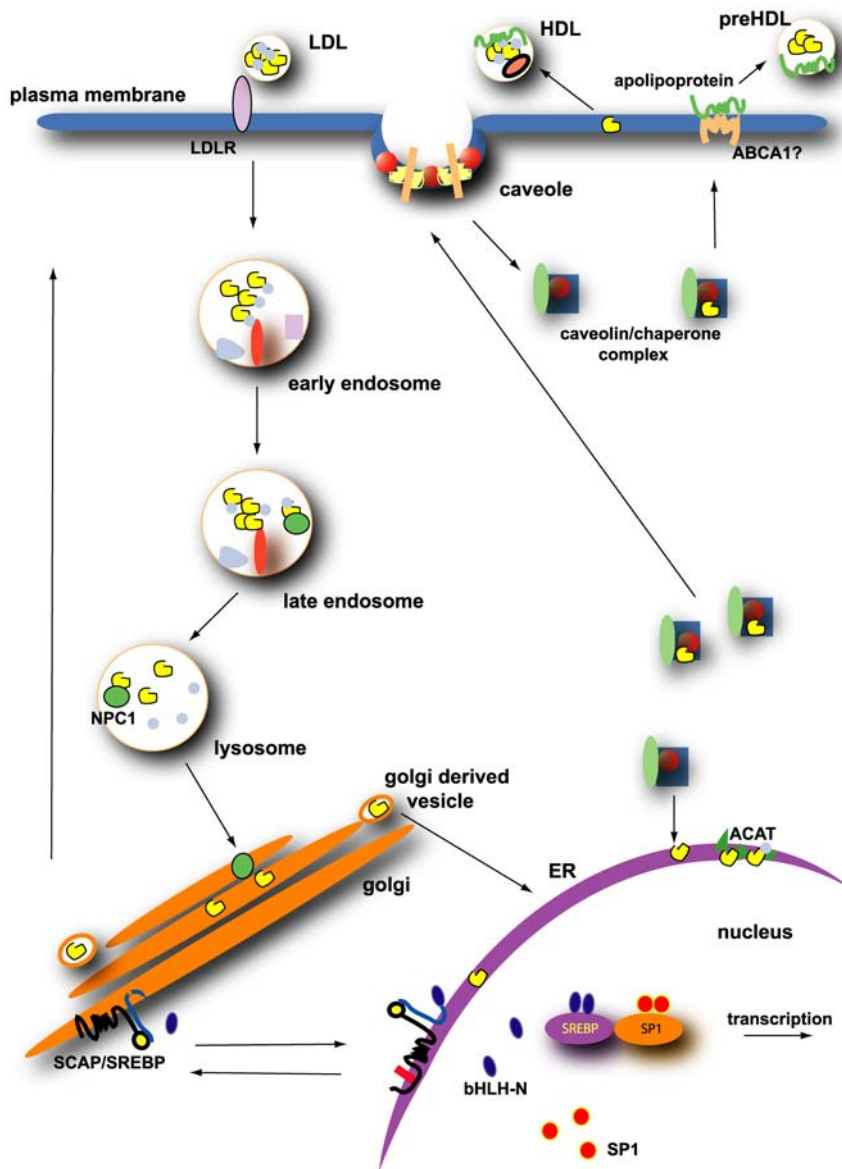


Figure 3. Regulation of cholesterol homeostasis in the cell. Figure presents mechanisms of cholesterol intake, synthesis and export as described in the text. Low-density lipoprotein (LDL) cholesterol (●) can be taken via LDL receptor (LDLR) localized in the plasma membrane. Since LDL cholesterol is in esterified form it moves through the endosomal pathway to lysosomes where it is cleaved to free cholesterol (●). In early endosomes Vps, vesicular sorting proteins (■) play an important role in the molecular distribution. Niemann-Pick C1 (NPC1) protein plays a critical role in cholesterol movement from late endosomes to lysosomes and Golgi. Once cholesterol is transported to the Golgi it is distributed from there to the plasma membrane and the endoplasmic reticulum (ER). The cholesterol level in the cell influences *de novo* synthesis of cholesterol via SCAP/SREBP complex. If the cholesterol level is high SCAP/SREBP complex will stay bound to an anchor protein (■) in ER. If the cholesterol level drops the complex moves to the Golgi where bHLH-N, N terminal part of SREBP is cleaved off and

released to the nucleus. In the nucleus bHLH-N binds to SREBP responsive elements and SP1 to SP1 responsive elements of cholesterologenic genes and triggers its transcription. At the same time low level of cholesterol in plasma membrane leads to exclusion of caveolin (●) from caveolae. Free caveolin was suggested to form a complex with chaperon proteins (■) in the cytosol and to move to ER where it takes newly synthesized cholesterol and brings it to the caveolae. Beside the regulation of intake and synthesis, the cholesterol level is regulated also by esterification and export. Cholesterol export involves two independent mechanisms. One is non-specific diffusion-mediated cholesterol efflux from the cell surface, followed by cholesterol esterification on high-density lipoproteins (HDL). Lecithin:cholesterol acyltransferase, LCAT (○) is involved in the esterification process. The other is an apolipoprotein-mediated process to generate new HDL by removing cellular phospholipid and cholesterol. This process is mediated by interaction of lipid-free or lipid-poor apolipoproteins with the cell surface, most probably with ATP-binding cassette transporter 1 (ABCA1) in raft domains. As a result pre-HDL vesicles containing phospholipids and free cholesterol are formed. Caveolin-1 was suggested to play a role in transport of free cholesterol to HDL.

Excess of free cholesterol can be transferred to cholesterol ester and stored in the cytosol but also be transported out of the cell. High-density lipoproteins (HDLs) are believed to play a main role in the later process. Recently, two independent mechanisms were reported (**Yokoyama S. 2000**). One is non-specific diffusion-mediated cholesterol efflux from the cell surface followed by cholesterol esterification in HDL. This process causes a constant gradient of free cholesterol between HDL and the cell surface, which represents the driving force for the removal of cellular cholesterol. The other is an apolipoprotein-mediated process to generate new HDL by removing cellular phospholipids and cholesterol. This process is mediated by the interaction of lipid-free or lipid-poor apolipoproteins with the cell surface, most probably with raft domains. As a result preHDL vesicles containing phospholipids and free cholesterol are formed. Caveolin was suggested to play a role in the transport of free cholesterol to HDLs. Thus to maintain cholesterol homeostasis in the cell it is important to achieve a balance between cholesterol intake, removal and synthesis. **Figure 3** shows a summary of these processes involved in the preservation of cellular cholesterol homeostasis.

1.2. Ergosterol

Ergosterol is a major sterol in the plasma membrane of yeast cells and it is playing a similar role to that of cholesterol in mammalian cells. Extensive mutational and biochemical studies performed on enzymes involved in ergosterol biosynthesis led to complete elucidation of this pathway. It was observed that the first part of the pathway, up to the formation of zymosterol (**Figure 1**) is important for yeast growth and that mutations in this part lead to ergosterol auxotrophy (**Lees N.D. et al. 1995**). However, subsequent steps of the pathway are non-essential for yeast growth since the intermediates produced can substitute for ergosterol. Although yeast cells showed no absolute requirements for ergosterol, some changes in plasma membrane permeability could be observed if ergosterol was substituted by other sterols (**Gaber R.F. et al. 1989; Hemmi K. et al. 1995**).

1.2.1 Regulation of ergosterol biosynthetic enzymes

Unlike the enzymatic aspects of ergosterol biosynthesis, the regulation of this pathway is poorly understood. So far it was known that ergosterol as well as other sterols containing C-22=23 unsaturation and C-24 methylation had the ability to regulate endogenous sterol biosynthesis (**Casey W.M. et al. 1991**).

Recently, two transcription factors, UPC2 and ECM22 were found to be involved in this regulation but the exact mechanism of their activation is still not known (**Vik A. and Rine J. 2001**). Furthermore many points of the ergosterol biosynthetic pathway are also regulated by oxygen and/or hem independently of the sterol status, which points to requirement for these co-factors in the pathway (**Kwast K.E. et al. 1998**).

1.2.2 Regulation of ergosterol homeostasis

Accumulation of ergosterol in yeast cells causes cytotoxicity and therefore regulation of the ergosterol level is an important process.

Under the normal aerobic conditions, *de novo* synthesis is the only ergosterol source in the cell, since yeast in those conditions can't take sterols from the environment (**Crowley J.H. et al. 1998**). Furthermore the export of sterols is unlikely to take place in yeast since no convincing apolipoprotein progenitor can be found in the yeast genome.

Therefore, ergosterol homeostasis in yeast is preserved through regulation of its synthesis, esterification and as recently has been shown of cellular localization (**Sturley S.L. 2000**).

Several genes were described to be involved in those processes although the mechanisms of action are not entirely elucidated. UPC2 and ECM22 have been already mentioned to regulate transcription of genes involved in ergosterol biosynthesis. Additionally UPC2 was reported to influence the intake of sterols under anaerobic conditions.

Recently, another protein called ARV1 (ARE2 required for viability 1) has been described to act as a sterol sensor and to mediate sterol uptake and distribution (**Tinkelenberg A.K. et al. 2000**). Yeast cells defective in the ARV1 gene were inviable if ACAT related enzyme 2 (ARE2) responsible for sterol esterification was deleted. With intact ARE2, ARV1 mutant showed significantly increased sterol levels in ER and vacuolar membrane. Additionally the mutant yeast cells were inviable under anaerobical conditions, which suggested impaired sterol uptake. Although it was reported in this case that esterification is important for prevention of sterol cytotoxicity, yeast viability was not impaired in ARE1 and ARE2 single mutants (**Yang H. et al. 1996**). Moreover, reduction of sterols by YAH1 and ARH1 in mitochondria was also suggested to play role in detoxification (**Manzella L. et al. 1998; Barros M.H. and Nobrega F.G. 1999**). So far the results implied that although yeast cells regulate ergosterol level, this regulation involves different mechanisms than those acquired in mammalian cells.

1.3 17β - hydroxysteroid dehydrogenase type 7 (17β -HSD7)

17β -HSD7 was first identified in rat, as a 32 kD microsomal phosphoprotein associated with a short form of prolactin receptor and therefore named Prolactin Receptor Associated Protein (PRAP). PRAP was abundantly expressed in ovarian corpus luteum (CL) of pregnant rat and showed no expression in any other steroidogenic and nonsteroidogenic tissue. Up regulation of expression was detected from the mid to the late pregnancy and was shown to be estradiol (E2) and prolactin (PRL) dependant (**Parmer T.G. et al. 1992; Duan W.R. et al. 1996 and 1997**).

The same protein was later identified in mouse as a novel estrogenic 17β -hydroxysteroid dehydrogenase. The mouse protein shares 89% identity with rat PRAP and the same expression pattern, with some additional lower expression in ovary of nonpregnant mouse, placenta, mammary gland, liver, kidney, testis, uterus, brain and small intestine.

Activity measurements for mouse and rat protein, revealed 17β -hydroxysteroid dehydrogenase activity, with estrone (E1) as a preferable substrate (**Nokelainen P. et al. 1998 and 2000**).

Human 17β -HSD7 shares 78% and 79% identity with rat and mouse 17β -HSD7, respectively. The tissue distribution for human enzyme was identified using *in silico* Northern blot and RT-PCR and corresponds to that of rat and mouse. In addition to that human 17β -HSD7 ESTs were detected in germinal B cells, thymus, fetal liver, and several neural tissues like retina, neuronal precursors and infant brain. Promoter analysis of human 17β -HSD7 gene revealed the presence of several lymphoid and brain specific transcription factors binding sites and, strikingly, complete absence of steroid responsive elements (**Krazeisen A. et al. 1999**), which is unusual for an enzyme that is considered to be involved in steroid metabolism.

Human 17β -HSD7, together with its closest vertebrate homologues, belongs to the short chain alcohol dehydrogenase (SCAD) family of proteins as determined by phylogenetic analysis. However, it has 2 unique features which it shares solely with ERG27, a recently identified 3-ketosteroid dehydrogenase from yeast involved in ergosterol biosynthesis and with no other SCAD protein (**Figure 4**). These are a 28 amino acid insert following the conserved NAG motif, which forms a loop near the substrate binding site and a hydrophobic helix on the C-terminus, which is presumably membrane associated according to homology-based molecular modeling (**Breitling R. et al. 2001**).

All these facts, the structural features, the high conservation between ERG27 and 17β -HSD7, the expression in fetal liver and brain which are tissues of intensive cholesterol biosynthesis and the absence of homologues in *Drosophila melanogaster* and *C.elegans* which are cholesterol auxotrophic organisms, point to a possible physiological role for 17β -HSD7 in cholesterol biosynthesis rather than in steroid hormone metabolism.

```

rathSD7      MMRKVVLITGASSGIGLALCGRLLAEDDD---LHLCLACRNLSKAGAVRDALLASHP--- 54
mouseHSD7    -MRKVVLITGASSGIGLALCGRLLAEDDD---LHLCLACRNLSKARAVRDTLLASHP--- 53
humanHSD7    -MRKVVLITGASSGIGLALCKRLLAEDDE---LHLCLACRNMSKAEAVCAALLASHP--- 53
rabbitHSD7   -MRKVVLITGASSGIGLALCKRLLTVDDG---LHLCLACRNMGKAKAARAALLASHS--- 53
ERG27        MNRKVAIVTGTNSNLGLNIVFRLIETEDTNVRLTIVVTSRTLPRVQEVINQIKDFYNKSG 60

rathSD7      -----SAEVSIVQMDVSNLQSVVARGAEVKKRFQRLDYLYLNAGIMPNPQLNLKAFFCGI 109
mouseHSD7    -----SAEVSIVQMDVSSLQSVVARGAEVKKQFQRLDYLYLNAGILPNPQFNLKAFFCGI 108
humanHSD7    -----TAEVTIVQVDVSNLQSVFRASKELKQRFQRLDCIYLNAGIMPNPQLNIKALFFGL 108
rabbitHSD7   -----GAQVTMVQVDVGLDQSVFRAADELQRFQRLDYVYLNAGIMPNPQLNVRALFSGL 108
ERG27        RVEDLEIDFDYLLVDFTNMVSVLNAYYDINKKYRAINLYFVNAAQGIFDGLDWIGAVKEV 120

rathSD7      FSRNVIHMFSTAEGLLTQNDKITADGFQEVFETNLFQGHFILIRELEPLLCHSDNPSQLIW 169
mouseHSD7    FSRNVIHMFSTAEGILTQNDQSVTADGLQEVFETNLFQGHFILIRELEPLLCHADNPSQLIW 168
humanHSD7    FSRKVIHMFSTAEGLLTQGDKITADGLQEVFETNVFGHFILIRELEPLLCHSDNPSQLIW 168
rabbitHSD7   FSRKVIHMFSTAEGLLTQGDRLTADGLQEVFETNIFGHFILIRELEPLLCHSDTPSRLIW 168
ERG27        FTNPLEAVTNPTYKIQLVGVKSKDD-MGLIFQANVFGPYFYFISKILPQLTRG--KAYIVW 177

rathSD7      TSSRNAKSNFSLEDIQHAKGQEPYSSSKYATDLLNVALNRNFNQKGLYSSVTCPGVMT 229
mouseHSD7    TSSRNAKKNFSLEDIQHSKGPEPYSSSKYATDLLNVALNRNFNQKGLYSSVMCPGVMT 228
humanHSD7    TSSRSARKSNFSLEDFQHSKGKEPYSSSKYATDLLSVALNRNFNQGLYSSNVACPGTALT 228
rabbitHSD7   TSSRNARKSNFSLEDIQHSKGQEPYSSSKYATDLLNVALNRHYNQGLYSSVVCPTVLT 228
ERG27        ISSIMSDPKYLSLNDIELLKTNASYEGSKRLVDLLHLATYKDLKGLINQYVVQPGIFTS 237

rathSD7      NLTYGILPPFVWTL LLPVIWLLRFFAHAFT-VTPYNGAEALVWLFHQK-PESLNPLTKYL 287
mouseHSD7    NMTYGILPPFIWTL LLPIMWLLRFFVNALT-VTPYNGAEALVWLFHQK-PESLNPLTKYA 286
humanHSD7    NLTYGILPPFIWTL LMPAILLRFFANAFT-LTPYNGTEALVWLFHQK-PESLNPLIKYL 286
rabbitHSD7   NMTYGILPPFMWTL LLPFIWLLRFFANAFT-LTPYNGAEVLVWLFHQK-PESLNPLAKYM 286
ERG27        HSFSEYLNFFTYFGMLCLFYLARLLGSPWHNIDGYKAANAPVYVTRLANPNFEKQDVKYG 297

rathSD7      SGTGGLGTNYVKGQKMDVD--EDTAEKFKYKTLLELEKQVRITIQKSDHHS----- 335
mouseHSD7    SATSGFGTNYVTGQKMDID--EDTAEKFEVLELEKRVRTTVQKSDHPS----- 334
humanHSD7    SATTGFRNYIMTQKMDLD--EDTAEKQYKLELEKHIRVTIQKTDNQARLSGSL 341
rabbitHSD7   SATTGLGSNYITTQKMDID--EDTA----- 309
ERG27        SATSRDGMPIKIQEIDPTGMSDVFAIYQKKLEWDEKLDQIVETRTPI----- 347

```

Figure 4. Alignments of 17 β -HSD7 protein sequences from different organisms with ERG27. 17 β -HSD7 belongs to the SCAD family of proteins and shares the same cofactor-binding site (green), active center (blue) and NAGI motif (yellow) with other members of the family. However, two additional hydrophobic domains marked with red squares 17 β -HSD7 shares with ERG27, 3-ketosterol reductase from yeast involved in ergosterol biosynthesis. Those domains are not present in other members of the SCAD family of proteins.

1.4. C14orf1 and its yeast homologue ERG28-connection with sterol biosynthesis and cellular proliferation

Recent analysis of gene transcriptional regulation in *Saccharomyces cerevisiae* identified a novel gene now called *erg28* whose expression correlated with the expression of the ergosterol pathway genes. Deletion of this gene in yeast cells resulted in accumulation of 3-hydroxysterols, 3-ketosterols and carboxylic acid sterols (CAS) and lowering of ergosterol level. The similar sterol profile was reported for ERG27 and ERG26 mutants with the only difference that the ERG28 mutant was viable but with an impaired growth rate (**Gachotte D. et al. 2001**). Therefore, it was suggested that ERG28 might play role in the modification of ERG26 and ERG27 activity through complex formation and/or in tethering those enzymes to the ER. Furthermore, ERG28 was found to be highly conserved among the species that are not cholesterol auxotrophs. The human homologue called C14orf1 was reported to be highly expressed in testis and overexpressed in cancer cell lines and therefore connected to cellular proliferation (**Veitia R.A. et al. 1999**). However the exact role of C14orf1 in the cell is still not elucidated.

1.5. The aim of the study

During evolution eucaryotic cells developed complicated mechanisms to preserve optimal sterol levels and acquire normal functioning. Since those processes are dynamic so far the exact cholesterol level necessary for viability and proliferation was not determined. Therefore the primary intention in this study was to examine changes in free cholesterol level in dying cells. Furthermore, it was tested whether and how the substitution of cholesterol with ergosterol influences survival and growth of cholesterol auxotrophic cell lines.

De novo cholesterol biosynthesis was found to be important for embryonic development. Mutations in cholesterol biosynthetic enzymes lead to severe defects especially in the neural system development. Due to structural similarity to ERG27, 17 β -HSD7 became a potential candidate gene involved in cholesterol biosynthesis. The aim of this study was to determine the subcellular localization of 17 β -HSD7 and its ability to restore ergosterol biosynthesis in ERG27 knockout yeast. Furthermore, the connection between 17 β -HSD7 and 3-ketosterol reductase defect in U-937 and X-63 cholesterol auxotrophic cell lines was checked.

In yeast, a novel gene called ERG28 was suggested to modify activities of ERG26 and ERG27 by forming interactions with those proteins and the human homologue of ERG28, C14orf1 was suggested to be connected to cell proliferation. Since cholesterol in mammalian cells was also found to be important for cell proliferation, the intention was to determine whether yERG28 and C14orf1 indeed interact with yERG27 and h17 β -HSD7, respectively and therefore influence proliferation via cholesterol and ergosterol amount.

2. RESULTS

2.1. Analysis of cholesterol auxotrophic U-937 cells in media containing different sterols

2.1.1. Cell survival and proliferation

It was recently suggested that cholesterol localized in the plasma membrane might have an additional role in preventing a sodium leakage into the cell. This function was proposed to be made possible by the unique structure of cholesterol. Since phytosterols have a different structure from cholesterol and since they should be designed to prevent proton and not sodium leakage, they were predicted not to be able to compensate for cholesterol deficiency in animal cells (**Haines T.H. 2001**). To check this theory, the previously identified cholesterol auxotrophic mammalian cell line U-937 was cultured in media with reduced (0,1%) serum and the addition of either cholesterol (cholesterol conditioned medium) or ergosterol (ergosterol conditioned medium). The same cells, cultured in medium with 10% serum (normal conditions) were used as a positive control and in medium with 0,1% serum without supplement as a negative control. Cell survival and proliferation were checked at different time points.

HeLa cells were used as an additional positive control. They can synthesize cholesterol *de novo* and different conditioned media had no impact on cell survival (**Figure 5 A**).

U-937 cells however, survived best in medium supplemented with 10% serum as expected since those were normal growth conditions. Survival was 98-100% during the entire time course and didn't decrease even after 96 h (**Figure 5 B green line**). If the cells were cultured with 0,1% of serum cell survival decreased to only 30% after 48 h, followed by rapid and complete cell death 96 h after plating (**Figure 5 B red line**). Surprisingly, only slight improvement in cell survival, in comparison to negative control, was observed 48 h after plating if cells were grown in cholesterol conditioned medium (**Figure 5 B yellow line**).

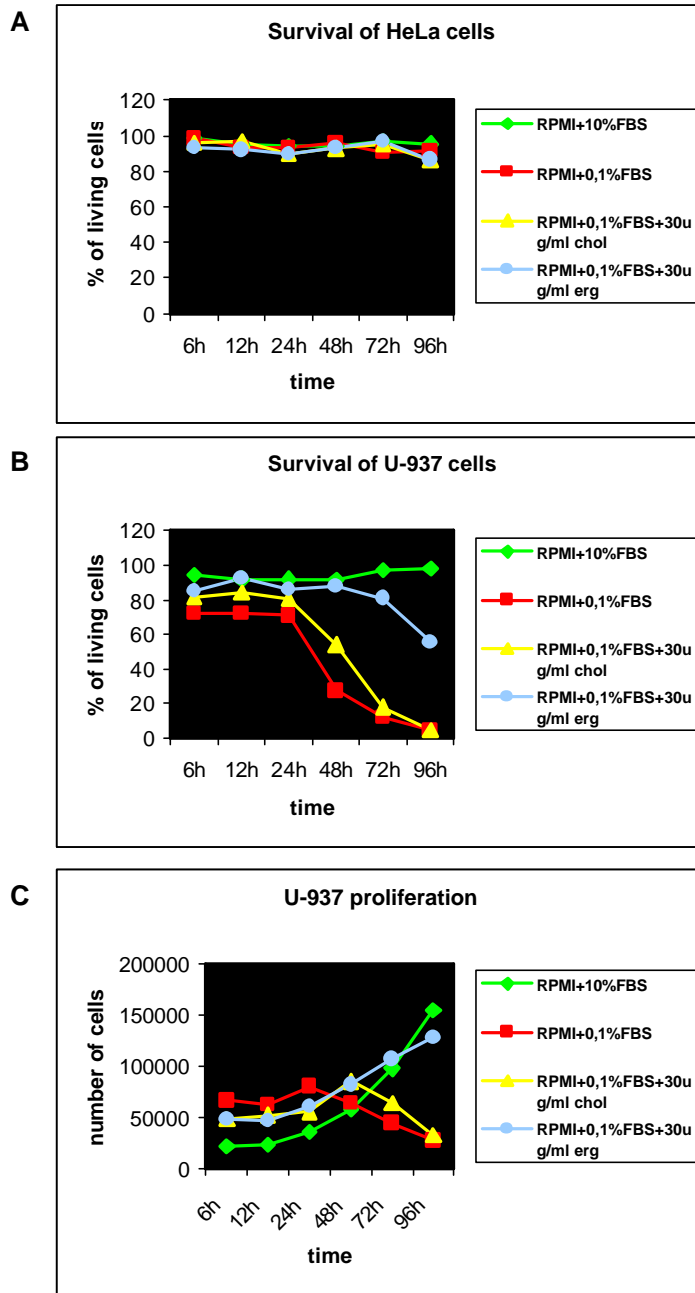


Figure 5. Survival and proliferation of HeLa and U-937 cells in different media. The averages of 5 experiments are presented. Survival of HeLa cells was not dependent on medium composition (A). U937 cells however, required addition of sterol in order to survive and proliferate (B). Note that U-937 cells could survive only 24 h without addition of sterol (red). Addition of cholesterol improved survival a bit (yellow) but much less as an addition of ergosterol (blue). No changes in survival could be observed in normal medium (green). The best proliferation of U-937 cells was in normal medium (green). Note that the proliferation rate in the first 24 h was the same in all cases (C). However, the cells that were grown in ergosterol conditioned medium (blue) or normal medium (green) could proliferate longer than the others.

This was not expected since the 30 µg/ml of cholesterol that was present in the cholesterol conditioned medium should be equivalent to the cholesterol amount in the normal medium.

Furthermore, if cells were grown in ergosterol conditioned medium 80% cell survival was observed in the first 72 h after plating, which was comparable to the control cells (**Figure 5 B blue line and green line**). Proliferation rates of U-937 cells during the first 24 h were the same no matter which media was used for culturing (**Figure 5 C**). Afterwards proliferation could be observed only if the cells were grown either in normal or ergosterol conditioned medium (**Figure 5 C green and blue line**). Furthermore the proliferation rate was still the same 48 h after the culturing if the cells continued to proliferate. 24 h later, however, the first differences in proliferation rate between cells grown in the normal conditions and cells grown in ergosterol conditioned medium could be observed (**Figure 5 C green and blue line 48-72h time point**). Cells that were grown in ergosterol conditioned medium started to proliferate more slowly most probably due to the reduced amount of growth factors in the reduced serum (**Figure 5 C blue line**).

The decrease in cell number that can be seen in **Figure 5 C, red and yellow lines**, was due to the shrinkage of dead cells which couldn't be recognized anymore under the microscope, so that in consequence less cells were counted. If cells were grown in the medium containing only a reduced amount of serum proliferation was supported only in first 24 h after plating (**Figure 5 C red line**). Surprisingly, cholesterol conditioned medium couldn't support cell growth longer than 48 h (**Figure 5 C yellow line**). However, it was observed that both, proliferation and survival in cholesterol conditioned medium depended on the cell number that was plated and varied between the experiments. Note that in some cases cells could survive as long as 72 h but only if cell number didn't exceed ~ 80000 cells/ml (**Figure 6 orange line**).

To be able to explain better the effect of cholesterol and ergosterol on cell survival, U-937 cells were cultured in either cholesterol conditioned medium with different concentrations of cholesterol, or in ergosterol conditioned medium with different concentrations of ergosterol.

Cell survival was found to depend on cholesterol concentration (**Figure 6 A**). The best survival was achieved if 30 µg/ml of cholesterol was present in the medium (**Figure 6 A orange line**). If 20 µg/ml of cholesterol was present in the medium, cells could survive only 48 h and then started to die (**Figure 6 A violet line**). If either 5 µg/ml or 10 µg/ml of cholesterol was present in the medium cells couldn't survive longer than 24 h, although a slightly improved survival could be observed if more cholesterol was present in comparison to the negative control (**Figure 6 A yellow, blue and orange lines**).

The cellular proliferation was also concentration dependent as shown in **Figure 6 B**.

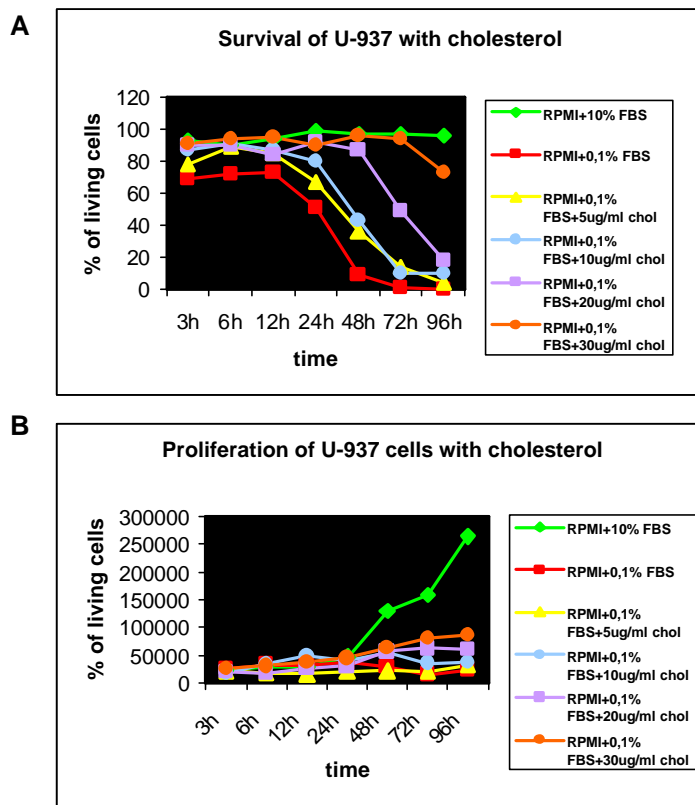


Figure 6. Survival and proliferation of U-937 cells with different concentrations of cholesterol. The averages of 3 experiments are presented. It is visible from the figure that survival of U-937 cells with cholesterol was concentration dependent (A). Note that the best survival was achieved with 30 $\mu\text{g/ml}$ of cholesterol (orange) which corresponds to the cholesterol amount in the normal medium (green). However this amount was enough only until cells reached ~ 80000 cells/ml (orange). Note also that cells started to die at the same time point. Cells couldn't proliferate with cholesterol amount less than 20 $\mu\text{g/ml}$ (B yellow and blue). The best proliferation was achieved with 30 $\mu\text{g/ml}$ (B orange). Note that the proliferation rates in first 48 h were the same for the cells that were grown in normal medium or in cholesterol conditioned medium with 30 $\mu\text{g/ml}$ of cholesterol (orange and violet).

The proliferation was possible only if either 10 $\mu\text{g/ml}$ or 20 $\mu\text{g/ml}$ of cholesterol was present in the medium and the proliferation rate was the same in both cases in the first 48 h after plating (**Figure 6 B orange and violet lines**). Afterwards, cells that were grown with a lower cholesterol concentration failed to proliferate (**Figure 6 B violet line 48h-72h**). If cells were grown with less than 20 $\mu\text{g/ml}$ of cholesterol no proliferation could be observed (**Figure 6 B yellow and blue line**). If cells were growing in ergosterol conditioned medium with different concentrations of ergosterol, in both, cell survival and proliferation, no concentration dependency was observed (**Figure 7A and B**).

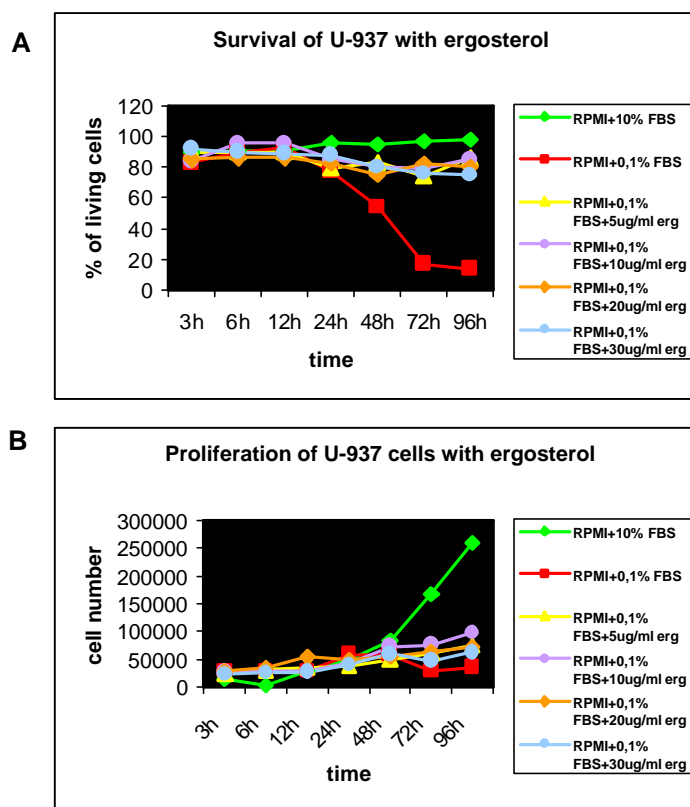


Figure 7. Survival and proliferation of U-937 cells with different concentrations of ergosterol. The averages of 2 experiments are presented. Note that survival of U-937 cells with ergosterol was not concentration dependable (A). The same was true for proliferation (B).

Cell survival was in all cases between 80% and 90% in the entire time course and didn't show any decrease after 96 h (**Figure 7A**).

To test the possibility that mutations, which restore the ability of U-937 cells to synthesize cholesterol, are responsible for the proliferation on ergosterol cells were transferred after 96 h to medium which contained only reduced serum and cell survival was monitored for 48 h. In first 24 h 50% reduction in cell survival was observed followed by survival decrease to 18% in next 24 h (data not shown). This indicated that the ability of cholesterol biosynthesis was not restored.

The results presented here revealed that even if cholesterol was added to the medium at the level of 30 $\mu\text{g/ml}$, which corresponded to normal conditions, the cells could not restore the survival rate observed for the positive control once the certain cell number was reached (**Figure 5 and Figure 6**).

RESULTS

Furthermore, it seems that ergosterol was more tolerable to the cells and could support cell survival and proliferation at all concentrations, since no concentration dependency was observed (**Figure 5 and Figure 7**). This suggested that the intake of LDL cholesterol, free cholesterol and ergosterol might be different. Additionally, the different sterol sources could have a different impact on the regulation of cell proliferation and death.

2.1.1. Cholesterol and ergosterol levels

The data presented here raised the question which processes inside the cells, caused different survival, once the sterols were taken up from the media. At the same time, it was necessary to determine whether ergosterol was kept in its original form inside the cells or it was metabolized further to be tolerable to the cells. The obvious next step was to detect the presence and amount of cholesterol and ergosterol in cell lysates and to search for potential changes leading to cell death.

U-937 cells were grown in different conditioned media as already described above. It should be emphasized that in this case the serum batch was changed and, therefore, cells grown in media containing reduced serum amounts failed to proliferate (**Figure 8 B**). Proliferation inability had an impact on cell survival. It was observed that in both cases, when the cells were grown with either cholesterol or ergosterol, they survived only first 48 h after plating (**Figure 8 A yellow and blue line**). Furthermore, the impact of both sterols on cell survival was the same and this did not correlate with previous results (**compare Figures 5 and 8**). However, since the intention was to answer first, whether ergosterol was kept in its original form and/or was metabolised further inside the cell and second, what the differences in free (non esterified) cholesterol level between living and dieing cells are, gass chromatography/ mass spectrometry (GC/MS) measurements were performed despite these discrepancies.

Cells were collected at different time points and the level of cholesterol and ergosterol was determined from cell lysates and media with GC/MS as explained in Materials and Methods. It should be noted that only free, non modified cholesterol and ergosterol could be measured with this method.

The initial values of cholesterol and ergosterol in media are presented as percentages of the free cholesterol level in RPMI+10% FBS (**Figure 9**). Cholesterol and ergosterol levels in both, cell lysates and media, measured at different time points are presented as a percentage of initial values (cholesterol and ergosterol levels in cells grown in normal condition before plating in different conditioned media).

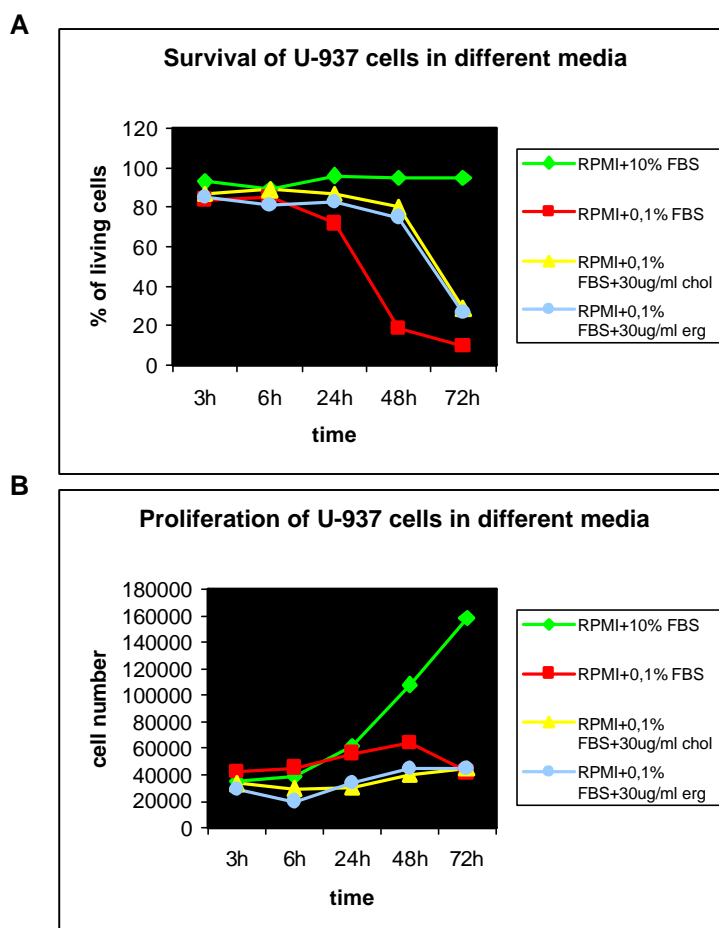


Figure 8. Survival and proliferation of U-937 cells used for GC/MS measurements
Both cholesterol (yellow) and ergosterol (blue) had the same impact on cell survival in this case. It should be noted that results presented here don't correlate with the previous results. Cells that were growing in media with reduced serum could not proliferate and this was probably due to different serum batch used in this case. The impaired cell proliferation is most likely to be a cause for different survival ability if compared to previous results.

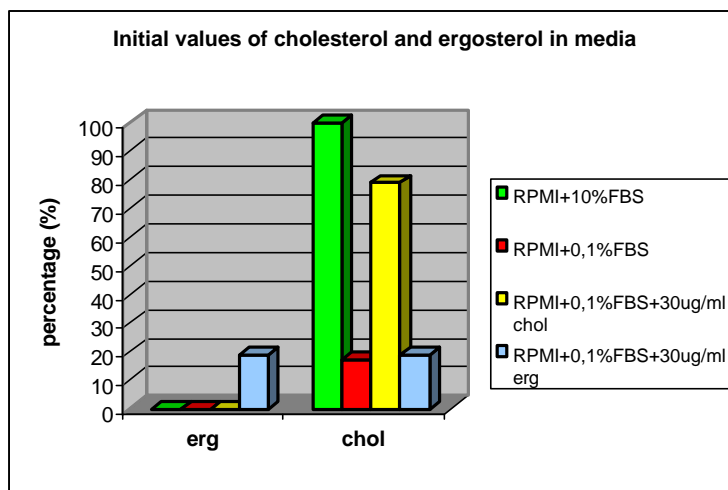


Figure 9. Initial levels of cholesterol and ergosterol in differently conditioned media measured with GC/MS. Free cholesterol and ergosterol levels were measured before U-937 cells were plated. The values are presented as a percentage of the measured cholesterol level in RPMI+10% FBS. Note that free cholesterol level in cholesterol conditioned medium (yellow) was 75% of the cholesterol level in normal medium (green). In RPMI+0,1% FBS, only 15% of cholesterol level is present. Note that ergosterol level in the same medium was very low. This is probably due to very poor ergosterol solubility. GC/MS spectra are presented in the Appendix.

It can be seen from the **Figure 9 (red)** that cholesterol level was low in medium that contained reduced amount of serum (15% of control). Furthermore, the ergosterol amount in ergosterol conditioned medium was surprisingly low, probably due to a very low ergosterol solubility. In cholesterol conditioned medium, the cholesterol amount was 30 $\mu\text{g}/\text{ml}$. This should be equivalent to the cholesterol amount in normal medium. However, a somewhat lower amount of cholesterol (75%) was measured in comparison to normal medium (**Figure 9 green and yellow**), but It should still be sufficient to satisfy cellular needs. However, the results presented here show that cholesterol could not support cell survival in comparison to normal conditions.

Therefore, it was checked whether cells were able to take cholesterol from the medium in the required amount. After 6 hours almost no free cholesterol could be detected in cholesterol conditioned medium (**Figure 10 A yellow**). This could imply that all cholesterol was taken up by the cells until the observed time point.

The same observation was made also for cells that were grown in other media. Note that in all cases almost no cholesterol can be detected in the medium already 6 h after plating (**Figure 10 B**) if compared to the initial values (**Figure 9**). The cholesterol level inside the cells was higher at the 3 h time point if the cells were grown in cholesterol conditioned medium in comparison to other media. Interestingly, no substantial changes in cholesterol level in those cells could be observed during the entire time course (**Figure 10 B yellow**).

If cells were grown in ergosterol conditioned medium, ergosterol could be detected inside the cells 6 h after plating. Interestingly no ergosterol was detected in later time points (**Figure 10 B blue**). However, it was observed that the cholesterol amount was much more increased in those cells at the 6 h time point in comparison to cells grown in other conditions. At later time points the cholesterol amount continued to increase until 9-fold elevation in its level occurred, 48 h after plating (**Figure 10 B blue**). If compared to cell survival the elevation in cholesterol level was followed by rapid cell death (**Figure 8 A blue**).

The same 9-fold elevation in cholesterol level was also observed in the cells, which were grown in a medium with reduced serum, only that it occurred earlier, 24 h after plating (**Figure 10 B red**) and was followed by rapid cell death as well (**Figure 8 A red**).

If cells were grown in normal medium, a low and fairly steady cholesterol level was detected in cell lysates during the observed time course. However slight elevation in cholesterol level occurred 6 h and 48 h after plating (**Figure 10 B green**). If compared with cell proliferation results (**Figure 8 B green**) it was observed that those elevations in cholesterol level were followed by substantial increase in cell number. Therefore, it can be concluded that the observed elevation in cholesterol level was required for cell proliferation.

Since cellular cholesterol homeostasis is partly regulated by cholesterol export from the cell (**Yokoyama S. 2000**), media in which cells were grown were collected in different time points and ergosterol and/or cholesterol amounts were measured.

It could be observed that substantial cholesterol export was present only from cells that were grown in normal conditions at 72 h time point. In this case initial cholesterol level was restored in the medium (**Figure 10 A green**). Furthermore, almost no cholesterol export could be observed from cells that were grown in cholesterol conditioned medium (**Figure 10 A red**). If cells were grown in ergosterol conditioned medium, only cholesterol export was detected and no ergosterol was present in the medium. It was observed in addition that elevated cholesterol level inside those cells (**Figure 10 B blue**) were accompanied with substantial cholesterol export to the medium 24 h after plating (**Figure 10 A blue**). However, it seems that once the cholesterol level exceeded a certain point (9-fold elevation) the export was aborted.

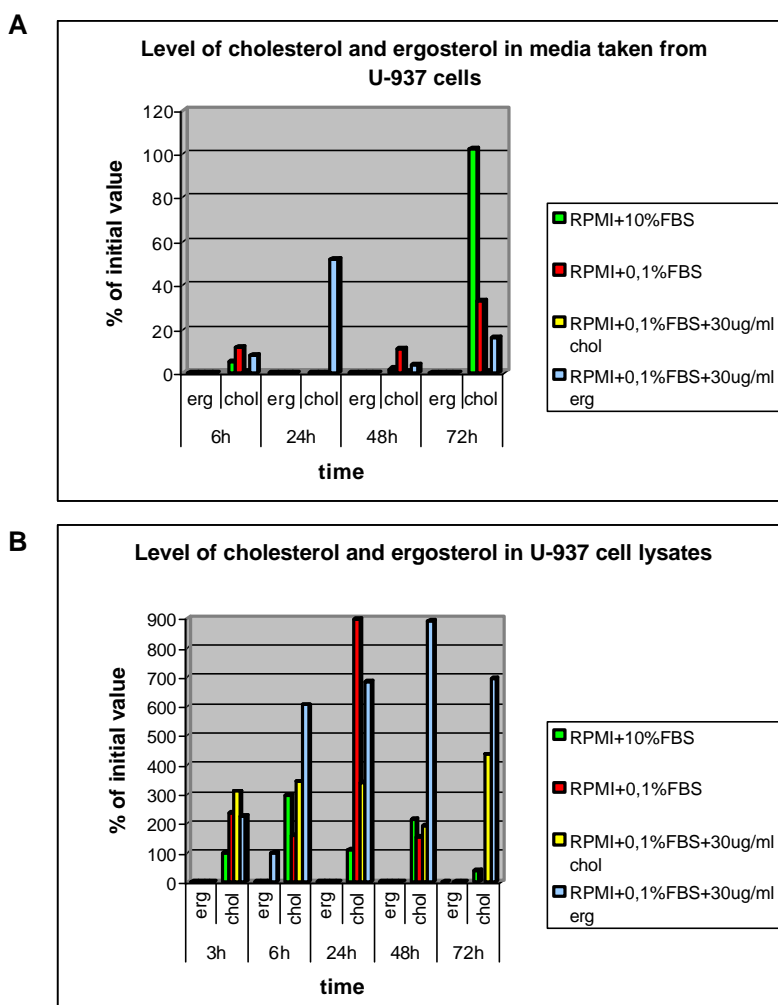


Figure 9. Free cholesterol and ergosterol level measured from media and U-937 cell lysates in different time points. Free cholesterol levels measured from media before cells were plated were taken as initial levels. In case of cell lysates the values obtained from the cells grown in normal medium before they were transferred in different conditioned media are taken as initial values. Values obtained from other time points are presented as % of initial value for each growing condition. Note that cells, which were growing in normal medium kept free cholesterol level low (B green). No changes in cholesterol level during the entire time course could be observed for cells that were grown in cholesterol conditioned medium (B yellow). Free cholesterol level reached 9 times elevation in cells that were growing with reduced serum (red) and with ergosterol (blue) at 24 h and 48 h of culturing. Note that substantial cholesterol export out of the cells was present only in positive control (A green). Almost no cholesterol export could be detected out of the cells that were grown in cholesterol conditioned medium (A yellow). More detailed description can be found in the text. GC/MS was used for measurements and the spectra are presented in the Appendix.

2.2 Identification of 17 β -HSD7 as a cholesterogenic enzyme

2.2.1. Expression of 17 β -HSD7 in cholesterol auxotrophic cell lines

U-937 human histiocytic lymphoma and X63 mouse myeloma cell lines were previously described as cholesterol auxotrophs due to deficiency in 3-ketosteroid reductase activity (**Billheimer J.T. et al. 1987**; **Sato J.D. et al. 1988**). Since it was suggested recently that 17 β -HSD7 might act as 3-ketosteroid reductase (**Breitling R et al. 2001**), it was checked whether the identified deficiency in 3-ketosteroid-reductase activity might be caused by mutations in 17 β -HSD7. Therefore, the genomic organization and expression of this gene was analyzed in both cell lines by PCR.

Neither in X63, nor in U-937 cells 17 β -HSD7 expression could be detected, even when cells were grown with reduced amount of serum, which should turn on the expression of cholesterogenic genes (**Figure 11**).



Figure 11. Expression of 17 β -HSD7 in U-937 (A) and X63 (B) cells. Expression was checked by PCR. In figure A, lanes 1, 4 and 8 represent water (negative controls); 2 and 3 represent expression of IDI 1 (~400 bp; used as a control for cholesterogenic gene expression) with normal serum amount and with reduced serum amount, respectively; 5, 6, 7 represent 17 β -HSD7 positive control (pGEX/hHSD7; ~900 bp) and 17 β -HSD7 expression in U937 cells that were grown with normal and reduced serum amount respectively; 9 and 10 represent glyceraldehyde-3-phosphate dehydrogenase (GAPDH) expression (~400 bp; control for RNA quality). In figure B lane 1 represents water (negative control); 2 is positive control for 17 β -HSD7 (pGEX/hHSD7; ~900 bp); 3 and 4 represent 17 β -HSD7 expressions with normal and reduced amount of serum; 5 represents GAPDH expression (~700 bp). Primers are listed in the Appendix.

RESULTS

Since no 17 β -HSD7 expression was detected, a possible gene deletion was checked. Genomic DNA was isolated from U-937 cells and the 17 β -HSD7 gene fragments were amplified (**Figure 12**). All exons could be detected and were of the right size. Intronic sequences were more hard to amplify due to repetitive sequences and in some cases no PCR could be obtained or the reaction was unspecific even with the positive control (17 β -HSD7 PAC clone). However, since all exons are preserved it can be suggested that no gene deletion occurred and that the structure of 17 β -HSD7 gene was preserved. Additionally, for exon 2, containing the cofactor binding site and exon 5, with the active center, it was possible to obtain sequences and no mutations could be found in these regions. However since not all exons and introns could be sequenced it was not excluded that some mutations leading to inappropriate RNA processing and therefore RNA instability existed in those cell lines. The other explanation could be the inability of U-937 and X63 to control 17 β -HSD7 expression due to either mutations in the promoter region or lack of some crucial control element.



Figure 12. PCR-products of the 17 β -HSD7 gene from genomic DNA of U-937 cells. Lanes: 1 and 2 represent exon 1 (~400 bp); 3 and 4 intron 1 (~900 bp); 5 and 6 exon 2 (~1150 expected size, note that amplification was unspecific; band of the correct size was cut out and sent for sequencing); 7 and 8 intron 2 (~400 bp); 9 and 10 exon 3 and 4 (~1500 bp); 11 and 12 intron 4 (~1400 bp); 13 and 14 exon 5 (~700 bp); 15 and 16 exon 6 (~850 bp); 17 and 18 intron 6 (~300 bp); 19 and 20 exon 7 (~400 bp); 19 and 20 intron 7 (note that no PCR was observed even in the positive control); 21 and 22 exon 8 (~970 bp) and 23 and 24 exon 9 (~1100 bp). First lane in all pairs is positive control (17 β -HSD7 PAC) and second is amplification product out of genomic DNA isolated from U-937 cells. In some cases, where several bands are present, amplification was unspecific.

2.2.2. Complementation assay

To assign the physiological role for 17β -HSD7 in cholesterol biosynthesis, its ability to complement for the defect of ergosterol biosynthesis in the SDG110 yeast strain was checked. Since 17β -HSD7 is homologous to yERG27, which is deleted in SDG110 strain, it was presumed that it might catalyze the same reaction, conversion of zymosteron to zymosterol and restore ergosterol biosynthesis.

Yeast cells were transformed as described in Materials and Methods with following constructs: pYES2.1/yERG25, pYES2.1/yERG27, pYES2.1/hHSD7, pYES2.1/hHSD7tr. (contains only first 214 amino acids and therefore the entire C-terminus is missing; see Figure 4), pYES2.1/mHSD7 and pESC/hERG28/hHSD7 (double construct having both hC14orf1 and h 17β -HSD7). Growth was maintained for 3 weeks on complementation selection plates. The results are presented in **Figure 13**.

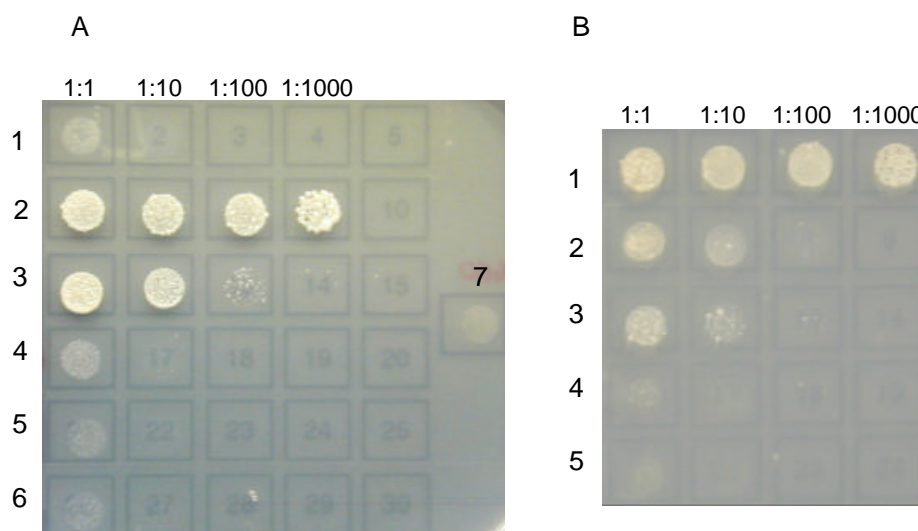


Figure 13. Yeast complementation assay. A) SDG110 yeast transformed with pYES2.1/yERG25 (1), pYES2.1/yERG27 (2), pYES2.1/hHSD7 (3), pESC/hERG28/hHSD7 (4), pYES2.1/hHSD1 (5), pYES2.1/hHSD5 (6) and nontransformed SDG110 (7). B) SDG110 transformed with pYES2.1/yERG27 (1), pYES2.1/hHSD7 (2), pYES2.1/mHSD7 (3), pESC/hERG28/hHSD7 (4) and pYES2.1/hHSD7tr. (5). In the names of the constructs HSD7 represents 17β -HSD7; HSD7tr. represents 17β -HSD7tr. which is missing the C-terminus; hERG28 represents C14orf1; HSD1 represents 17β -HSD1; HSD5 represents 17β -HSD5; h=human; m=mouse; y=yeast. Pictures of constructs used in complementation assay are presented in Appendix. Note that only yERG27 (A2 and B1), h 17β -HSD7 (A3 and B2) and m 17β -HSD7 (B3) could restore yeast growth on complementation selection plate without addition of sterol.

RESULTS

Only in yERG27 and both, h17 β -HSD7 and m17 β -HSD7 transformants ergosterol biosynthesis was restored and yeast were able to grow on plates without addition of sterol (**Figure 13 A2, A3, B1, B2 and B3**). yERG25 was used as a negative control. It is not catalyzing the same reaction as yERG27 and therefore couldn't complement the defect (**Figure 13 A1**).

Since it was observed before that 17 β -HSDs can use different substrates and catalyze different reactions, two additional members of this family were included in the experiment to check the specificity of 17 β -HSD7 action. Neither 17 β -HSD1 which has 17 β -reductase activity nor 17 β -HSD5 which has 17 β and 3 α -keto reductase activity could restore yeast growth (**Figure 13 A5 and A6**). Complementation inability was also observed for a truncated form of 17 β -HSD7 (**Figure 13. B5**). This was expected, since it showed no catalytic activity toward estrone in *in vitro* activity assays (Völkl A. personal comm.).

The results undoubtedly showed that the reaction catalyzed by 17 β -HSD7 was specific. However, the growth of 17 β -HSD7 transformants was not optimal. SDG110 transformed with ERG27 formed visible colonies already after 3 days in culture. For both, human and mouse 17 β -HSD7 transformants it took 3 weeks to grow. Therefore, a double transformant having hC14orf1 in addition to h17 β -HSD7 was included in the experiment. hC14orf1 is homologous to yERG28, which was described as a protein potentially involved in facilitating the interaction between yERG26 and yERG27 and tethering the complex to the ER (**Gachotte D et al. 2001**). Since the yeast system is not optimal for human proteins some of necessary interactions may not be optimal either. However, hC14orf1 in addition to 17 β -HSD7 couldn't restore normal growth. Double transformants failed to form visible colonies even after 3 weeks in culture. Although colony formation was observed at the beginning of incubation under the microscope, it seemed that eventually the yeast stopped to grow.

Since no improvement in growth rate of 17 β -HSD7 transformants could be achieved, the next step was to check the expression level and activity of human proteins in the SDG110 yeast strain. All human proteins except h17 β -HSD5 were very poorly expressed as it is shown in **Figure 14**. Additionally, in the case of the double transformant it seems that h17 β -HSD7 was expressed at extremely low levels since no signal could be detected with antibodies against myc epitope fused to the h17 β -HSD7 sequence (**Figure 14 B**). This can very well explain the inability of this yeast transformant to grow. hC14orf1 was expressed however, although two bands instead of one appeared when checked with antibodies against FLAG epitope fused to the sequence (**Figure 14 B**). The lower band corresponded in size to hC14orf1 (17 kd) but the upper band was around 50 kd and was probably due to unspecific crossreaction.

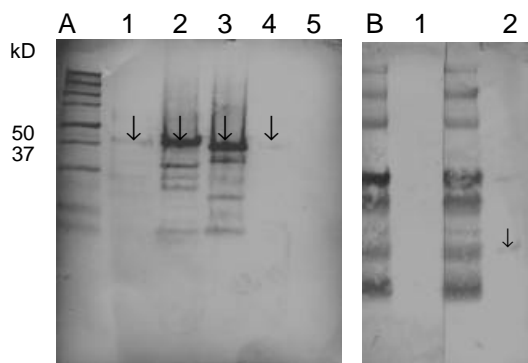


Figure 14. Western blot. Figure A shows the expression of h17 β -HSD1 (1), h17 β -HSD5 (2), yERG27 (3) and h17 β -HSD7 (4) in SDG110. In all cases the most upper bands correspond in size to indicated proteins. Lane 5 represents nontransformed yeast (- control). Figure B shows the expression of h17 β -HSD7 (1) and hC14orf1 (2) in double transformed yeast. Only hC14orf1 was expressed (lower band ~17 kD). h17 β -HSD7 could not be detected (Figure B1). Proteins presented in Figure A were detected with anti-V5 antibodies. In Figure B, C14orf1 was detected with anti-FLAG and h17 β -HSD7 was detected with anti-myc antibodies. The expected proteins are marked with arrows.

	Estrone %	Estradiol%
SDG110	99,4	0,6
SDG110/ yERG27	90,1	9,9
SDG110/ h17 β -HSD7	95,8	4,2

Table 1. Conversion of estrone to estradiol. SDG110 yeast were used as a control to measure background for the conversion. In all cases the same number of yeast cells was used. No further normalization of the measured values was done. The conversion was measured after one hour of incubation with estrone as a substrate. Conversion was normalized to cell number.

Activity measurements using extract of SDG110 yeast expressing yERG27 and h17 β -HSD7 with estrone as a substrate, showed substantial conversion of estrone to estradiol only in yERG27 and h17 β -HSD7 transformants (**Table 1**). Very poor conversion efficiency if compared to that observed for m17 β -HSD7 expressed in mammalian cells, suggested that estrone might not be the best substrate for human enzyme, which additionally supported the hypothesis that h17 β -HSD7 might have a different catalytical role in vivo from that previously reported (**Nokelainen P. et al. 1998**).

Activity measurements together with the protein expression results indicate that slow growth rate in case of SDG110 transformed with h17 β -HSD7 was most probably due to low protein level in the yeast cells and therefore not enough of the end product ergosterol to support the growth. The same situation was also observed in a ERG28 deficient yeast strain (**Gachotte D. et al. 2001**). Furthermore, although the expression level of h17 β -HSD7 was very low the protein was active suggesting that restored ability of yeast transformant to grow without addition of sterol was entirely due to h17 β -HSD7 activity.

RESULTS

2.2.3. Cellular localization

Until now it is known that the last steps of cholesterol biosynthesis take place in endoplasmic reticulum, although recent studies speculate about the possible cholesterol synthesis also in peroxisomes (**Olivier L.M. and Krisans S. 2000**). So far it was observed that the cholesterol biosynthetic pathway was distributed among multiple cellular compartments and that some of the steps could be carried out in more of them rather than only one. Accordingly, some of the enzymes involved in the pathway were found in various localizations in the cell. If 17β -HSD7 is indeed able to catalyze the conversion of zymosteron to zymosterol, one of the last steps in cholesterol biosynthesis, the enzyme is likely to be localized in the ER. However, the ability of mouse and rat 17β -HSD7 to catalyze the conversion of estrone to estradiol together with the expression in ovaries and placenta, place them among steroidogenic enzymes that are mostly localized in the cytosol, mitochondria and peroxisomes. To further elucidate the real physiological role for cholesterologenic or steroidogenic 17β -HSD7, its cellular localization was checked.

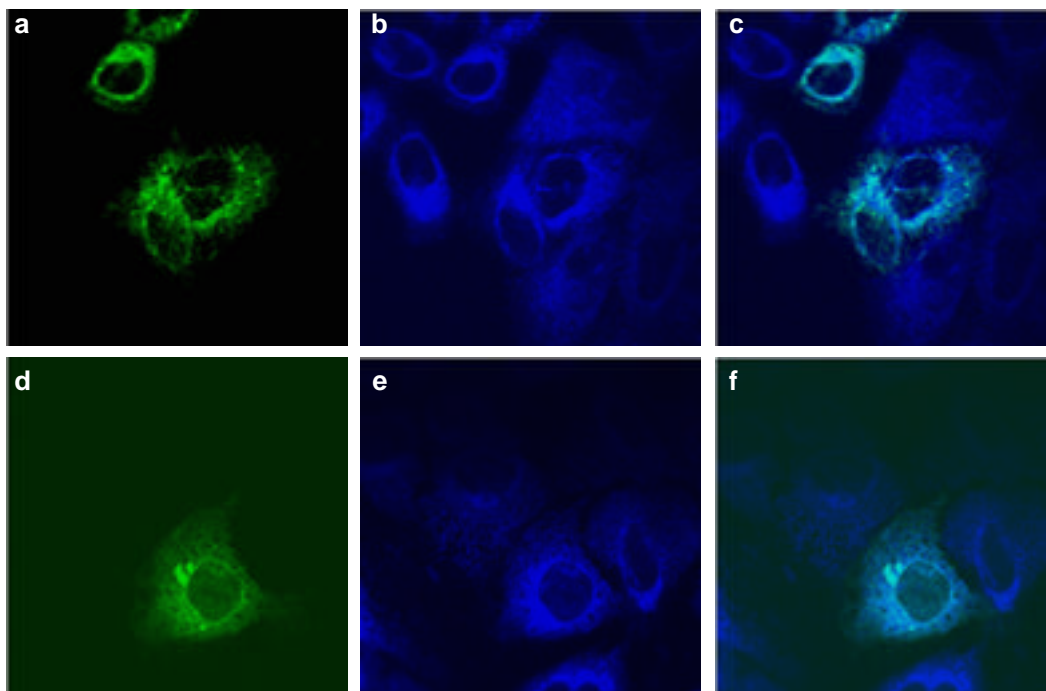


Figure 15. Localization of pEGFP/hHSD7 (a-c) and pEGFP/mHSD7 (d-f) in ER. Figure a, d represent GFP fluorescence and b, e ER-Tracker fluorescence respectively. Figure c and f represent an overlay of both fluorescences. Note that colocalization is presented in light blue. HSD7 = 17β -HSD7; GFP = green fluorescent protein; h=human; m=mouse. Plasmid constructs are presented in the Appendix.

Both human and mouse 17β -HSD7 cDNA was fused at the N-terminus to GFP and transfected into HeLa cells. The fusion proteins were exclusively localized in the ER (**Figure 15**). In addition to those results PSORT prediction classified 17β -HSD7 as a possible ER membrane protein with the N-terminal motif RKVV, which represents an ER membrane retention signal. Homology-based molecular modeling studies carried out previously on 17β -HSD7 emphasized the importance of the C-terminal part of the protein, which contains a hydrophobic helix that is presumably membrane associated (**Breitling R. et al. 2001**). It was already presented in this study that h 17β -HSD7tr. without C-terminus could not restore ergosterol biosynthesis in SDG110 yeast strain (**Figure 13 B**). Additionally, in vitro activity measurements with estrone as a substrate did not show any conversion to estradiol (results not shown). Those results implied that the protein was inactive and that the C-terminus is important for the activity. Taking all this into account, it is possible that the C-terminus also plays role in ER localization either by forming the interaction with some resident ER protein or by containing an additional, so far unidentified signaling motif.

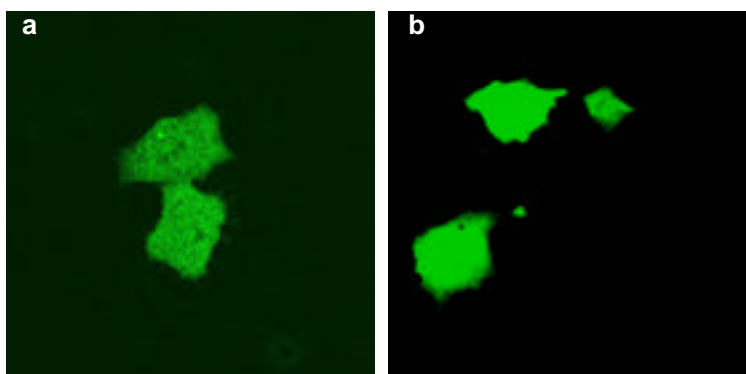


Figure 16. Localization of pEGFP/hHSD7tr (a) and pEGFP/yERG27stop (b) in HeLa cells. Deletion of the C-terminus of h 17β -HSD7 leads to protein mislocalization to cytosol and nucleus as presented at figure a. GFP/yERG27stop has a point mutation generated spontaneously during PCR amplification, which leads to a premature stop signal so that the entire C-terminal part of the protein is not present. This caused the same effect in yERG27 localization as in 17β -HSD7tr localization. Here HSD7tr. stands for 17β -HSD7tr. which is missing C-terminus; h=human; y=yeast.

To check this hypothesis, the same truncated form of 17 β -HSD7 as used in the complementation experiment, was fused to GFP with its N-terminal part. This protein was completely dislocalized to the cytosol and even to the nucleus (**Figure 16a**). The same result was obtained when CFP was fused to the C-terminus of 17 β -HSD7 (not shown), suggesting that the C-Terminus is indeed important for proper localization. This is also true for yERG27 (**Figure 16 b**).

2.3. Identification of C14orf1 as a possible 17 β -HSD7 interactor and its role in cholesterol biosynthesis

2.3.1. *In vitro* and *in vivo* interactions with C14orf1

It was already mentioned that yERG28 might be the protein that is responsible for tethering of yERG27 to the ER membrane. Since 17 β -HSD7 is sharing the same structural features (**Figure 4**) and is probably playing the same physiological role as yERG27, the possible interaction with C14orf1, human homologue of yERG28 was checked.

In vitro interaction studies using a pull down assay revealed possible interactions between 17 β -HSD7 and C14orf1 in both cases, human and mouse (**Figure 17 A**). Furthermore, deletion of the C-terminus in the case of h17 β -HSD7 tr. did not influence the interaction. The signal was however much weaker, because of the smaller amount of protein used in the study due to a very low solubility (**Figure 17 A and B**). GST alone was used as a negative control and did not interact with any of the tested proteins. Zyxine and its interactor Pax9 were used exclusively as a positive control in the pull down assay and were not used further in the study. Interaction between yERG27 and yERG28 could not be checked in the *in vitro* assay, because it was not possible to purify ERG27 in active form out of both yeast and bacterial cells.

The next step was to check whether the same interactions were also taking place *in vivo*, using a yeast Two-hybrid system. Although 17 β -HSD7 and C14orf1 could interact *in vitro*, in the yeast, none of those interactions was observed (**Figure 18**). Even the interaction between yERG27 and yERG28 was spurious since in all cases the β -galactosidase assay gave negative results.

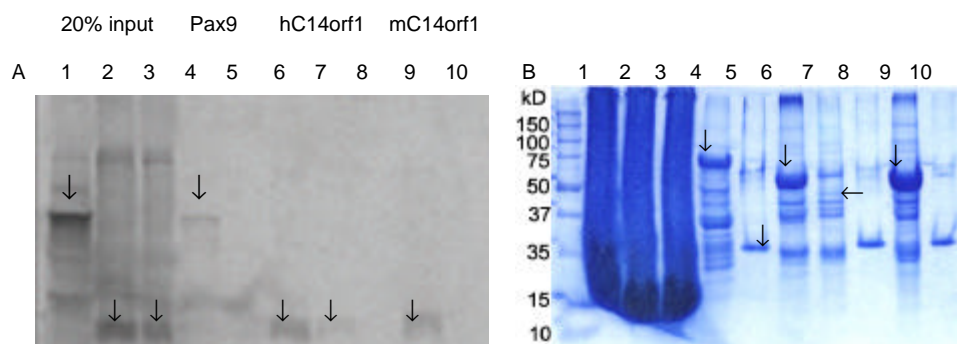


Figure 17. Pull down assay. Lanes 1, 2, 3 represent 20% input of in vitro translated Pax9, hC14orf1 and mC14orf1 respectively. Lanes 5, 8, 10 represent GST only and lanes 4, 6, 7 and 9 represent pGEX/zyxine, pGEX/hHSD7, pGEX/hHSD7 tr. and pGEX/mHSD7. Figure A shows results of pull down with interaction partners written above the numbers and figure B represents coomassie stained gel showing the amount of proteins used in the study. In the names of the constructs used for this experiment HSD7 stands for 17 β -HSD7 and HSD7tr. for 17 β -HSD7 lacking the entire C-terminus; h=human; m=mouse. Pax9 and its interaction partner zyxine were used in the experiment as a control. Note that all of the tested proteins could form interactions in vitro. The weaker signal obtained in the pull down assay for interaction between 17 β -HSD7tr. and hC14orf1 (A7) was due to much lower protein amount that could be purified and used in the experiment in comparison to other proteins (B7). The bands of the proteins are marked by arrows.



Figure 18. In vivo interactions in yeast. Lanes 1a and 1b represent yeast cotransformed with pGBKT7/hHSD7 and pGADT7/hERG28. In lanes 1c and 1d yeast cotransformed with pGBKT7/hHSD7 and pGADT7/yERG28 are shown and in lanes 1e and 1f are yeast cotransformed with either pGBKT7/hHSD7 and pGADT7 or pGBKT7 and pGADT7/hERG28, used as a negative controls. Lanes 2a-f represent in the same order yeast transformants with mouse homologues of the same proteins. Lanes 3a and 3b represent yeast cotransformed with pGBKT7/yERG27 and pGADT7/yERG28. In lane 3e yeast transformant with pGBKT7/hHSD7tr. and pGADT7/hERG28 is shown and in lane 3f is a negative control having pGBKT7/hHSD7tr. HSD7 = 17 β -HSD7; HSD7tr. = 17 β -HSD7 without C-terminus; hERG28 = hC14orf1; mERG28 = mC14orf1; h=human; m=mouse; y=yeast.

RESULTS

All constructs were checked by sequencing and found to be correct, so inability of transformed yeast cells to grow on selection plate was entirely due to a lack of interactions under the physiological conditions.

2.3.2. Cellular localization of C14orf1 and yERG28

Since yERG28 was suggested to act as a tether for yERG27 at the ER but no interactions could be observed between those proteins and also their human homologues, the subcellular distribution of yERG28 and C14orf1 was checked in HeLa cells.

Human and mouse C14orf1 were both localized in ER (**Figure 19**). Yeast ERG28 however, showed punctate pattern in the cytosol (**Figure 20 a**). Additionally, the cellular localization of yERG27 was checked in HeLa cells to see whether yeast proteins could be properly localized in mammalian cells. The result is shown at **Figure 20 b-d**.

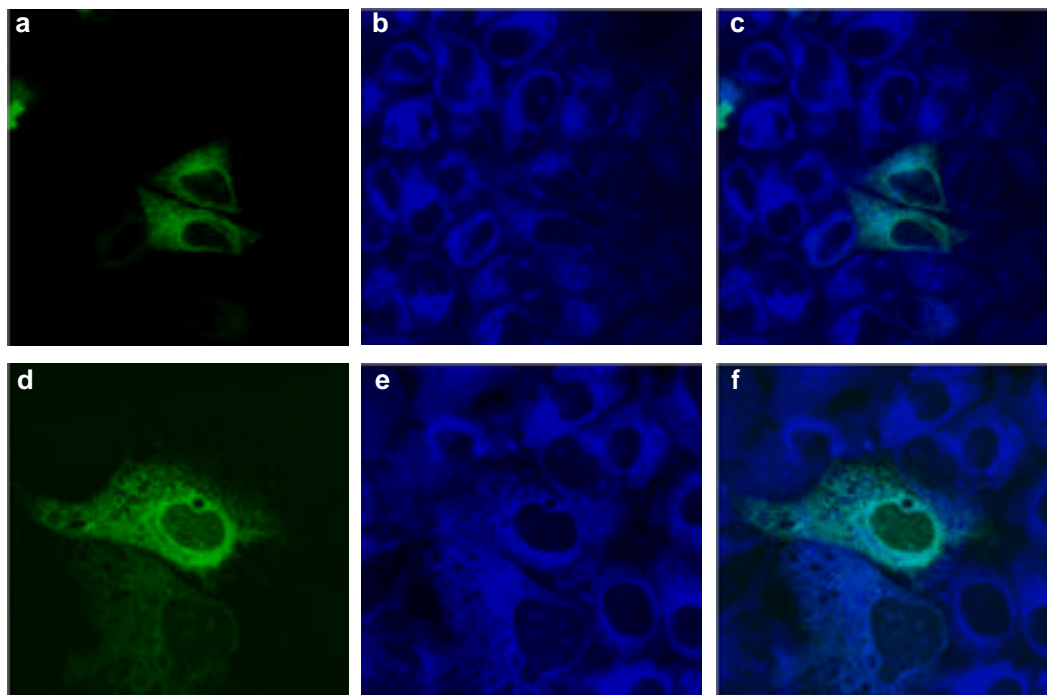


Figure 19. Localization of pEGFP/hERG28 (a-c) and pEGFP/mERG28 (d-f) in ER. Figure a, d represent GFP fluorescence and b, e ER-Tracker fluorescence separately. Figure c and f represent an overlay. Note that colocalization is presented in light blue. hERG28 stands for human C14orf1 and mERG28 stands for mouse C14orf1.

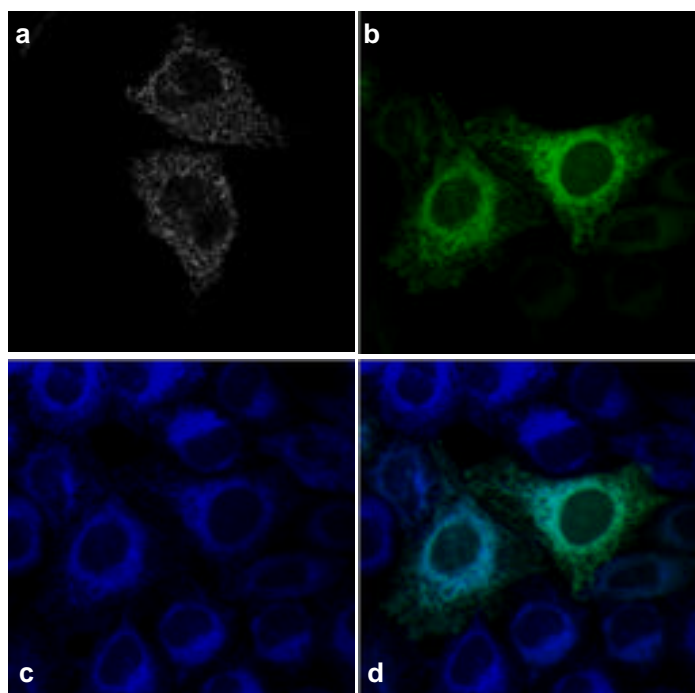


Figure 20. Localization of pEGFP/yERG28 (a) and pEGFP/yERG27 (b-d) in HeLa cells. Figure b and c represent GFP and ER-Tracker fluorescence separately and figure d represents an overlay. Note that colocalization is presented in light blue.

yERG27 was localized in the ER in HeLa cells. The same localization pattern was observed in yeast as well (**Baudry K. et al. 2001**). Since yERG28 was not localized in the ER as previously suggested and human and mouse C14orf1 were, the existence of ER localization signals was checked by PSORT. hC14orf1 has two ER membrane retention signals, SRFL and QKKR, positioned on both the N and the C-terminus, respectively. yERG28 however has no known localization signal and it is predicted to be localized in the cytosol. Recently, a possible interactor of yERG28, CHM2 was identified (**Uetz P. et al. 2000; Ito T. et al. 2001**). It belongs to a family of proteins involved in vesicular transport in yeast. It is known that human homologues of the yeast vesicular sorting protein (Vps) family are localized to early endosomes (**Howard T.L. et al. 2001**). Taking this into account, it might be that the punctate structures of yERG28 that were detected in HeLa cells were actually endosomes.

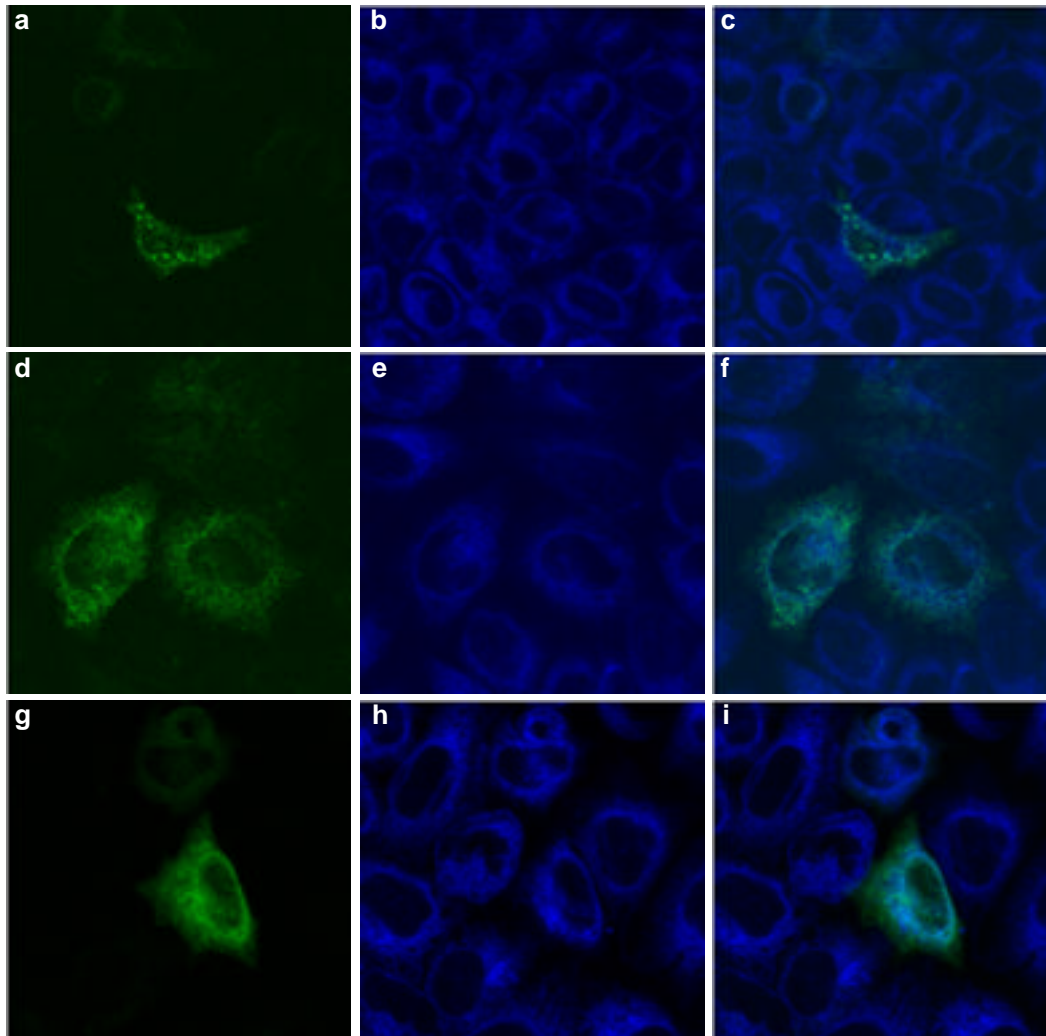


Figure 21. Cholesterol influenced changes in cellular localization of GFP/yERG28 in HeLa cells. Figure a-c represent punctuated localization of GFP/yERG28 in cells cultured with 10% serum. If amount of serum is reduced to 0,1%, punctate pattern starts to diminish (d-f) and the fusion protein finally accumulates in ER (g-i). Figures a, d, g and b, e, h represent GFP and ER-Tracker fluorescence separately. Figures c, f and i represent the overlays of both fluorescence. Note that colocalization is presented in light blue.

2.3.3. Cholesterol influenced changes in C14orf1 and yERG28 cellular localization

It is known that endosomes play an important role in cholesterol trafficking. This rises the possibility that yERG28 may also be involved in this process. Since it was observed that proteins involved in cholesterol transport are changing cellular localization according to cholesterol requirements and its flow within the cell, it was checked whether this would be the case also with yERG28 if exogenous cholesterol supplies to cells were reduced.

Both, hC14orf1 and yERG28 were fused to GFP with their N-terminal parts and transfected into HeLa cells. The cells were grown in media with 10% and 0,1% serum for 24 and 48 h and then checked with the confocal microscope.

As is visible from **Figure 21** yERG28 was changing its localization in HeLa cells depending on the serum amount in the medium. In normal condition, when 10% serum was added, yERG28 was localized in the punctated pattern in the cell (**Figure 21 a-c**). If the serum amount was reduced to 0,1% and therefore cholesterol supplies from outside were also reduced, the punctated structures started to diminish and yERG28 acquired a more cytosolic localization (**Figure 21 d-f**). At the end it accumulated merely in the ER (**Figure 21 g-h**). This was observed in the cells 24h after transfection. After 48h however, decrease in survival of cells expressing both human and yeast fusion proteins was observed no matter whether they were overexpressed or expression level was very low. Since chromophores fused to the proteins can interfere with protein localization, it was necessary to check whether localization would change if the chromophore was placed at the C-terminus. yERG28 with YFP fused to the C-terminus was localized in cytosol and nucleus, quite similar to YFP alone, suggesting that C-terminal fusion of the chromophore probably caused the observed mislocalization (**Figure 22 c**).

RESULTS

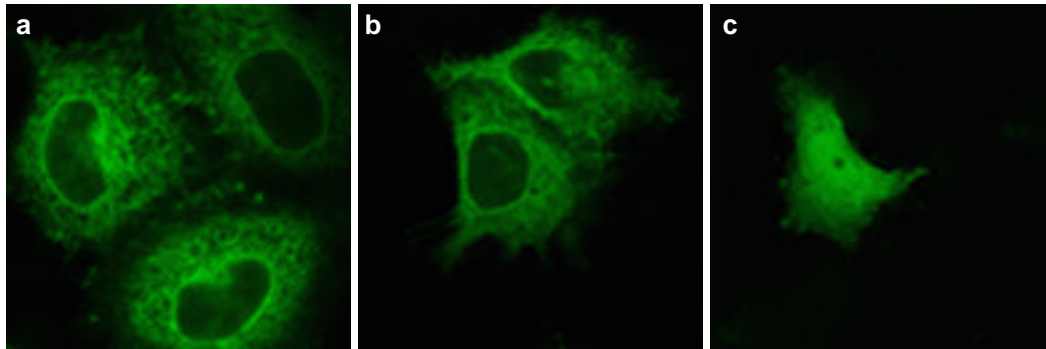


Figure 22. Cellular localization of pEGFP/hERG28 in ER of HeLa cells (a, b) and mislocalization of yERG28/YFP (c). Figure a) represents HeLa cells cultured with 10% serum and on figure b) are HeLa cultured with only 0,1% serum. hERG28 stands for human C14orf1.

Therefore, only results with pEGFP/yERG28 were considered for further discussion. Human homologue C14orf1 did not show any changes in localization due to reduced supplies of cholesterol from outside. In all cases it was localized in the ER (**Figure 21 a, b**). The same localization was obtained no matter whether the chromophore was fused to the N- or C-terminus. This corresponded very well to the presence of two ER localization signals on both sides of the protein. Taking all this into account it seems that C14orf1 is a ER resident protein and yERG28 can change its cellular localization in response to sterol levels.

3. DISCUSSION

3.1. Cellular requirements for cholesterol

Sterols are the major components of the plasma membrane and are involved in modulation of its permeability. It was suggested recently that the cholesterol structure might play an additional important role in the plasma membrane namely in the preservation of the normal cell function through prevention of the proton leakage into the cell (**Haines T.H. 2001**).

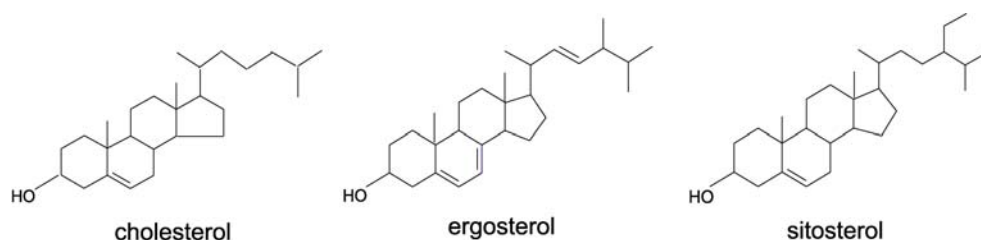


Figure 23. Differences between structures of mammalian sterol cholesterol, fungal sterol ergosterol and plant sterol sitosterol.

This would suggest that other sterols like ergosterol or sitosterol wouldn't be suited for this role and couldn't substitute for cholesterol in mammalian cells. Structures of the all three sterols are presented at **Figure 23**. It was however reported that yeast ergosterol auxotrophs could survive normally with other sterols if tiny amounts of ergosterol (insufficient for growth) were added to the medium (**Rodriguez R.J. et al. 1982.**). Normal survival was also observed for the yeast ergosterol auxotrophs that were using closest ergosterol intermediates. However, in this case slight disadvantage in the cell growth was observed (**Lees N.D. et al. 1999; Smith S.J et al. 1996; Geber A. et al. 1995**).

This led to the conclusion that other sterols can substitute the structural role of ergosterol in the cell membrane but cannot have the “sparking” function of regulatory nature, which is specific for ergosterol.

A similar effect was reported in mammalian cells if cholesterol was substituted with ergosterol. It was observed that the cellular cholesterol level has an impact on cell cycle progression (**Martinez-Botas J. et al. 1999; Suarez Y. et al. 2002**). Ergosterol could support cell survival but was ineffective in restoring proliferation of cells in which cholesterol synthesis was blocked. However, if only slight amounts of cholesterol were present, the ergosterol could restore the control conditions (**Suarez Y. et al. 2002**).

The same results were obtained in this study. It is visible from the **Figures 5 and 7** that ergosterol could support U-937 cell growth for 96 h if added to the medium with reduced serum which contained around 15% of the normal cholesterol amount (**Figure 8**). The reduced cholesterol amount itself was not enough to support the cell growth longer than 24h (**Figure 5-7**). It has to be mentioned, however, that the ergosterol impact on cell survival was serum depending and varied with the different serum batches that were used in different experiments (**Figure 5, 7 and 8**). Those results implied the contribution of some additional factors to the cell survival. Furthermore no dose response in both, cell survival and cell proliferation could be observed if U-937 cells were grown with different ergosterol concentrations (**Figure 7**). This correlated very well with the GC/MS results reported here. Although the cells imported exogenous ergosterol entirely, it was detected inside the cells only 6 h after the plating. Afterwards only free (non esterified) cholesterol could be detected in those cells. Additionally, the cholesterol level in the cells was much higher if compared to the control cells that were grown in normal conditions with 10% serum (**Figure 10**). One explanation for that could be that the ergosterol was converted to cholesterol to be tolerable to the cell. However, this is not likely, since ergosterol could not restore the proliferation in other cells, as previously reported by Suarez Y. and associates, if cholesterol biosynthesis was aborted and no cholesterol was present in the medium. It is therefore possible that ergosterol was not detected in the cells in the later time points because it was not kept in the free form and was not measurable any more by GC/MS method. Furthermore, it is possible that ergosterol could act in this case by triggering mobilization of the cellular cholesterol supplies. This is a very likely explanation, since a higher cholesterol level in comparison to that in the control cells could be detected already 6h after plating (**Figure 9**). The observation that ergosterol concentration had no impact on cell survival and proliferation additionally contributed to this theory.

It was previously reported that 30 µg/ml of free cholesterol added to the medium containing LDL deprived serum had the same effect on the cell survival as LDL derived cholesterol (**Suarez Y. et al. 2002**).

It was observed that the cholesterol effect on cell proliferation was concentration depending but cell viability was not affected at least in the time range of 72 h.

In this study however both, the cell viability as well as the cell proliferation has been shown to be dependent on cholesterol concentration. The cholesterol ability to support cell survival for a certain period of time correlated with the cell number used in the experiments (**Figure 5 and 6**). Even 30 $\mu\text{g/ml}$ of cholesterol which should present the cholesterol amount in the normal conditions, couldn't support cell growth after the cell number reached ~ 80000 cells/ml. GC/MS results revealed that all cholesterol has been taken up from the media by the cells, but the free cholesterol amount inside the cells did not change during the entire time course in comparison to the control cells or the cells that were grown with ergosterol. Additionally, no cholesterol export from the cells could be observed in this case either (**Figure 10**). It is therefore very likely that free cholesterol imported into U-937 cells was not properly distributed in the cell but was blocked instead. As a consequence cholesterol homeostasis was disturbed and cell survival and proliferation were reduced. Since the ability of cholesterol to support cell survival was observed to be dependant on the cell number and since it was found that all cholesterol was taken up from the media but only a very small amount of cholesterol was actually exported from the cells it is also possible that newly formed cells were deprived of external cholesterol supplies and therefore couldn't survive. Indeed, it was observed that although the control cells that were grown in the medium with 10% serum imported almost all of the external cholesterol 24 h after plating, the initial amount of cholesterol in the medium was restored at the end, which was probably due to the substantial cholesterol export from the cells (**Figure 10**). This was not the case in the medium with reduced serum and cholesterol. Together, those results emphasize the importance of the cholesterol balance in the cell and additionally support the explanation for the cholesterol inability to keep U-937 cells alive as presented in this study.

It was recently reported that inhibition of cholesterol production could trigger apoptosis in the nonproliferating cells (**Michikawa M. and Yanagisawa K. 1999**). The elevation in the sterol responsive gene transcription through activation of sterol regulatory element binding protein (SREBP) was also observed to be connected to apoptosis (**Higgins M.E. and Ioannou Y.A. 2001**). It was found that the sterol level did not actually influence this process but since cholesterologenic genes are activated by SREBP it was suggested that elevation of cholesterol level took place as a consequence and enabled the proper execution of the apoptotic program.

In this study it was observed that a 9-fold elevation in cholesterol inside the cell was connected to cell death.

In both cases, if U-937 cells were cultured in the medium with reduced serum only, or with addition of ergosterol, 9-fold elevation in the cellular cholesterol level was observed 24 h before the cells started to die (**Figure 8 and 10**). However, cell death was observed also in the case of U-937 cells that were growing in the cholesterol conditioned medium, although no elevation in the cellular cholesterol level could be measured (**Figure 8 and 10**). It is therefore possible that apoptosis can be triggered by different mechanisms of which one resulted in an elevated cholesterol level and the other was triggered by insufficient cholesterol amounts. However further studies have to be performed to elucidate the exact mechanisms by which sterols can execute the cell death.

3.2. Role of 17 β -HSD7 in cholesterol biosynthesis

Until now 17 β -HSD7 was identified in rat and mouse as a steroidogenic enzyme, which is catalyzing the conversion of estrone to estradiol (**Nokelainen P. et al. 2000**). The major expression in steroidogenic tissues like ovaries and placenta was supporting those findings. However, homology based molecular modeling revealed great similarity to yeast ERG27, the enzyme involved in synthesis of zymosterol, one of the intermediates in ergosterol and cholesterol biosynthesis (**Breitling R. et al. 2001**). Additionally, it was found by *in silico* Northern blot and later by *in situ* experiments on mouse embryos that in addition to steroidogenic tissues, 17 β -HSD7 was expressed also in the embryonic nervous system and liver, the places of extensive cholesterol biosynthesis, together with other cholesterologenic genes (**Krazeisen A. et al. 1999; Laubner D. personal comm.**). Furthermore, no homologues of 17 β -HSD7 was found in *C.elegans* and *Drosophila melanogaster*, which are known as cholesterol auxotrophic organisms. All this highlighted 17 β -HSD7 as a potential candidate for cholesterol biosynthesis. In this study it has been shown for the first time experimentally that 17 β -HSD7 indeed act as a cholesterologenic enzyme.

3.2.1. Ability of 17 β -HSD7 to restore ergosterol synthesis in yeast complementation assay

Since 17 β -HSD7 is homologous to yERG27, it was convenient to check its function in yeast complementation assay. SDG110 yeast cells used in this study are ergosterol auxotrophs due to targeted disruption of ERG27 and therefore show impaired conversion of zymosterone to zymosterol.

Only an enzyme, which can catalyze zymosterol synthesis, would be able to reverse the yeasts' requirements for exogenously supplied ergosterol.

The results presented here revealed that only native ERG27 and 17 β -HSD7 could restore ergosterol biosynthesis. All other genes, including another short chain alcohol dehydrogenase (SCAD) member and the steroidogenic enzyme 17 β -HSD1, as well as 17 β -HSD5, which has the 3 α -ketosterol activity, failed to abolish SDG110 auxotrophy (**Figure 13 A and B**). The same was observed if the truncated 17 β -HSD7 protein (17 β -HSD7tr.) containing only first 214 amino acids (**Figure 4**) was used (**Figure 13 B**). Those results emphasize the specificity of the 17 β -HSD7 catalyzed reaction and in addition the importance of the C-terminus for its catalytic activity, as it was already suggested by modeling studies (**Breitling R. et al. 2001**). However, although 17 β -HSD7 could abolish ergosterol auxotrophy in SDG110 yeast, severe growth retardation was observed in comparison to the ERG27 transformant. This observation implied that the system might not be optimal. Indeed, the expression level of 17 β -HSD7 was found to be very low (**Figure 14 A**), which probably led to insufficient ergosterol production. Since proliferation is controlled by the ergosterol amount, the low ergosterol level could cause slower growth of 17 β -HSD7 transformed yeast. (**Gachotte D. et al. 2001; Lees N.D. et al. 1999; Smith S.J et al. 1996; Geber A. et al. 1995**).

3.2.2. 17 β -HSD7 activity in yeast

Slower growth of h17 β -HSD7 yeast transformant could additionally be caused by possible lower activity of the human enzyme if expressed in yeast. Since the suggested substrate zymosterone is not available commercially, the well-characterized conversion of estrone to estradiol was measured instead-in yeast extracts containing either yERG27 or h17 β -HSD7,- and the results were compared. Very poor substrate conversion was observed in both cases. Additionally, 2-fold lower conversion activity for h17 β -HSD7 was measured in comparison to yERG27 activity (**Table 1**). Since h17 β -HSD7 expression in the same amount of the yeast cells was approximately 10 times lower than the yERG27 expression, it can be concluded that estrone is a better substrate for h17 β -HSD7 than for yERG27 (**Figure 14 A**). However, the estrone activation with h17 β -HSD7 was much worse in this case than that previously measured for the mouse enzyme expressed in mammalian cells (**Nokelainen P. et al. 1998**). This result additionally supports the involvement of human 17 β -HSD7 in sterol synthesis as it was found here by yeast complementation assay.

However, the possibility that 17 β -HSD7 might also be involved in the steroid conversion shouldn't be entirely excluded, since the yeast cells were shown not to be the ideal system for human proteins. Further experiments that are currently going on in our lab should additionally elucidate 17 β -HSD7 role in cholesterologenesis.

3.2.3 Cellular localization of 17 β -HSD7

Localization of 17 β -HSD7 in the endoplasmic reticulum (ER) also suggested its role in cholesterol biosynthesis rather than steroid metabolism, since this is the cellular compartment in which the last steps of this process take place. Furthermore the C-terminus was found to be important for localization since 17 β -HSD7tr. in which it was deleted showed mislocalization to the cytosol and the nucleus (**Figure 15 a**). However, no ER targeting signal could be found in the C-terminal part of the 17 β -HSD7 sequence. The only motif present is the ER membrane retention signal RKVV, which is localized close to the N-terminus and which was proven in this study not to be sufficient for the ER localization. Therefore, it is not excluded that 17 β -HSD7 has to form an interaction via the C-terminus with some ER resident protein in order to be properly localized. Recently, it was suggested that an additional protein identified in yeast and called yERG28 could be involved in tethering yERG26 and yERG27 in the ER (**Gachotte D et al. 2001**). However, the results presented in the present study show that neither C14orf1, the human homologue of yERG28, nor yERG28 itself, could form interactions with 17 β -HSD7 nor yERG27, respectively, and therefore they can be excluded as candidate proteins.

3.2.4. Expression of 17 β -HSD7 in cholesterol auxotrophic cell lines

The first intention at the beginning of this study was to perform the complementation experiment in a mammalian system instead in the yeast. Human U-937 and mouse X63 cholesterol auxotrophic cell lines were analyzed for this purpose since they were reported to have a defect in 3-ketosterol reductase (**Billheimer J.T. et al. 1987; Sato J.D. et al. 1988**). It was unfortunately not possible to perform the complementation experiment due to very poor transformation efficiency and inability to get stable transformants. However, some progress towards understanding the molecular defect of those cells was made: 17 β -HSD7 expression could not be detected in both cell lines although the gene seems to be intact (**Figure 11**).

Since in other cells like HeLa, HepG2 and human skin fibroblasts, which are not cholesterol auxotrophs, detectable levels of 17 β -HSD7 were always present, the absence of its expression from U-937 and X63 cells is likely to be connected to a defect in 3-ketosterol reductase associated with cholesterol auxotrophy.

Altogether the results presented here identify 17 β -HSD7 primarily as a cholesterogenic rather than steroidogenic enzyme. However, it is not excluded that the enzyme can also be involved in sterol activation in steroidogenic tissues, since it is highly expressed in ovaries, which are suggested to derive the majority of their cholesterol supplies from plasma, rather than synthesizing it *de novo*.

3.3. Role of C14orf1 and ERG28 in sterol metabolism

Recently, yeast ERG28 was identified as a new enzyme involved in ergosterol biosynthesis probably by facilitating complex formation between yERG26 and yERG27 and by tethering this complex to ER (**Gachotte D. et al. 2001**). The conclusion was based on observation that yeasts disrupted in the ERG28 gene were accumulating the same intermediates as ERG26 and ERG27 knockouts and had a lower amount of ergosterol but were not ergosterol auxotrophs.

The human homologue of ERG28 called C14orf1 had been identified previously not in connection to cholesterol biosynthesis but to a high rate of proliferation (**Veitia R.A. et al. 1999**). The highest expression of this gene was found in testis and in the majority of cancer cells. Since cholesterol is necessary for membrane formation and cell cycle progression its connection with cell proliferation through involvement in cholesterol biosynthesis was not excluded. However the results presented in this study showed that both, yERG28 and C14orf1 were not likely to influence cholesterol biosynthesis through interaction with cholesterogenic enzymes.

3.3.1. C14orf1 and ERG28 as possible interaction partners of 17 β -HSD7 and ERG27

Pull down experiments presented in this study revealed that an interaction between 17 β -HSD7 and C14orf1 was possible *in vitro* (**Figure 17 A**).

Since the C-terminus was found to be necessary for 17 β -HSD7 activity and ER localization it was expected that C14orf1 would interact with this part of the protein in order to control it. However this was not the case since interaction efficiency between 17 β -HSD7 as well as its C-terminal truncated form and C14orf1 was the same (**Figure 17 A and B**).

None of the tested proteins could interact in *in vivo* experiments in yeast (**Figure 18**). It should be taken into account that poor 17 β -HSD7 expression in yeast cells could lead to an insufficient level of interaction and consequently to an inability of transformants to grow under the high selection. To overcome that problem it would be necessary to check the interactions between human proteins in mammalian cells. Florescence resonance energy transfer (FRET) would be a suitable method for that purpose. Unfortunately, due to technical limitations it was not possible to perform this experiment. However, since no interactions could be observed also for the yERG27 and yERG28, it is very likely that the *in vivo* results obtained for the human homologues in this study are more reliable than the *in vitro* ones.

3.3.2. Cellular localization and potential involvement in sterol trafficking

It has been proven by now that yERG28 can influence ergosterol production and most precisely the last steps of the pathway (**Gachotte D. et al. 2001**). Since both C14orf1 and yERG28 consist almost entirely of transmembrane domains (predicted by transmembrane region detection programs; <http://www.expasy.ch/tools/#transmem>), any enzymatic activity can be virtually excluded for those proteins. Additionally, only C14orf1 was found to have an ER membrane retention signal on both the C-terminal and N-terminal part (PSORT prediction; <http://psort.nibb.ac.jp/>) and is presented in this study to be actually localized there (**Figure 19 a-c**).

yERG28 expressed in HeLa cells gave a punctate pattern in the cytosol that resembled some vesicular structures. Furthermore the localization was dependent on the position of the chromophore fused for detection. Since no known localization signal was found in the yERG28 sequence this result suggested that its localization might be directed by protein-protein interactions. Recently, CHM2 was identified as a possible interactor of yERG28 in a Two-hybrid screen (**Ito T. et al. 2001**). This protein is a member of the vesicular sorting protein (Vps) family that directs movement of proteins, which are destined for degradation in lysosomes or recycling to the cell surface through the vesicular pathway (**Howard T.L. et al. 2001**).

It is also known that the same pathway is used for the distribution of cholesterol and probably ergosterol and that this process is very important for the preservation of sterol homeostasis (**Blanchette-Mackie E.J. 2000; Millard E.E. et al. 2000; Sturley S.L. 2000; Higgins M.E. et al. 1999**).

The results presented in this study imply that yERG28 may be involved in sterol trafficking and/or may be a part of some sterol sensing complex, since its localization in mammalian cells seems to be depending on cholesterol supplies from outside. Under reduced serum conditions the punctate cytosolic pattern was diminishing and at the end ERG28 acquired ER localization (**Figure 21**). It should be mentioned in addition that localization of the yeast protein in mammalian cell could be impaired. However, it has been shown here that yERG27 protein, which is highly conserved between species, localized in the ER in mammalian cells as reported previously for its localization in the yeast (**Baudry K. et al. 2001**). It is therefore likely that the highly conserved yERG28 would also show the same cellular distribution in both mammalian cells and yeast.

In a yERG28 knock-out yeast a lower ergosterol amount is one result of the impaired zymosterone to zymosterol conversion (**Gachotte D. et al. 2001**). Also, it was reported that this block was not due to the low yERG26 and yERG27 amount, since almost all ergosterol biosynthesis genes were upregulated in those mutants (**Hughes T.R. et al. 2000**). Therefore it was suggested that yERG28 forms a complex with yERG26 and yERG27 and modulates their activity (**Gachotte D. et al. 2001**). This is however not likely since the results presented in this study revealed no interactions between yERG27 and yERG28. Taking this into account it is more likely that yERG28 influences ergosterol homeostasis via different mechanism than suggested before.

A possible new mechanism of action is presented in **Figure 23**. Until there is enough ergosterol in the cell ERG28 is bound to the vesicular sorting protein (Vps) like CHM2 in late endosomes which are involved in ergosterol distribution. Since yERG28 localization was connected to the cholesterol level in the cell as presented at **Figure 21** and yERG28 itself has no sterol-sensing domain (SSD), yERG28 is likely to be a part of some complex that serves as a cholesterol sensor. When the ergosterol level drops, the complex moves to the cytosol. It was previously reported that CHMP1, a member of the human Vps family, which is localized in endosomes can also be localized in nucleus where it influences gene transcription. Therefore, it is possible that once the yERG28 leaves the endosomes, it interacts with another protein in the cytosol, which results in the release of the CHM2 from the complex and its subsequent translocation to the nucleus, where it could influence transcription of the genes involved in ergosterol biosynthesis. The complex containing yERG28 moves to ER. Since yERG28 itself does not interact with yERG27 as was shown in this study, it is possible that another protein, which is a part of the complex, forms these interactions that bring yERG26 and yERG27 in closer proximity. This could optimize catalytic efficiency.

The rest of the complex might act as an ergosterol sensor, and when enough ergosterol is produced the complex leaves ER with its ergosterol cargo and transfers to the Golgi. From there ergosterol is distributed in the cell. In the yeast little is known about the mechanism of this distribution.

In mammalian cells, the cholesterol distribution was reported to involve Golgi derived vesicles, endosomes and caveolins. Therefore, it is likely that yeast might also use Golgi derived vesicles as well as endosomes to which the yERG28 complex would be directed. The suggested mechanism correlates well with the phenotype reported for the yERG28 knock-out. If yERG28 is not present, more of Vps could enter the nucleus, which would result in upregulation of the genes involved in the ergosterol biosynthesis as it was observed in microarray experiments (**Hughes T.R. et al. 2000**). Additionally, yERG26 and yERG27 would not be efficient enough if a modulator protein is not present in the ER. This would result in a very low zymosterol production, inefficient amount of ergosterol and therefore slower growth. However, further experiments are needed to check this hypothesis.

It was already mentioned that C14orf1 is highly expressed in proliferating cells and tissues. Additionally, cellular proliferation was reported to depend on cholesterol level (**Martinez-Botas J et al. 1999**). The ER is the place where cholesterol and ergosterol are synthesized *de novo*. In mammalian cells this is also the place from which cholesterol synthesis is controlled via SREBP/SCAP complex (**Osborne T.F. et al. 1998; Sakakura Y. et al. 2000; Yang T et al. 2000**). Since C14orf1 is a human homologue of yERG28 it would be expected to have the same physiological role in the cell. The results presented here suggest that if this is indeed the case, C14orf1 would have a different mechanism of action, since its localization was not dependable on exogenous cholesterol supplies (**Figure 22**). Additionally, it is known that ergosterol biosynthesis and homeostasis is controlled differently from cholesterol biosynthesis. The exact mechanisms involved in this process are still not entirely elucidated (**Sturley S.L. 2000; Vik A. and Rine J. 2001**) but it could be expected that yERG28 and C14orf1 would act via different mechanisms if they were involved in the same process.

A suggested mechanism for C14orf1 action is presented in **Figure 24**. It was discovered recently that caveolin-1 plays an important role in trafficking of endogenously synthesized cholesterol. Furthermore it was found to acquire different localization in different cell types (**Li W.P. et al. 2001**). Under normal conditions, when the cholesterol level is optimal, the majority of caveolin-1 is localized in the plasma membrane caveolae. If the cholesterol level changes, caveolin-1 is leaving the caveolae and associates in the cytosol with chaperon proteins. This complex is directed to the ER where it bind newly synthesized cholesterol and returns back to the plasma membrane. The exact mechanism of this process is not known but it is known that it doesn't take place via the Golgi (**Smart E.J. et al. 1996**).

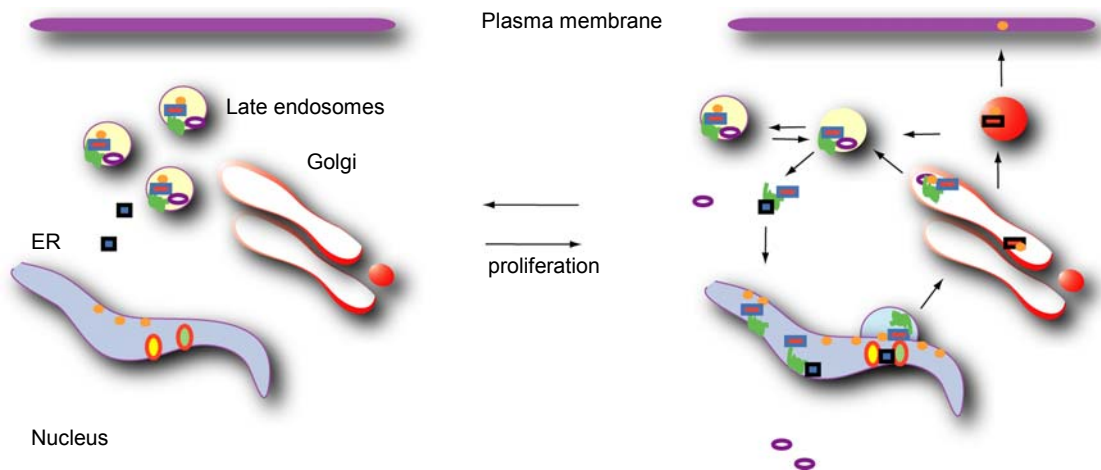


Figure 23. Suggested mechanism of action for ERG28 in ergosterol homeostasis. If ergosterol level drops, a possible complex of yERG28 (green) and Vps and/or other proteins leaves the endosomes and goes to the cytosol (■). In the cytosol another complex is formed (■) and Vps member (○) is released to the nucleus. The rest of the complex goes to ER. In the ER one protein from the complex (■) interacts with ERG26 (●) and ERG27 (●). At the same time the rest of the complex (■) collects ergosterol (●) and translocates to Golgi. Cholesterol is further distributed via Golgi formed vesicles and the initial endosomal complex of ERG28 is reformed. If ergosterol level is high complex will stay bound to it in late endosomes.

C14orf1 was reported to be expressed in some level in the majority of tissues examined but high expression was seen only in testis (Veitia R.A. et al. 1999). Furthermore, it was overexpressed in the majority of cancer cell lines. Those data implied the role for C14orf1 in cell proliferation. Additionally, as an yERG28 homologue it is likely to be involved in cholesterol homeostasis. This correlates well since the cholesterol level influences proliferation.

In the present study C14orf1 was found to be localized in the ER. It is possible that it serves there as a docking protein for a caveolin-chaperon complex and enables it to take newly synthesized cholesterol from the ER. If the cholesterol level drops or more cholesterol is needed then more of C14orf1 would be produced. Furthermore, C14orf1 can have an additional role in activating the SREBP/SCAP complex. The existence of a protein that anchors SREBP/SCAP complex to the ER when the cholesterol level is optimal has been suggested recently (Yang T et al. 2000).

DISCUSSION

If the cholesterol level drops the complex is released to the Golgi, but the exact mechanism how the complex leaves the anchor is still not known. Therefore, it might be possible that C14orf1 interacts with the anchor protein, which results in the release of the SREBP/SCAP complex from the anchor and its subsequent movement to the Golgi. To elucidate the exact physiological role of C14orf1 additional experiments are necessary.

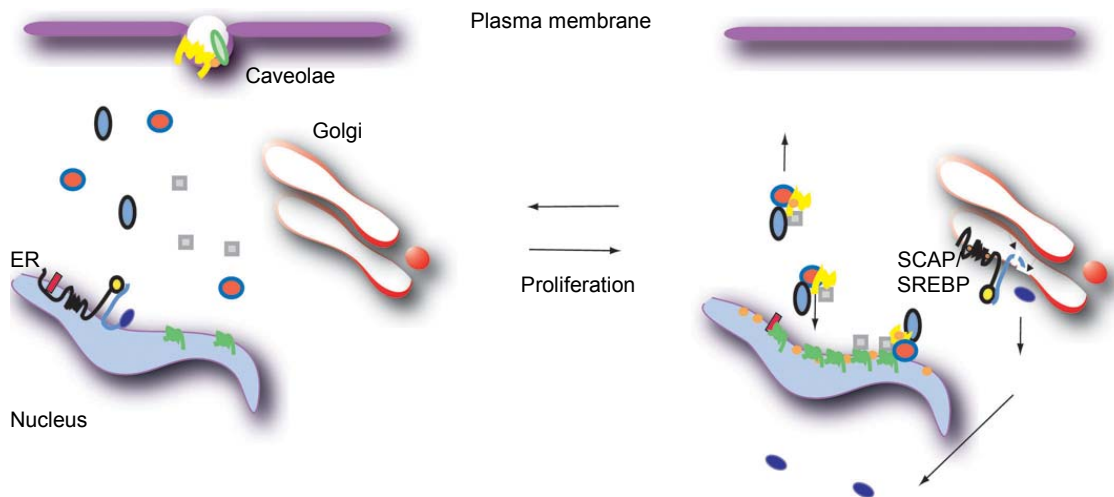


Figure 24. Suggested mechanism of action for C14orf1 in cholesterol homeostasis.

It is very likely that caveolins are also involved in this process since they have been described as proteins responsible for cholesterol transport from ER. If sufficient cholesterol is present, the majority of caveolins (yellow) are localized in caveolae in the plasma membrane bound to cholesterol (orange). They act as cholesterol sensors, so if cholesterol level drops they leave the plasma membrane and form a complex with chaperon proteins (blue) in the cytosol. The complex translocates to the ER and collects cholesterol. C14orf1 (green) may act at this step as a docking protein. At the same time it may help releasing the SCAP/SREBP complex to the Golgi by forming interaction with SCAP/SREBP anchor protein (red). SREBP N-terminal domain (blue) is cleaved off in the Golgi and translocated to the nucleus where it triggers transcription of cholesterologenic genes. After collecting cholesterol caveolin/chaperon complex returns to the plasma membrane where caveolin forms caveolae and helps cholesterol distribution in the rest of the membrane.

3.4. Conclusions

The following main conclusions can be drawn from the results presented in this work.

First, cholesterol auxotrophic U-937 cells do not require exogenous cholesterol supplies exclusively in order to survive. This is shown in the first part of this work, which presents a detailed examination of the cellular requirements for cholesterol and its influences in major cellular processes such as survival, proliferation and apoptosis. The yeast sterol ergosterol, in combination with reduced serum, could support both cellular growth and survival. It was, however, shown that ergosterol was not kept in the free form inside the cells and, therefore, might act predominantly via triggering mobilization of internal cholesterol supplies.

Second, it was also observed that free cholesterol level in the cell was kept low under the normal conditions. A relatively minor elevation in cholesterol level (9-fold) resulted in cell death. This is a very interesting observation since the cholesterol role in triggering of apoptosis was recently discussed.

Third the hypothetical role of 17β -HSD7 in cholesterol biosynthesis was proven experimentally in this study for the first time. In addition the C-terminus of 17β -HSD7 was found to be important for both protein activity and its proper localization in the endoplasmic reticulum.

Finally, the involvement of two previously identified proteins, γ ERG28 and its human homologue C14orf1 in sterol biosynthesis was shown to be unlikely. Instead it is hypothesized that both proteins are involved in cholesterol trafficking and preservation of its homeostasis in the cell.

4. MATERIALS AND METHODS

4.1. METHODS

4.1.1. Working with nucleic acids

Plasmid DNA preparation from bacteria

Bacterial cells were incubated in LB-medium with either ampicillin or kanamycin over night at 37°C with shaking (200 rpm). Depending on the desired amount of DNA the culture volume was set to 5 ml (DNA concentration \cong 100-150 ng/ μ l) or 50 ml (DNA concentration \cong 1 μ g/ μ l). For the plasmid DNA isolation from a of 5 ml culture the NucleoSpin Plasmid-Kit (Macherey-Nagel #740 588.50) was used. The larger amount of plasmid DNA out from 50 ml of culture was obtained using the Nucleobond AX 100-Kit (Macherey-Nagel #740573). In both cases the procedure was done according to the manufacturer's protocol. The amount of isolated plasmid DNA was measured on a Beckman DU 530 spectrophotometer. An aliquot of the sample was diluted 1:100 in water and extinction at 260 nm was measured. Multiplication of the measured result by 50 (double stranded DNA concentration at OD₂₆₀=1) and by 100 (dilution factor) gives DNA concentration in μ g/ml.

Plasmid DNA preparation from yeast

Two yeast colonies were scrapped of the plate and resuspended in 1 ml of 1 \times TE buffer, followed by centrifugation at 3500 rpm for 10 min. The pellet was resuspended in 0,5 ml S-buffer and incubated at 37°C for 30 min.

0,1 ml of lysis solution was added, vortexed and incubated at 65°C for 30 min. After that, 166 µl of 3M sodium acetate was added and chilled 10 min on ice, followed by centrifugation at 15000xg for 10 min. The supernatant was transferred into a new eppendorf tube and DNA was precipitated with 0,8 ml of cold 100% EtOH for 10 min on ice. The sample was centrifuged afterwards for 10 min at 15000 g and the pellet was washed with 0,5 ml of 70% EtOH. The sample was centrifuged again and the pellet was dried on air. It was dissolved in 40 µl of sterile water and additionally purified with the PCR purification kit (Qiagen).

RNA preparation from mammalian cells

Up to 8×10^5 cells were used for total RNA isolation with StrataPrep Total RNA Microprep Kit (Stratagene #400752) according to the manufacturer's protocol. Cells were collected, centrifuged and washed with PBS. After lysis and centrifugation the supernatant was mixed with binding buffer and ethanol and applied to the column. An additional DNase treatment was carried out on the column for 15 min on 37°C. The column was washed with different buffers and the RNA was eluted from the column into an RNase free eppendorff tube. RNA concentration and purity were measured on a Beckman DU 530 spectrophotometer. The sample was diluted 1:100 in 10 mM TRIS buffer and extinction at 260 nm and 280 nm was measured. Multiplication of the measured result at 260 nm by 40 (RNA concentration at $OD_{260}=1$) and 100 (dilution factor) gives the RNA concentration in µg/ml. OD_{260} / OD_{280} ratio gives information on the purity of the RNA (if 1,7 and more the purity is good).

RNA preparation from yeast cells

Up to 5×10^7 yeast cells were used for total RNA isolation with RNeasy Mini Kit (QIAGEN #74104) according to manufacturer's Enzymatic Lysis Protocol (RNeasy Mini Protocol for Isolation of Total RNA from yeast). Yeast cells were centrifuged and the supernatant removed. The spheroplasts were prepared by resuspending the cells in appropriate buffer (supplied with the kit). After that the cells were lysed and centrifuged. The supernatant was mixed with ethanol and applied to the column. The column was treated with series of different buffers so that only RNA remained bound. RNA was eluted from the column into RNase free eppendorf tube. The concentration was calculated as described above.

cDNA synthesis

cDNA can be synthesized by reverse transcriptase action from RNA template. The synthesis was done using Oligo-d(T)-Primer and reverse transcriptase from Ready To Go T-Primed First-Strand Kit (Amersham Pharmacia Biotech Inc. #27-9263-01) according to the manufacturer's protocol.

PCR reaction

Any specific DNA fragment can be amplified using polymerase chain reaction (PCR) method. The method is based on the ability of DNA polymerase for template-based (i.e. complementary) elongation of a short stretch of deoxyribonucleotides (primer) bound to a denatured (single stranded) DNA template. Primers are designed to flank the region of interest that will be amplified. The first step is denaturation of a double stranded DNA template at 95°C for 30 sec. Then the annealing of forward and reverse primers takes place for 30 sec at a temperature that is specific for each pair of primers. Elongation is carried out by thermostable Taq polymerase at 72°C with elongation time depending on the size of the desired amplification fragment (\cong 1 min per 1 kb). This procedure is repeated through a number of cycles until the amplified fragment is obtained in sufficient amount (usually 28-35 cycles, during which the number of desired DNA molecules increases approx. exponentially). The procedure was done in PE 9600-PCR machine (Perkin Elmer). Typical reaction conditions for a 20 μ l reaction (final concentrations):

- 2-20 ng of DNA template
- 0,2 mM of each dNTP
- 1 \times reaction buffer with (NH₄)₂SO₄ (MBI Fermentas)
- 1,5 nM MgCl₂ (MBI Fermentas)
- 0,5 μ M of each primer
- 2 U of Taq polymerase (MBI Fermentas)

DNA electrophoresis

Due to negative charge DNA molecules can be separated according to their size by migration in an electric field. The DNA sample is mixed with loading dye and applied to an agarose gel. The gel is immersed in the chamber with buffer, and a constant voltage is applied across the gel.

The negatively charged DNA will travel toward the anode. DNA can be visualized afterwards by UV excitation (254 nm) of intercalated ethidium-bromide dye.

DNA purification

For some applications like restriction digestion and ligation, it can be necessary to purify the DNA sample after the PCR reaction. This can be done by cutting the DNA bands of the desired size out of the agarose gel and extracting them with the QIA-quick Gel Extraction Kit (QIAGEN). Alternatively, the PCR mixture can be applied directly to the column of the QIA-quick PCR Purification Kit (QIAGEN). Both methods were used according to the manufacturer's protocol.

Restriction digestion of DNA

The method is based on the ability of bacterial enzymes called restriction endonucleases to recognize and cut palindromic sequences in foreign DNA with high specificity, which results in DNA fragmentation. This method is used for cloning of DNA fragments into the vectors. The typical reaction conditions used per 10 μ l reaction (final concentrations):

- ~ 1 μ g of DNA
- 1 \times or 2 \times buffer* (MBI Fermentas)
- 1 U of enzyme (MBI Fermentas)

*The amount and type of used buffer depended on the restriction enzyme(s). The reaction was carried out for 1 h or longer on 37°C. Some of the enzymes can be inactivated later at 65°C for 20 min. The cutted DNA was analyzed by electrophoresis and if desired purified by previously described methods.

Ligation

It is possible to ligate different DNA fragments that were cut with the same restriction endonucleases with the help of T4 DNA ligase. The typical reaction conditions used per 15 μ l of reaction (end concentrations):

- ~ 150 μ g of PCR fragment
- ~ 50 μ g of vector

1× T4 ligase buffer (MBI Fermentas)
40 U Of T4 DNA ligase (MBI Fermentas #EL0331)

The reaction was carried out at room temperature for 1-2 h or over night on 14°C. For direct ligation of PCR products carrying A extensions produced by Taq polymerase, to pYES2.1, pCR2.1 and pcDNA3.1 vectors TOPO cloning was used according to the manufacturer's protocol (Invitrogen).

Cloning

Into yeast expression vector pYES2.1/V5/His (Invitrogen)

yErg25, yErg27, h17 β -Hsd7, h17 β -Hsd7 tr., h17 β -Hsd1, h17 β -Hsd5 and m17 β -Hsd7 were amplified by PCR using primers listed in Appendix out of the following templates*:

pYES2.1 / yERG25 #15	for yErg25
pYES2.1 / yERG27 #17	for yErg27
pYES2.1 / hHSD7 #90	for h17 β -Hsd7
pQB / hHSD1	for h17 β -Hsd1
pGEXhHSD5 BamHI/KpnI #11	for h17 β -Hsd5
pGEX / mHSD7	for m17 β -Hsd7

The TOPO cloning kit (Invitrogen) was used for ligation of the PCR products to the vector.

Into yeast expression vector pESC-URA (Stratagene)

PCR was done by using the pYES2.1 / hHSD7 #90 and cDNA isolated from 293 cells as a template for h17 β -Hsd7 and hC14orf1 amplification respectively. The primers used in the reactions are listed in Appendix. The first step was the cloning of hC14orf1 into the pESC-URA vector, done by cutting both vector and gel extraction purified PCR product with EcoRI and NotI. After cutting the vector was purified by gel extraction, and the PCR product by PCR purification kit. This was followed by the ligation reaction. The positive clone pESC / hERG28 was used for second step cloning of h17 β -Hsd7 with BamHI and Sall restriction endonucleases. The procedure was same as in the first step.

Into eucariotic expression vector pEGFP-C1 (Clontech)

yErg27, yErg28, h17 β -Hsd7, h17 β -Hsd7 tr. and hC14orf1 were amplified by PCR using primers listed in Appendix, out of the following templates*:

pYES2.1 / yERG27 #17	for yErg27
pGEX / hHSD7	for h17 β -Hsd7
pGEX / yERG28 #14	for yErg28
pESC / hERG28/hHSD7	for hC14orf1
pYES / hHSD7tr	for h17 β -Hsd7 tr.

yErg27 and h17 β -Hsd7 PCR products were first cloned into pCR2.1 by TOPO cloning and then subcloned into pEGFP-C1 by cutting with EcoRI and BamHI in case of yErg27 and HindIII and BamHI in the case of h17 β -Hsd7. All other PCR products were purified by gel extraction and cut with EcoRI and BamHI except h17 β -Hsd7 tr. which was cut with Sall and BamHI. In all cases the vector was purified after cutting by gel extraction, and the PCR product was purified with PCR purification kit.

Into eucariotic expression vector pECFP-N1 (Clontech)

yErg27 and h17 β -Hsd7 were amplified by PCR out of the templates mentioned above and using the primers listed in the Appendix. h17 β -Hsd7 was first ligated to pCR2.1 by TOPO cloning and then subcloned into pECFP-N1 by cutting it out with HindIII and BamHI. yErg27 PCR product was first purified through gel extraction and then cut with EcoRI and BamHI. After cutting with the required enzymes and prior to ligation, vector and h17 β -Hsd7 were purified through gel extraction and yErg27 with PCR purification kit.

Into eucariotic expression vector pEYFP-N1 (Clontech)

yErg28 and hC14orf1 were amplified by PCR from pESC / hERG28 / hHSD7 and pEGFP / yERG28 respectively, using the primers listed in the Appendix. Both PCR products were first purified through gel extraction and then cut with EcoRI and BamHI in case of yERG28 and XhoI and BamHI in case of hC14orf1. After cutting with required enzymes and prior to ligation, vector was purified through gel extraction and both PCR products with PCR purification kit.

Into bacterial expression vector pGEX

h17 β -Hsd7 tr. was amplified by PCR out of pYES2.1/ hHSD7tr. #6 using the primers listed in the Appendix. PCR product was purified through gel extraction and cut with EcoRI and BamHI. After cutting and prior to ligation vector was purified through gel extraction and PCR product with PCR purification kit.

Into eucariotic expression vector pcDNA3.1/V5/His (Invitrogen)

yErg28, hC14orf1 and mC14orf1 were amplified by PCR out of pEGFP/yERG28, pEGFP/hERG28 and pEGFP/mERG28 respectively with the primers listed in Appendix. All PCR products were ligated to the vector by TOPO cloning.

Into yeast expression vector pGBKT7 (Clontech)

yErg27, h17 β -Hsd7, h17 β -Hsd7 tr. and m17 β -Hsd7 were amplified by PCR with the primers listed in Appendix and out of the following templates*:

pYES2.1 / yERG27 #17	for yErg27
pYES2.1 / hHSD7 #90	for h17 β -Hsd7
pYES2.1 / hHSD7 tr. #6	for h17 β -Hsd7 tr.
pYES2.1 / mHSD7 #4	for m17 β -Hsd7

All PCR products were purified through gel extraction prior to cutting with restriction enzymes. yErg27 was cut with EcoRI and BamHI as well as m17 β -Hsd7. h17 β -Hsd7 and h17 β -Hsd7 tr. were cut with BamHI and Sall. The vector cut with required enzymes was purified after cutting and prior to ligation through gel extraction. Cut PCR products were purified with PCR purification kit.

Into yeast expression vector pGADT7 (Clontech)

yErg28, hC14orf1 and mC14orf1 were amplified by PCR out of pEGFP/yERG28, pEGFP/hERG28 and pEGFP/mERG28 respectively, with the primers listed in Appendix. The purification procedure was done as mentioned above. All PCR products as well as vector were cut with EcoRI and BamHI.

*all constructs that are not listed in the Appendix were made previously and not for the purpose of this study.

- The constructs were sequenced by Dr. W. Metzger (Sequiserie).

4.1.2. Protein chemistry

Expression and purification of recombinant proteins

Overnight cultures of bacteria transformed with the constructs:

pGEX / hHSD7
pGEX / h HSD7 tr.
pGEX / mHSD7
pGEX / yERG27

were diluted 1:10 with LB-medium and incubated further for 2 h until $OD_{600} \cong 0,5$. Induction of protein expression was done by addition of 0,25 mM IPTG for 2-4 h at 37°C. After induction the culture was centrifuged at 4°C and 1000xg for 10 min and the pellet was resuspended in 200 μ l of PBS (per 50 ml culture). Since all expressed proteins were insoluble, 20 μ l of 10% Triton, 1ml of PBS and 2 μ l of protease inhibitor, PI (1000 \times) were added to bacterial suspension and incubated on ice for 10 min. After that 2,4 μ l of lysozyme (0,2 mg/ml final conc.) was added and incubated at room temperature for 10 min to break the cell wall. To break cells completely sample was freeze shortly in liquid nitrogen and then immediately thawed in a water bath. This was repeated 3 times. To remove released genomic DNA, 3 mM $MgCl_2$ and 30 U of benzonase were added and incubated at room temperature for 5 min followed by centrifugation for 15 min at 15000xg and 4°C. The supernatant was transferred into a new eppendorf tube and frozen immediately or kept on ice until used. GST fusion protein can be purified through Glutathione Sepharose 4B beads (Amersham Pharmacia Biotech AB #17-0756-01). Prior to protein addition 100 μ l of beads was transferred into a 1,5 ml eppendorf tube and centrifuged for 2 min at 3500 rpm. The supernatant was discarded and 3 \times washing with 1 ml of ice cold PBS was done. After the washing step PBS was added to the pellet in 1:1 ratio. To purify the protein 30 μ l of previously prepared beads were mixed with 170 μ l of protein suspension and incubated over night at 4°C with shaking. The next day the mixture was centrifuged for 2 min at 1000xg and the supernatant was transferred to another eppendorf tube. To remove unbound proteins beads were washed 3 \times with 500 μ l of cold PBS and in the end resuspended in 50 μ l of PBS and analyzed on the gel. It is also possible to elute the bound protein with GSH containing buffer and to remove the tag by thrombin cleavage.

Polyacrylamid gel electrophoresis (PAGE)

This method is used to separate proteins solubilized in SDS in electric field on the basis of their molecular weights. All samples were mixed 1:1 with 5× Laemmli buffer and incubated for 5 min at 95°C. Electrophoresis was done in a two buffer system for the 10% tricine gels and in 1× Tris-glycin-SDS buffer for commercial polyacrylamid gradient gels 4%-20% (Biorad) which were used in pull down experiment to separate proteins with size difference of only 4 kD. Tricine gels were run at 90 V for 1,5 h and gradient gels at 120 V for 2,5-3 h. To visualize the protein bands, gels were incubated with Coomassie stain for 30 min-1 h at RT and destained afterwards by boiling in 7% acetic acid.

Western blotting

Proteins separated by PAGE can be transferred to PVDF membrane and analyzed with specific antibodies. Before transfer a membrane cut to the size of the gel was wet with methanol and immersed together with the gel in blotting buffer for 30 min. The membrane was put with 2 pieces of filter paper soaked with blotting buffer onto the lower electrode of a BioRad Trans-Blot SD device, followed by the gel and two more pieces of filter paper, all soaked with blotting buffer. The upper electrode was put on top and blotting was carried out for 30 min at 20 V. After blotting, the gel was transferred into Coomassie stain and the membrane was blocked with 5% milk suspension in PBS with addition of 0,05% Tween 20 to prevent unspecific binding. Prior to incubation with antibodies membrane was washed with PBS for 5 min at room temperature with shaking. Primary Anti-V5 antibody (Invitrogen #46-0705) was diluted 1:5000 in PBS and the membrane was incubated with antibody solution overnight at 4°C with shaking. Next day the membrane was washed with PBS 3 times, each time for 5 min and secondary Peroxidase-conjugated AffiniPure Goat Anti-mouse antibody (Dianova #115-035-068) diluted 1:2000 in PBS was added. The incubation was carried out for 1h at room temperature. After washing with PBS 3 times for 5 min, staining reaction was performed. 25 ml of staining buffer was mixed with 1mg of diaminobenzidine and 100 µl of cobalt-chloride solution (10mg/ml). To start the reaction 10 µl of H₂O₂ was added. The membrane was incubated in staining mix for 5-10 min, washed with distilled water and dried on a piece of paper. When 2 primary antibodies were used, membrane was first incubated 2 h at RT with Anti-FLAG antibodies (Stratagene), diluted 1:5000 in milk suspension. After the washing step the membrane was incubated over night at 4°C with the same dilution of Anti-Myc (Invitrogen) antibodies. The rest of the procedure was the same as described above.

In vitro translation

TNT T7 Coupled Reticulocyte Lysate System (Promega #L 4610) was used for in vitro translation of pcDNA3.1 / hERG28 #2, pcDNA3.1 / mERG28 #4, pcDNA3.1 / yERG28 #1 according to manufacturer's protocol. The proteins were labeled by incorporation of Redivue ³⁵S-methionine (Amersham-Pharmacia Biotech #AG1094).

Pull down assay

To check protein interactions, 5 µl of in vitro translated protein resuspended in 190 µl of binding buffer was added to GST fusion protein bound to glutathion sepharose beads and was incubated for 2 h at 4°C with shaking (950 rpm). After incubation was finished, beads were washed 4× with 500 µl of wash buffer. Each washing step was carried out for 20 min at 4°C with shaking, followed by centrifugation for 2 min at 1000xg. Beads were resuspended in 10 µl of Laemmli buffer after the final washing, denatured for 5 min at 95 °C and loaded on a PAA gradient gel. After the run gel was soaked in solution containing 50% MeOH, 12% acetic acid and 0,05% formaline for 20 min. Before drying, gel was additionally soaked for 10 min in 20% EtOH and 2% glycerol solution. Drying was done for 55 min at 80°C in Gel dryer, model 583 (Biorad). Dried gel was exposed to an imaging plate BAS-MS 2325 (FUJI PHOTO FILM CO., LTD). After overnight exposure the plate was analyzed with Image analyzer FLA-3000 (Fuji).

4.1.3. Working with bacteria

Storage and growing

For the long time storage 0,75 ml of over night growing bacterial suspension were mixed with 0,5 ml of autoclaved 80%-100% glycerol in cryo-vial (Nunc, #375418) and frozen immediately at -80°C. For the short time storage up to 1 month, bacterial suspension or plates were stored at 4°C. Bacterial cells were grown in LB medium with or without antibiotics depending on the strain resistance.

The following procedure was used: a little amount of glycerol stock or 50 μ l of bacterial suspension was transferred in LB medium (5-50 ml) and left over night at 37°C with shaking (200 rpm).

Heat-shock transformation

In majority of cases TOP 10 competent E.Coli cells (Invitrogen) or DH5 α were used for transformation and plasmid production. For protein expression BL21 (DE3) (Stratagene) strain was used. Transformation procedure was the following: 2 μ l of plasmid solution or 10-20 μ l of ligation mix were transferred on the top of 100 μ l of chemically competent bacterial cells and kept on ice for 30 min. After heat-shock was carried out at 42°C for 30 sec, bacteria were grown for 1 h in 250 μ l of SOC medium at 37°C with shaking (200 rpm). Usually, the entire suspension was plated on selection plate and left over night on 37°C.

4.1.4. Working with yeast

Storage and growing

To store yeast for longer period of time, 0,5 ml of yeast suspension was mixed with 0,5 ml of autoclaved 15% glycerol in cryo-vial and frozen at -80°C. Yeast were stored in suspension or on the plates at 4°C up to 1 month. To grow them, 200 μ l of glycerol stock (completely thawed on ice) or 2-3 colonies from the plate were transferred to the required media and left on 30°C with shaking (200 rpm) for liquid culture. If yeast were grown on the plate, up to 100 μ l of yeast suspension was transferred per small Petri dish and equally distributed on the agar.

Growing yeast in media with different sterols

yeast strain SDG110 was grown in YPDA medium with addition of 20 μ g/ml cholesterol or ergosterol in liquid culture or on plates.

Both cholesterol and ergosterol were solubilized in 100% EtOH: Tween 20 = 1:1. Yeasts were grown on plates in serial dilution 1:1, 1:10, 1:100, 1:1000 at 30°C until colonies were visible. For liquid culture 1 ml of yeast suspension $OD_{600} = 0,4$ was added to medium and incubated at 30°C with shaking (200 rpm). Yeast suspension was grown to saturation. Growth was checked by measuring OD_{600} .

Transformation

For transformation, yeasts were grown in liquid culture until $OD_{600} > 1$. Two different transformation procedures were applied:

a) Transformation with LiAc

The culture was diluted to $OD_{600} = 0,4$ in 50 ml of YPDA medium and incubated for 3 h at 37°C with shaking. After incubation yeasts were centrifuged at 2500 rpm for 5 min. The pellet was resuspended in 25 ml of 1×TE buffer and centrifuged again. Supernatant was discarded and the pellet was resuspended in up to 2 ml of 1×LiAc/1×TE and left for 10 min at room temperature to make the yeast competent for transformation. Transformation was done the following way: up to 2 µg of plasmid DNA was mixed with 6 µl of salmon sperm DNA (Sigma #D-9156) in an eppendorf tube. 100 µl of competent yeast cells were added to the mixture and vortexed. Final 600 µl of 40% PEG-3350/LiAc/TE was added, vortexed for 10 sec and incubated at 30°C and 500 rpm on table shaker for 30 min. Following incubation, 88 µl of DMSO was added, mixed by inverting the tube and incubated at 42°C for 15 min in water bath. After heat-shock the sample was centrifuged for 10 sec at 15000xg and the pellet was resuspended in 100 µl of 1×TE. 1:10 and 1:100 dilutions were made and plated on proper selection plates.

b) Transformation with BIO 101 kit (BIO 101.Inc)

SDG110 yeast strain used in complementation experiment was transformed according to the manufacturer's protocol for transformation of yeast grown in suspension.

Complementation Assay

The method is based on the ability of the gene of interest to complement the specific defect in the yeast strain it was transformed to, which changes yeast requirements for the specific medium. The method is especially useful for analyzing gene homologues. SDG110 yeast were grown in YPDA + cholesterol medium up to $OD_{600} \cong 3$. Transformation was done with the BIO 101 kit using the following plasmid constructs:

pYES2.1 / yERG25
pYES2.1 / yERG27
pYES2.1 / hHSD7
pYES2.1 / hHSD7 tr.
pYES2.1 / mHSD7
pYES2.1 / hHSD1
pYES2.1 / hHSD5
pESC / hERG28 / hHSD7

After transformation the entire reaction mixture from each transformant was plated on transformation selection plates (-HIS-URA+cholesterol+glucose) and incubated on 30°C for 3 days until colonies formed. Two colonies from each plate were picked, resuspended in 20 μ l and checked for the plasmid by PCR. 5 μ l of each positive colony was spotted onto a new transformation selection plate and incubated for 3 more days at 30°C. After enough amount of each yeast transformant was obtained, the yeast clones were resuspended in 50 μ l of sterile water and serial dilutions were made (1:1, 1:10, 1:100, 1:1000). 5 μ l of each dilution of one clone was plated on one field of the same horizontal row on the complementation selection plate (-HIS -URA -cholesterol + galactose + raffinose). The plates were incubated at 30°C up to 3 weeks.

Sample preparation for activity measurements and western blotting

One clone of each yeast transformant that grew on complementation selection plate was transferred to 50 ml of the same liquid media. For control SDG110 nontransformed yeasts were grown in the same amount of YPDA+cholesterol. After 3 days of shaking at 30°C yeasts were harvested by centrifugation and resuspended in 5 ml of PBS. Cell number was counted under the microscope. For activity measurements, around 590×10^6 cells were taken and vortexed with 1 volume of acid washed glass beads (425-600 μ ; Sigma) 10 times for 30 sec with the 30 sec break in between. Cells were additionally sonified. The procedure was the same for the PAGE and Western blotting only that yeast amount was adjusted to $OD_{600}=1$ instead of cell number.

Two-hybrid assay

This method is used for the identification of protein interactions *in vivo*. The method is based on cotransformation of the yeast with potential protein interactors cloned in 2 different vectors, so-called bait and prey vector. The coding DNA cloned into the bait vector is fused to the DNA binding domain of the yeast transcription factor Gal4. The second coding DNA cloned into the prey vector is fused to the Gal4 transactivation domain. Only if the two cloned proteins interact the Ade, His and lacZ reporter genes will be activated.

The method was done the following way: AH109 yeast strain was grown overnight in YPDA medium until $OD_{600} > 1$. Then yeasts were transformed with the plasmids

pGBKT7
pGBKT7 / yERG27
pGBKT7 / hHSD7
pGBKT7 / hHSD7 tr.
pGBKT7 / mHSD7

and plated onto SD/-Trp selection plates. After 3 days of incubation at 30°C 3 colonies were picked from each plate, resuspended in 50 ml of SD/-Trp liquid medium and incubated at 30°C with shaking until $OD_{600} > 1$. The yeast were then transformed the following way:

AH109 / pGBKT7 / yERG27 with pGADT7 / yERG28
AH109 / pGBKT7 / hHSD7 with pGADT7 / hERG28
AH109 / pGBKT7 / hHSD7 with pGADT7 / yERG28
AH109 / pGBKT7 / hHSD7 tr. with pGADT7 / hERG28
AH109 / pGBKT7 / mHSD7 with pGADT7 / mERG28

Yeast transformants containing pGBKT7 plasmid constructs were also transformed with pGADT7 vector only and AH109 strain containing the pGBKT7 vector was transformed with each of the pGADT7 plasmid constructs as negative controls. After transformation yeasts were plated on SD/-Leu/-Trp plates and incubated at 30°C until colonies formed. One colony from each plate was resuspended in 20 μ l of sterile water and 5 μ l was transferred to a numbered field on QDO plate. The plate was incubated on 30°C until colonies formed.

β-Galactosidase Assay

This is an additional way to prove protein interactions. Only the yeasts, which carry the proteins that are interacting the activation of the lacZ reporter gene will occur and β-galactosidase will be produced. The following procedure was done to prove protein interactions: a sterile Whatman filter paper (#1005 125) was put into a 10 cm Petri dish and soaked with 2,5-5 ml Z-buffer / X-Gal solution. A sterile nitrocellulose filter was shortly pressed on top of a QDO plate with yeast colonies and then removed. The colonies stuck to the filter. To break the yeast cells the filter was immersed for 10 sec into liquid nitrogen, then thawed and put with the yeast exposed side on top of the previously prepared Whatman paper. The incubation was carried out at room temperature until a blue color appeared, but not more than 8 hours.

4.1.5. Working with mammalian cells

Storage and growing

For storage of mammalian cells for the longer period of time, they were collected in certain number, depending on the cell type, centrifuged and mixed with 1 ml of freezing medium in cryo-vial. They were left in the Cryo 1°C Freezing Container (NALGENE #5100-0001) filled with 4°C isopropanol for 1 day at -80°C. The cells can remain frozen at -80°C up to 6 months but for the longer period they should be transferred to -160°C in liquid nitrogen.

To grow stored cells they were thawed quickly from -160°C to 37°C, centrifuged 5 min at 1000xg and transferred to the culture flask filled with appropriate medium. All cells were grown at 37°C with 5% CO₂ in a humid atmosphere until confluence. When confluent, adherent cells were trypsinized and splitted into more culture flasks for further growing. Cells growing in suspension were collected by centrifugation for 5 min at 1000xg, resuspended in medium and splitted into more culture flasks.

U-937 cells and **X63** cells were maintained in 80 cm² flasks (Nunc #178891) filled with 20 ml of RPMI 1640 MEDIUM WITH GLUTAMAX-I (GIBCO BRL #61870-010) with addition of 10% Fetal Bovine Serum (GIBCO BRL #26140-079) and 1% Penicillin /Streptomycin solution (GIBCO BRL #15140-122). They were splitted 1:2 every 2 days.

HeLa and **NIH3T3** cells were maintained in 80 cm² flask filled with 20 ml of RPMI-1640 MEDIUM WITH GLUTAMAX-I + 10% FBS + 1% Penicillin /Streptomycin until confluence. They were splitted 1:20 every week using Trypsin-EDTA (GIBCO BRL #25300-054) to detach them from the surface.

Growing cells in media containing different sterols

U-937 cells were plated in 6 well MULTIWELL plates (FALCON #353046) filled with 5 ml of RPMI-1640 MEDIUM WITH GLUTAMAX-I with addition of 1% Penicillin /Streptomycin and:

- 10% FBS
- 0,1% FBS
- 0,1% FBS + 5 µg/ml cholesterol
- 0,1% FBS + 10 µg/ml cholesterol
- 0,1% FBS + 20 µg/ml cholesterol
- 0,1% FBS + 30 µg/ml cholesterol
- 0,1% FBS + ≅ 5 µg/ml ergosterol
- 0,1% FBS + ≅ 10 µg/ml ergosterol
- 0,1% FBS + ≅ 20 µg/ml ergosterol
- 0,1% FBS + ≅ 30 µg/ml ergosterol

Cholesterol (Sigma #C-3045) and ergosterol (Sigma E-6510) were solubilized in 45% water solution of 2-Hydroxypropyl-β-cyclodextrin (Sigma #C-0926) at 80°C over night. In media with 10% FBS and 0,1% FBS only, the same amount of 45% water solution of 2-Hydroxypropyl-β-cyclodextrin was added. The number of plated cells was ≅ 20000 cells/ml for U-937 cells. In case of HeLa cells confluent cultures were trypsinized in 5 ml and 2 drops of HeLa cells in Trypsin were added per well. They were left to proliferate for 96 h. To see how good cells could survive and proliferate in different media, they were collected 3 h, 6 h, 12 h, 24 h, 48 h and 96 h after plating and the percentage of living cells was calculated as discussed below.

Calculating cell survival

10 µl of U-937 cell suspension was mixed with 10 µl of Trypan-blue stain 0,4% (GIBCO BRL #15250-061) and left for 1 min at room temperature. The mixture was then transferred to Neubauer chamber (MARIENFELD) and cells were counted under the microscope.

The number of cells within all four 16 square areas was divided by 4 to get the average and multiplied by 2500 to obtain the number of cells per 1 ml. The percentage of living cells was calculated by dividing the number of white cells with the overall number of cells (blue and white) and multiplying it by 100.

Cell transfection

HeLa and NIH 3T3 cells were grown in 35 mm Coated Glass Bottom Microwell Dish (MatTek Corporation) filled with 2 ml of medium until 50% confluence. Transfections were made with following constructs:

pEGFP / hHSD7	pEGFP / mHSD7
pEGFP / hHSD7 tr.	pEGFP / mERG28
pEGFP / yERG27	
pEGFP / yERG27 stop	
pEGFP / yERG28	
pEGFP / hERG28	
yERG28 / YFP	
hERG28 / YFP	
in HeLa cells	in NIH 3T3 cells

FuGENE 6 Transfection Reagent (Roche) was used according to the manufacturer's protocol.

ER staining

The staining was done with 300 nmol of ER-Tracker Blue-White DPX (Molecular Probes) according to the manufacturer's protocol. The absorption of the ER-Tracker Blue-White DPX is 353 nm, while the peak fluorescence emission is variable and ranges from 430 nm to 640 nm.

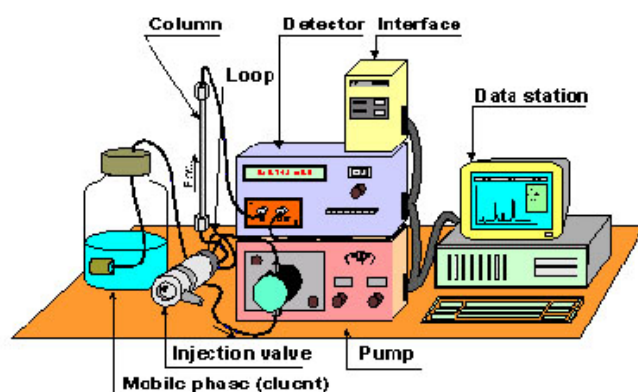
4.1.6. Analytical methods

Confocal microscopy

With the help of confocal microscope it is possible to scan through different planes of the same object and to reconstruct its 3D model. The principle of the method lies in ability to observe only the plane, which is in focus of the laser light. The observed plane is changed simply by changing the focus. The laser scanning microscope LSM 410 (Zeiss) was used to check cellular localization of GFP and YFP fusion proteins. GFP fluorescence was excited at 488 nm and YFP fluorescence at 510 nm.

HPLC

High Pressure Liquid Chromatography (HPLC) is a method in which a liquid phase containing dissolved mixtures travels through a column with a solid stationary phase. The active ingredients of the sample migrate in a differential way according to their polarity and their density. The high-pressure pumps are used to accelerate the separation. The method can be used for separation, identification, quantification and purification of the compounds (here used for separation of steroids).



Sample preparation for conversion of steroids

Reaction mixture:

10 μ l of homogenized cells
440 μ l of 10mM KP-buffer pH 8
0,5 μ l of (6, 7- 3 H)-estrone (final conc. 40 nM)
50 μ l of NADPH (final conc. 7mM)

The samples were incubated 1h in a water bath at 37°C with shaking.

Afterwards, 100 μ L of stop solution (0,21 M ascorbic acid in 1% mixture of EtOH and acetic acid) was added and the samples were purified through Strata C18-E columns (Phenomenex). The elution of steroids was done with 250 μ l of MeOH, HPLC grade.

Separation of steroids

Separation of steroids was done on a Beckman HPLC system using the following conditions:

column: Hibar® Fertigsäule RT, 250-4, Lichrosolv, RP-18, 5 μ m (Merck, #50333)

liquid phase: acetonitrile: H₂O = 1: 1

sample volume applied to column: 20 μ l

flow rate: 1ml / min

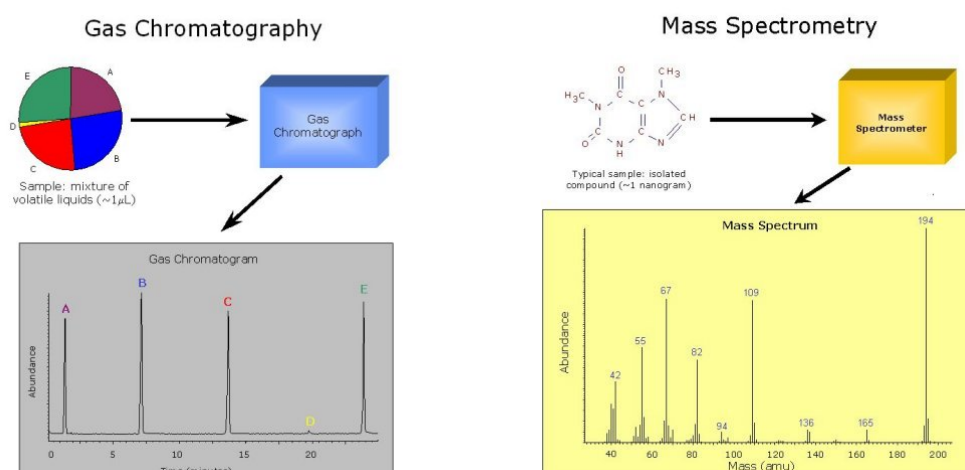
Liquid eluated from the column was mixed 1:1 with scintillation cocktail. Light flashes induced by radioactive compounds were measured online by a flow through scintillation counter. Signal detection and integration was done by the 32Karat software (Beckman). Percentage of conversion was calculated from the areas below the educt and the product peak.

GC/MS

Gas chromatography / mass spectroscopy (GC/MS) is a powerful method used for separation and identification of single compounds out of the mixture. The sample is evaporized and injected into a gas chromatograph producing a separation with respect to time versus the absorption of the ions.

MATERIALS AND METHODS

Next, these isolated ions are injected into a mass spectrometer where they become separated on the bases of the mass versus charge ratio. This way qualitative as well as quantitative information for the compounds can be obtained.



Here the sterols, ergosterol and cholesterol were extracted from the mammalian and yeast cells, as well as from the media in which the cells were grown and applied to GC/MS. Agilent 5890 Series II gas chromatograph and Finnigan SSQ 7000 mass spectrometer were used.

Sample preparation:

Mammalian cells and media

Cell pellets were resuspended in 400 µl of sterile water. 2 ml of 100% EtOH and 2,5 ml of n-hexane were added. Samples were shaken for 30 sec, briefly vortexed and left until phase separation occurred.

The hexane phase was transferred into a new tube and hexane extraction was repeated. Afterwards the tubes with combined hexane phases were dried under vacuum and 150 µl of BSTFA / TMCS in a ratio 4:1 was added into each tube. The tubes were left 1h at room temperature and then 100 µl of n-hexane was added. 1 µl of each sample was used per measurement.

4.2. MATERIALS

4.2.1. Buffers and media

Standard buffer

1 x PBS 10 mM Sodium phosphate, 150 mM NaCl, pH 7,4

SDS-PAGE

5 X Laemmli buffer 50% glycerol, 4% SDS, 0,2 M Tris-HCl,
0,1% G250, pH 6,8

Gel buffer 3 M Tris, 0,3% SDS, pH 8,45

Stacking gel (4%) 3,6 ml water, 0,67 ml gel buffer, 0,67 ml acrylamide,
10 µl TEMED, 45 µl 10% APS

Resolving gel (10%) 1 ml water, 3 ml gel buffer, 3,3 ml acrylamide
2,5 ml glycine, 20 µl TEMED, 60 µl 10% APS

Two-system buffer 0,1 M Tris, 0,1 M Tricine, 0,1% SDS (catode)
0,2 M Tris-HCl, pH 8,9 (anode)

Protein staining
(Coomassie) 200 ml methanol, 5 ml acetic acid, 295 ml water
500 mg Coomassie blue G250 (filtrate)

Western blotting

Blotting buffer 48 mM Tris, 33 mM Tricine, 1,3 mM 10% SDS,
20% methanol

Staining buffer 0,225 g NaH₂PO₄, 1,59 g Na₂HPO₄, 11 g NaCl,
8,5 g imidazol, 625 µl Tween 20, 250 ml water,
pH 7,5

Cobalt chloride
solution 10 mg/ml CoCl₂

MATERIALS AND METHODS

Pull down assay

Binding buffer	50 mM potassium phosphate, 100mM NaCl, 1 mM MgCl ₂ , 10% glycerol, 0,1% Tween 20, 1,5 % BSA, pH 7,4
Washing buffer	50 mM potassium phosphate, 100 mM NaCl, 1 mM MgCl ₂ , 10% glycerol, 0,1% Tween 20, pH 7,4

Yeast transformation

10 x TE	100 mM Tris-HCl, 10mM EDTA, pH 7,5
10 x LiAc	1 M lithium acetate, pH 7,5 (with acetic acide)
1 x LiAc / 0,5 x TE	100 mM lithium acetate, 5 mM Tris-HCl, 0,5 mM EDTA
50% PEG-3350	50g PEG-3350 dissolved in 100 ml distilled water (autoclaving at 121°C for 20 min.)
1 x LiAc/ 40% PEG-3350/ 1 x TE	10 ml of 10 X LiAc, 10 ml of 10 x TE, 80 ml of 50% PEG-3350 (prepare fresh immediately before use)

Plasmid isolation out of yeast cells

S-buffer	10 mM potassium phosphate, 10mM EDTA, 50 mM β-mercaptoethanol, 50 μg/ml zymolase
Lysis-buffer SDS	25 mM Tris-HCl pH 7,5, 25 mm EDTA, 2,5%

β-Galactosidase assay

Z-buffer	16,1 g/l Na ₂ HPO ₄ , × 7 H ₂ O, 5,5 g/l NaH ₂ PO ₄ , 0,75 g/l KCl, 0,246 g/l MgSO ₄ × 7 H ₂ O
Z-buffer / X-Gal	100 ml Z-buffer, 0,27 ml β-mercaptoethanol, 1,67 ml X-gal (20 mg/ml in DMSO) solution

Media for bacterial culture

LB-Medium 10 g BACTO Peptone, 5 g Yeast Extract, 10 g NaCl and 1 l Milli-Q-water;
for plates additional 20 g/l Bacto-agar (autoclaving)
with Ampicillin or After cooling the medium add 50 mg/l of antibiotics
Kanamycin

For X-Gal-IPTG plates: 0,04% (w/v) X-Gal, 40 mmol/l IPTG

Media for yeast culture

Stock solutions:

Glucose	50% glucose (autoclaved)
Galactose	25% galactose (autoclaved)
Raffinose	25% raffinose (steril filtrated)
1% Leucine	1 g of leucin in 100 ml water (sterile filtrated)
0,1% Adenine	0,1 g of adenin in 100 ml water (sterile filtrated)
1% Triptophan	1 g of tryptophan in 100 ml water (sterile filtrated)
Drop-out mix	2,5g adenin, 1,2 g L-arginin, 6,0 g L-aspartat, 6,0 g L-glutamat, 1,8 g L-isoleucin, 1,8 g L-lysin, 1,2 g L-methionin, 3,0 g L-phenylalanin, 22,5 g L-serin, 12 g L-threonin, 1,8 g L-tyrosin, 9,0 g of L-valin
YPDA	10 g Yeast extract, 10 g Bacto Peptone and up to 1 l Milli-Q-water (autoclaving). After cooling down 40 ml 50% glucose and 2 ml 1% adenin solution was added.
with Cholesterol or Ergosterol	before autoclaving 20 µg/ml of sterol was added
SDG110 selection medium (-His+chol)	1,675 g Yeast Nitrogen Base, 0,15 g QDO mix (- His/ -Leu/ -Trp/ -Ade), 0,125 g Cholesterol, 232 ml Milli-Q-water (autoclaving). 1,5 ml 1% leucine, 5 ml 0,1% adenine, 1 ml 1% tryptophan, 10 ml 50% glucose was added afterwards

MATERIALS AND METHODS

Transformation Selection medium (-His-Ura+chol)	1,675 g Yeast Nitrogen Base, 0,25 g Drop-out mix, 0,125 g Cholesterol, 237,5 ml Milli-Q-water (autoclaving). Afterwards 10 ml 50% glucose, 1 ml of 1% triptophan and 1,5 ml of 1% leucine was added.
Complementation selection medium (-His-Ura-chol+gal +raf.)	1,68 g Yeast Nitrogen Base, 0,25 g Drop-out mix, 207,5 ml of Milli-Q-water (autoclaving). Afterwards 1 ml % triptophan, 1,5 ml 1% leucine, 20 ml of 25% galactose and 20 ml of 25% raffinose was added.
SD/-Trp/-Leu	0,64 g DO supplement (-Leu/ -Trp), 6,7 g Yeast Nitrogen Base, 950 ml Milli-Q-water (autoclaving). After cooling 40 ml 50% glucose was added
SD/-Trp	The same as the SD/-Trp/-Leu only that 6 ml/l of 1% leucine was added after cooling
QDO	0,6 g QDO (- Ade/ -His/ -Leu/ -Trp), 6,7 g Yeast Nitrogen Base, 950 ml Milli-Q-water (autoclave). After cooling 40 ml 50% Glucose was added.

In all cases if plates were made 25 g/l Agar was added before autoclaving.

4.2.2. Chemicals

General

Acrylamide	Biomol
Ammoniumperoxodisulphate (APS)	Merck
Ascorbic acid	Merck
Bovine serum albumin (BSA)	Merck
Cholesterol	Sigma
Coomassie blue G250	Biomol
Ergosterol	Sigma
Ethanol	Merck
Ethylenediamine tetraacetic acid (EDTA)	Biomol
Glycerol	Biomol
Glycine	Biomol
³ H-estrone	NEN
Hydrochloric acid (HCl)	Merck
2-Hydroxypropyl- β -cyclodextrin	Sigma
Imidazol	Biomol
Isopropyl thiogalactopyranosid (IPTG)	DCL
Lithium acetate	Merck
Magnesium chloride	Merck
Methanol	Merck
N,O-Bis(trimethylsilyl)trifluoro-acetamid (BSTFA)	Fluca
β -merkaptoethanol	Merck
Peroxid 30% (H ₂ O ₂)	Merck
Polyethylen glycol 3350 (PEG-3350)	Merck
Potassium chloride	Merck
Potassium phosphate	Merck
Redivue ³⁵ S-Methionin	Amersham-Pharmacia
Salmon sperm DNA	Sigma
Sodium chloride	Merck
Dodecyl sulfate sodium salt (SDS)	Merck
Sodium-dihydrogen phosphate	Merck
Sodium phosphate	Merck
Sodium-hydrogen phosphate	Merck
TEMED	Sigma
Tricine	Biomol
Trimethyl-chlorosilane (TMCS)	Fluca
Tris	USB
Triton X-100	Sigma
Tween 20	Merck

Chemicals for bacterial and yeast media

Adenin	Merck
Ampicillin	Biomol
Amino acids	Sigma
Bacto agar	Difco
Bacto peptone	Difco
DO supplement	Clontech
Galactose	Merck
Glucose	Merck
Kanamycin	Sigma
QDO supplement	Clontech
Raffinose	Sigma
X-Gal	Biomol

Media and chemicals for mammalian cell culture

DMEM Medium	Gibco BRL (Invitrogen)
Dimethyl sulfoxide	Sigma
ER-Tracker Blue-White DPX	Molecular Probes
Fetal Bovine Serum (FBS)	Gibco BRL (Invitrogen)
FuGENE 6 Transfection Reagent	Roche
Penicillin/Streptomycin	Gibco BRL (Invitrogen)
RPMI-1640 Medium with GLUTAMAX I	Gibco BRL (Invitrogen)
Trypsin-EDTA	Gibco BRL (Invitrogen)
Trypan Blue Stain	Gibco BRL (Invitrogen)

4.2.3 Antibodies

Primary:

Anti-V5 antibody	Invitrogen
Anti-FLAG antibody	Stratagene
Anti-Myc antibody	Invitrogen

Secondary:

Peroxidase-conjugated AffiniPure Goat Anti-mouse antibody	Dianova
Peroxidase-conjugated Goat anti Rabbit IgG (H+L)	Sigma

4.2.4 Enzymes

Endonuclease (Bensonase)	Sigma
Lysozym	Sigma
Turbo Pfu	Gibco BRL
T4 ligase (cohesiv end)	MBI Fermentas
Taq polimerase	MBI Fermentas
Zymolase	Sigma

Restriction endonucleases

BamHI	MBI Fermentas
EcoRI	MBI Fermentas
HindIII	MBI Fermentas
Sall	MBI Fermentas
XhoI	MBI Fermentas

4.2.5 Cells

Bacterial

One Shot TOP10 Competent Cells: F⁻ *mcrA* Δ (*mrr-hsdRMS-mcrBC*) Φ 80/*lacZ* Δ M15 Δ *lacX74* *deoR* *recA1* *araD139* Δ (*ara-leu*)7697 *galU* *galK* *rpsL* (STR^R) *endA1* *nupG*
Invitrogen

Epicurian Coli BL21 (DE3): E.Coli B, F⁻ *ompT* *hsdS*(r_B⁻m_B⁻) *dcm* + Tet^r *gal* λ (DE3) *endA* Hte (*argU* *proL* Cam)
Stratagene

Yeast

SDG110: MAT a *upc2* *ade2* *his3* *ura3-52* *erg27D::HIS3*
Provided by Dr.Martin Bard,Ph.D

Mammalian cells

HeLa, human cervix carcinoma	DSMZ
U-937, human histiocytic lymphoma	DSMZ
NIH-3T3, Swiss mouse embryo	DSMZ
X63AG8.653, mouse myeloma	DSMZ

4.2.6. Vectors

pcDNA3.1/V5/His	Invitrogen
pcDNA3.1	Invitrogen
pCR2.1	Invitrogen
pECFP-N1	Clontech
pEGFP-C1	Clontech
pEYFP-N1	Clontech
pESC-URA	Stratagene
pGADT7	Clontech
pGBKT7	Clontech
pGEX 2TBamHI*	Pharmacia

*additional restriction sites were added into original pGEX 2T

pYES2.1/V5/His	Invitrogen
----------------	------------

4.2.7. Kits

BIO101 kit	BIO101.Inc
NucleoSpin Plasmid-Kit	Macherey-Nagel
Nucleobond AX 100-Kit	Macherey-Nagel
QIA-quick Gel Extraction Kit	QIAGEN
QIA-quick PCR Purification Kit	QIAGEN
Ready To Go T-Primed First-Strand Kit	Amersham Pharmacia
Rneasy Mini Kit	QIAGEN
StrataPrep Total RNA Microprep Kit	Stratagene
TNT T7 Coupled Reticulocyte Lysate System	Promega

4.2.8. Other material

Biodyne A transfer membrane	Pall
Cry 1°C Freezing Container	NALGENE
Filter paper	Whatman
Glutathione Sepharose 4B beads	Amersham Pharmacia
Imaging plate BAS-MS 2325	Fuji
Multiwell plate	FALCON
Pall fluorotrans W membrane	Pall
Polyacrylamid gradient gels	BioRad
Neubauer chamber	Marienfeld
Strata C18-E columns	Phenomenix

4.2.9. Devices

DU 530 spectrophotometer	Beckman
Gel dryer, model 583	BioRad
Image analyser FLA-3000	Fuji
LSM 410	Zeiss
PE 9600-PCR machine	Perkin Elmer
SSQ 7000 mass spectrometer	Finnigan
Trans-Blot SD device	BioRad
5890 Series II gas chromatograph	Aglient
HPLC-System Gold [®]	Beckman
HPLC-radioactivity monitor LD 506 D	Berthold

LITERATURE

Barros M.H. and Nobrega F.G. YAH1 of *Saccharomyces cerevisiae*: a new essential gene that codes for a protein homologous to human adrenodoxin.

Gene. 1999 Jun 11;233(1-2):197-203.

Baudry K.; Swain E.; Rahier A.; Germann M.; Batta A.; Rondet S.; Mandala S.; Henry K.; Tint G.S.; Edlind T.; Kurtz M.; Nickels J.T.Jr. The Effect of the *erg26-1* Mutation on the Regulation of Lipid Metabolism in *Saccharomyces cerevisiae*

J Biol Chem. 2001 Apr 20;276(16):12702-11.

Billheimer J.T., Chamoun D., Esfahani M. Defective 3-ketosteroid reductase activity in a human monocyte-like cell line.

J Lipid Res. 1987 Jun;28(6):704-9.

Blanchette-Mackie E.J. Intracellular cholesterol trafficking: role of the NPC1 protein.

Biochim Biophys Acta. 2000 Jun 26;1486(1):171-83.

Breitling R., Krazeisen A., Moller G., Adamski J. 17 β -hydroxysteroid dehydrogenase type 7--an ancient 3-ketosteroid reductase of cholesterologenesis.

Mol Cell Endocrinol. 2001 Jan 22;171(1-2):199-204.

Casey W.M., Burgess J.P., Parks L.W. Effect of sterol side-chain structure on the feed-back control of sterol biosynthesis in yeast.

Biochim Biophys Acta. 1991 Feb 5;1081(3):279-84.

Clayton P.T. Disorders of cholesterol biosynthesis.

Arch Dis Child. 1998 Feb;78(2):185-9.

Crowley J.H., Leak F.W., Shianna K.V., Tove S., Parks L.W. A mutation in a purported regulatory gene affects control of sterol uptake in *Saccharomyces cerevisiae*.

J Bacteriol. 1998 Aug;180(16):4177-83.

Duan W.R., Linzer D.I., Gibori G. Cloning and characterization of an ovarian-specific protein that associates with the short form of the prolactin receptor.

J Biol Chem. 1996 Jun 28;271(26):15602-7.

Duan W.R., Parmer T.G., Albarracin C.T., Zhong L., Gibori G. PRAP, a prolactin receptor associated protein: its gene expression and regulation in the corpus luteum.

Endocrinology. 1997 Aug;138(8):3216-21.

Gaber R.F., Copple D.M., Kennedy B.K., Vidal M., Bard M. The yeast gene ERG6 is required for normal membrane function but is not essential for biosynthesis of the cell-cycle-sparking sterol.

Mol Cell Biol. 1989 Aug;9(8):3447-56.

Gachotte D., Eckstein J., Barbuch R., Hughes T., Roberts C., Bard M. A novel gene conserved from yeast to humans is involved in sterol biosynthesis.

J Lipid Res. 2001 Jan;42(1):150-4.

Garver W.S., Erickson R.P., Wilson J.M., Colton T.L., Hossain G.S., Kozloski M.A., Heidenreich R.A. Altered expression of caveolin-1 and increased cholesterol in detergent insoluble membrane fractions from liver in mice with Niemann-Pick disease type C.

Biochim Biophys Acta. 1997 Oct 24;1361(3):272-80.

Geber A., Hitchcock C.A., Swartz J.E., Pullen F.S., Marsden K.E., Kwon-Chung K.J., Bennett J.E. Deletion of the *Candida glabrata* ERG3 and ERG11 genes: effect on cell viability, cell growth, sterol composition, and antifungal susceptibility.

Antimicrob Agents Chemother. 1995 Dec;39(12):2708-17.

Haines T.H. Do sterols reduce proton and sodium leaks through lipid bilayers?

Prog Lipid Res. 2001 Jul;40(4):299-324.

Hemmi K., Julmanop C., Hirata D., Tsuchiya E., Takemoto J.Y., Miyakawa T. The physiological roles of membrane ergosterol as revealed by the phenotypes of *syr1/erg3* null mutant of *Saccharomyces cerevisiae*.

Biosci Biotechnol Biochem. 1995 Mar;59(3):482-6.

Higgins M.E., Davies J.P., Chen F.W., Ioannou Y.A. Niemann-Pick C1 is a late endosome-resident protein that transiently associates with lysosomes and the trans-Golgi network.

Mol Genet Metab. 1999 Sep;68(1):1-13.

Higgins M.E. and Ioannou Y.A. Apoptosis-induced release of mature sterol regulatory element-binding proteins activates sterol-responsive genes.

J Lipid Res. 2001 Dec;42(12):1939-46.

Howard T.L., Stauffer D.R., Degnin C.R., Hollenberg S.M. CHMP1 functions as a member of a newly defined family of vesicle trafficking proteins.

J Cell Sci. 2001 Jul;114(Pt 13):2395-404.

Hughes T.R., Marton M.J., Jones A.R., Roberts C.J., Stoughton R., Armour C.D., Bennett H.A., Coffey E., Dai H., He Y.D., Kidd M.J., King A.M., Meyer M.R., Slade D., Lum P.Y., Stepaniants S.B., Shoemaker D.D., Gachotte D., Chakraburttty K., Simon J., Bard M., Friend S.H.

Functional discovery via a compendium of expression profiles.

Cell. 2000 Jul 7;102(1):109-26.

Ito T., Chiba T., Ozawa R., Yoshida M., Hattori M., Sakaki Y.

A comprehensive two-hybrid analysis to explore the yeast protein interactome.

Proc Natl Acad Sci U S A. 2001 Apr 10;98(8):4569-74.

Krazeisen A., Breitling R., Imai K., Fritz S., Moller G., Adamski J.

Determination of cDNA, gene structure and chromosomal localization of the novel human 17beta-hydroxysteroid dehydrogenase type 7(1).

FEBS Lett. 1999 Oct 29;460(2):373-9.

Kuwabara P.E. and Labouesse M. The sterol-sensing domain: multiple families, a unique role?

Trends Genet. 2002 Apr;18(4):193-201.

Kwast K.E., Burke P.V., Poyton R.O. Oxygen sensing and the transcriptional regulation of oxygen-responsive genes in yeast.

J Exp Biol. 1998 Apr;201 (Pt 8):1177-95.

Lees N.D., Skaggs B., Kirsch D.R., Bard M. Cloning of the late genes in the ergosterol biosynthetic pathway of *Saccharomyces cerevisiae*--a review.

Lipids. 1995 Mar;30(3):221-6.

Li W.P., Liu P., Pilcher B.K., Anderson R.G. Cell-specific targeting of caveolin-1 to caveolae, secretory vesicles, cytoplasm or mitochondria.

J Cell Sci. 2001 Apr;114(Pt 7):1397-408.

Manzella L., Barros M.H., Nobrega F.G. ARH1 of *Saccharomyces cerevisiae*: a new essential gene that codes for a protein homologous to the human adrenodoxin reductase.
Yeast. 1998 Jun 30;14(9):839-46.

Martinez-Botas J., Suarez Y., Ferruelo A.J., Gomez-Coronado D., Lasuncion M.A. Cholesterol starvation decreases p34(cdc2) kinase activity and arrests the cell cycle at G2.
FASEB J. 1999 Aug;13(11):1359-70.

Michikawa M. and Yanagisawa K. Inhibition of cholesterol production but not of nonsterol isoprenoid products induces neuronal cell death.
J Neurochem. 1999 Jun;72(6):2278-85.

Millard E.E., Srivastava K., Traub L.M., Schaffer J.E., Ory D.S. Niemann-pick type C1 (NPC1) overexpression alters cellular cholesterol homeostasis.
J Biol Chem. 2000 Dec 8;275(49):38445-51.

Moebius F.F., Fitzky B.U., Glossmann H. Genetic defects in postsqualene cholesterol biosynthesis.
Trends Endocrinol Metab. 2000 Apr;11(3):106-14.

Nokelainen P., Peltoketo H., Vihko R., Vihko P. Expression cloning of a novel estrogenic mouse 17 beta-hydroxysteroid dehydrogenase/17-ketosteroid reductase (m17HSD7), previously described as a prolactin receptor-associated protein (PRAP) in rat.
Mol Endocrinol. 1998 Jul;12(7):1048-59.

Nokelainen P., Peltoketo H., Mustonen M., Vihko P. Expression of mouse 17beta-hydroxysteroid dehydrogenase/17-ketosteroid reductase type 7 in the ovary, uterus, and placenta: localization from implantation to late pregnancy.
Endocrinology. 2000 Feb;141(2):772-8.

Olivier L.M. and Krisans S.K. Peroxisomal protein targeting and identification of peroxisomal targeting signals in cholesterol biosynthetic enzymes.
Biochim Biophys Acta. 2000 Dec 15;1529(1-3):89-102.

Osborne T.F. and LaMorte V.J. Molecular aspects in feedback regulation of gene expression by cholesterol in mammalian cells.
Methods. 1998 Sep;16(1):42-8.

Parmer T.G., McLean M.P., Duan W.R., Nelson S.E., Albarracin C.T., Khan I., Gibori G. Hormonal and immunological characterization of the 32 kilodalton ovarian-specific protein.
Endocrinology. 1992 Nov;131(5):2213-21.

Pol A., Luetterforst R., Lindsay M., Heino S., Ikonen E., Parton R.G. A caveolin dominant negative mutant associates with lipid bodies and induces intracellular cholesterol imbalance.
J Cell Biol. 2001 Mar 5;152(5):1057-70.

Rodriguez R.J., Taylor F.R., Parks L.W. A requirement for ergosterol to permit growth of yeast sterol auxotrophs on cholestanol.
Biochem Biophys Res Commun. 1982 May 31;106(2):435-41.

Roux C., Wolf C., Mulliez N., Gaoua W., Cormier V., Chevy F., Citadelle D. Role of cholesterol in embryonic development.
Am J Clin Nutr. 2000 May;71(5 Suppl):1270S-9S.

Roy S., Luetterforst R., Harding A., Apolloni A., Etheridge M., Stang E., Rolls B., Hancock J.F., Parton R.G. Dominant-negative caveolin inhibits H-Ras function by disrupting cholesterol-rich plasma membrane domains.
Nat Cell Biol. 1999 Jun;1(2):98-105.

Sakakura J., Shimano H., Sone H., Takahashi A., Inoue N., Toyoshima H., Suzuki S., Yamada N., Inoue K. Sterol regulatory element-binding proteins induce an entire pathway of cholesterol synthesis.
Biochem Biophys Res Commun. 2001 Aug 10;286(1):176-83.

Sato J.D., Cao H.T., Kayada Y., Cabot M.C., Sato G.H., Okamoto T., Welsh C.J. Effects of proximate cholesterol precursors and steroid hormones on mouse myeloma growth in serum-free medium.
In Vitro Cell Dev Biol. 1988 Dec;24(12):1223-8.

Schroeder F., Woodford J.K., Kavecansky J., Wood W.G., Joiner C. Cholesterol domains in biological membranes.
Mol Membr Biol. 1995 Jan-Mar;12(1):113-9.

Smart E.J., Ying Y., Donzell W.C., Anderson R.G. A role for caveolin in transport of cholesterol from endoplasmic reticulum to plasma membrane.
J Biol Chem. 1996 Nov 15;271(46):29427-35.

Smith S.J., Crowley J.H., Parks L.W. Transcriptional regulation by ergosterol in the yeast *Saccharomyces cerevisiae*.
Mol Cell Biol. 1996 Oct;16(10):5427-32.

Sturley S.L. Conservation of eukaryotic sterol homeostasis: new insights from studies in budding yeast.

Biochim Biophys Acta. 2000 Dec 15;1529(1-3):155-63.

Suarez Y., Fernandez C., Ledo B., Ferruelo A.J., Martin M., Vega M.A., Gomez-Coronado D., Lasuncion M.A. Differential effects of ergosterol and cholesterol on Cdk1 activation and SRE-driven transcription.

Eur J Biochem. 2002 Mar;269(6):1761-71.

Tinkelenberg A.H., Liu Y., Alcantara F., Khan S., Guo Z., Bard M., Sturley S.L. Mutations in yeast ARV1 alter intracellular sterol distribution and are complemented by human ARV1.

J Biol Chem. 2000 Dec 29;275(52):40667-70.

Uetz P., Giot L., Cagney G., Mansfield T.A., Judson R.S., Knight J.R., Lockshon D., Narayan V., Srinivasan M., Pochart P., Qureshi-Emili A., Li Y., Godwin B., Conover D., Kalbfleisch T., Vijayadamodar G., Yang M., Johnston M., Fields S., Rothberg J.M. A comprehensive analysis of protein-protein interactions in *Saccharomyces cerevisiae*.

Nature. 2000 Feb 10;403(6770):623-7.

Veitia R.A., Ottolenghi C., Bissery M.C., Fellous A. A novel human gene, encoding a potential membrane protein conserved from yeast to man, is strongly expressed in testis and cancer cell lines.

Cytogenet Cell Genet. 1999;85(3-4):217-20.

Vik A. and Reine J. Upc2p and Ecm22p, dual regulators of sterol biosynthesis in *Saccharomyces cerevisiae*.

Mol Cell Biol. 2001 Oct;21(19):6395-405.

Yang H., Bard M., Bruner D.A., Gleeson A., Deckelbaum R.J., Aljinovic G., Pohl T.M., Rothstein R., Sturley S.L. Sterol esterification in yeast: a two-gene process.

Science. 1996 May 31;272(5266):1353-6.

Yang T., Goldstein J.L., Brown M.S. Overexpression of membrane domain of SCAP prevents sterols from inhibiting SCAP.SREBP exit from endoplasmic reticulum.

J Biol Chem. 2000 Sep 22;275(38):29881-6.

Yokoyama S. Release of cellular cholesterol: molecular mechanism for cholesterol homeostasis in cells and in the body.

Biochim Biophys Acta. 2000 Dec 15;1529(1-3):231-44.

5. APPENDIX

5.1. Primers and constructs

Table 5.1a. Constructs made for the purpose of this study

Name	Plasmid	Primers	Restriction sites
pYES2.1/yERG25	pYES2.1	29281;yERG25r	-
pYES2.1/yERG27	pYES2.1	29277;35405	-
pYES2.1/hHSD7*	pYES2.1	29275;36257	-
pYES2.1/hHSD7tr.*	pYES2.1	29275;hHSD7tr.r	-
pYES2.1/mHSD7*	pYES2.1	23730;37111	-
pYES2.1/hHSD1*	pYES2.1	hHSD1f;hHSD1r	-
pYES2.1/hHSD5*	pYES2.1	hHSD5f;hHSD5r	-
pESC/hERG28/hHSD7*	pESC-URA	hERG28EcoRIf;hERG28NotI hHSD7BamHI f;hHSD7Sallr	EcoRI/NotI; BamHI/Sall
pEGFP/yERG27	pEGFP-C1	31898;31901	EcoRI/BamHI
pEGFP/yERG28	pEGFP-C1	37885;37886	EcoRI/BamHI
pEGFP/hHSD7*	pEGFP-C1	32039;31900	HindIII/BamHI
pEGFP/hHSD7tr.*	pEGFP-C1	38573;38574	Sall/BamHI
pEGFP/mHSD7*	pEGFP-C1	38569;38570	EcoRI/BamHI
pEGFP/hERG28*	pEGFP-C1	37884;37887	EcoRI/BamHI
pCR2.1/hHSD7*	pCR2.1	31899;32039	-
pCR2.1/yERG27	pCR2.1	31898;31901	-
pECFP/yERG27	pECFP-N1	32283;39719	EcoRI/BamHI
pECFP/hHSD7*	pECFP-N1	32039;39239	HindIII/BamHI
pEYFP/yERG28	pEYFP-N1	38576;37885	EcoRI/BamHI
pEYFP/hERG28*	pEYFP-N1	37884;39240	XhoI/BamHI
pGEX/hHSD7tr.*	pGEX	hHSD7BamHI f;hHSD7tr.EcoRIr	BamHI/EcoRI
pcDNA3.1/yERG28	pcDNA3.1/V5/His	37885;39521	-
pcDNA3.1/hERG28*	pcDNA3.1/V5/His	37884;39522	-
pcDNA3.1/mERG28*	pcDNA3.1/V5/His	38571;39523	-
pGBkT7/yERG27	pGBkT7	31898;31901	EcoRI/BamHI
pGBkT7/hHSD7*	pGBkT7	40089;40139	BamHI/Sall
pGBkT7/hHSD7tr.*	pGBkT7	40089;40090	BamHI/Sall
pGBkT7/mHSD7*	pGBkT7	38569;38570	EcoRI/BamHI
pGADT7/yERG28	PGADT7	37885;37886	EcoRI/BamHI
pGADT7/hERG28*	pGADT7	37887;40091	EcoRI/BamHI
pGADT7/mERG28*	pGADT7	38571;38572	EcoRI/BamHI

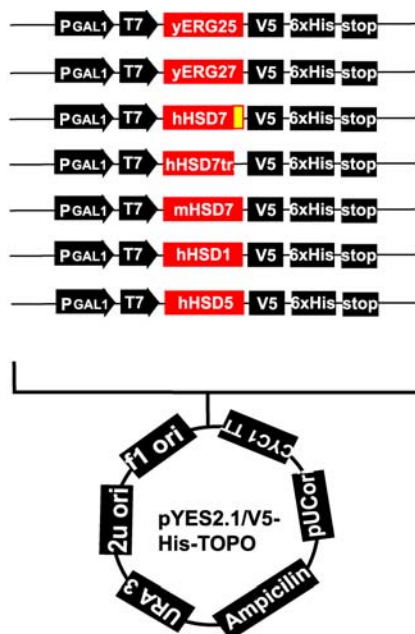
* HSD7 stands for 17 β -HSD7; HSD7tr. stands for 17 β -HSD7 without C-terminus; HSD1 stands for 17 β -HSD1; HSD5 stands for 17 β -HSD5; hERG28 and mERG28 stand for hC14orf1 and mC14orf1; h=human, m=mouse, y=yeast.

Table 5.1b. PCR and sequencing primers

Name	Internal number	Size	Sequence 5'-3'	Tm°C
yeastERG25for.	29281	26	ATGTCTGCCGTTTTCAACAACGCTAC	61,3
yERG25r.	-	18	GCTCAAAGAAGACTAAC	49,1
yeastERG27for.	29277	29	ATGAACAGGAAAGTAGCTATCGTAACGGG	61,0
yeastERG27mycr.	35405	26	AAATGCGGCCGCAATGGGGGTTCTAG	70,0
humanHSD7for.	29275	24	ATGCGAAAGGTGGTTTTGATCACC	60,0
hHSD7 myc r2	36257	22	AAAGCGGCCGCTAGGCATGAGC	65,1
hHSD7tr.EcoRI	-	26	AGAATTCCTGCTGGTTGAAGTTCCTG	63,2
mHSD7_start_for	23730	21	GGTGCAGGGCGTGAAGATGC	63,3
mHSD7r	37111	21	GCTCGGGTGATCCGATTTCTG	58,1
hHSD1f.	-	19	GATGCTGCAGGCCTTCCTG	61,0
hHSD1Xhol r.	36668	21	AAACTCGAGCTGCGGGGCGGC	67,9
hHSD5 f.	-	21	CTATGTGGCTCTACCTGGCGG	63,7
hHSD5 r.	-	19	GACTGCCTGGGCTGGTTT	61,0
hHSD7BamHI f.	-	20	TGGATCCATGCGAAAGGTGG	59,4
hHSD7Sall r.	-	23	AAAGTCGACTAGGCATGAGCCAC	62,4
hERG28EcoRI f.	-	22	TGAATTCATGAGCCGTTTCCTG	58,4
hERG28NotI r.	-	26	AAAGCGGCCGCGTTTCTCTTCTG	66,4
yERG27EcoRI f.	31898	28	GAATCCTATGAACAGGAAAGTAGCTAT	52,2
yERG27BamHI r.	31901	29	GGATCCTTATTATTAATGGGGGTTCTAG	57,4
yERG28EcoRI f.	37885	31	TTTTTGAATTCTATGTTTCAGCCTACAAGACG	61,6
yERG28BamHI r.	37886	29	AAAAGGATCCTTACCAAGCAACACCAGTG	63,2
hHSD7HindIII f.	32039	20	AAGCTTCGATGCGAAAGGTG	54,5
hHSD7BamHI r.	31900	26	CTATTAGAATTATAGGCATGAGCCAC	52,2
hHSD7tr.Sall f.	38573	31	TTTTGTGCGACATGCGAAAGGTGGTTTTGATC	68,3
hHSD7tr.BamHI r.	38574	29	AAAAGGATCCGTGCTGGTTGAAGTTCCTG	66,5
mHSD7EcoRI f.	38569	24	TTTTGAATTCGATGCGGAAGGTGG	62,7
mHSD7BamHI r.	38570	25	AAAAGGATCCTCAGCTCGGGTGATC	61,6
hERG28XhoI f.	37884	27	TTTTCTCGAGCTATGAGCCGTTTCCTG	63,5
hERG28BamHI r.	37887	32	AAAAGGATCCTCAGTTTCTTCTTCTGTCTG	61,9
yERG27EcoRI f.	32283	27	TTTGAATTCTATGAACAGGAAAGTAGC	53,8
yERG27BamHI r.	39719	35	AAAAGGATCCGCGGTTTTCAACAATTTGATCTTTCAG	70,5
hHSD7HindIII f.	32039	20	AAGCTTCGATGCGAAAGGTG	54,5
hHSD7BamHI r.	39239	28	TTTTGGATGCCGTAGGCATGAGCCACTG	69,4
yERG28EcoRI f.	37885	31	TTTTTGAATTCTATGTTTCAGCCTACAAGACG	61,1
yERG28BamHI r.	38576	26	AAATGGATCCCGCCAAGCAACACCAG	67,9
hERG28BamHI r.	39240	31	TTTTGGATCCCGGTTTCTTCTTCTGTCTG	66,6
yERG28stop r.	39521	32	CTATTACCAAGCAACACCAGTGTAGTATTCTC	58,5
hERG28stop r.	39522	27	GCTGGCCTCAGTTTCTTCTTCTTGTGTC	61,0
mERG28EcoRI f.	38571	26	TTTTGAATTCATGAGCCGCTTCCTG	64,8
mERG28	39523	27	GCTGGCCTCAATTTCTTCTTCTGTC	60,7
hHSD7BamHI y f.	40089	25	AAAAGGATCCGTATGCGAAAGGTGG	62,1
hHSD7Sall r.	40139	30	AAAAAGTCGACGGAATAGGCATGAGCCAC	67,0
hHSD7tr.Sall r.	40090	29	AAAAGTCGACGTGCTGGTTGAAGTTCCTG	65,9
mHSD7EcoRI f.	38569	24	TTTTGAATTCGATGCGGAAGGTGG	62,7
mHSD7BamHI r.	38570	25	AAAAGGATCCTCAGCTCGGGTGATC	61,6
yERG28BamHI r.	37886	29	AAAAGGATCCTTACCAAGCAACACCAGTG	63,2
hERG28EcoRI f.	40091	25	TTTTGAATTCATGAGCCGTTTCCTG	60,2
mERG28BamHI r.	38572	39	AAAAGGATCCTCAATTTCTTCTTCTGTCTGGATACTG	66,9

5.2. Figures of constructs used in the study

A



B

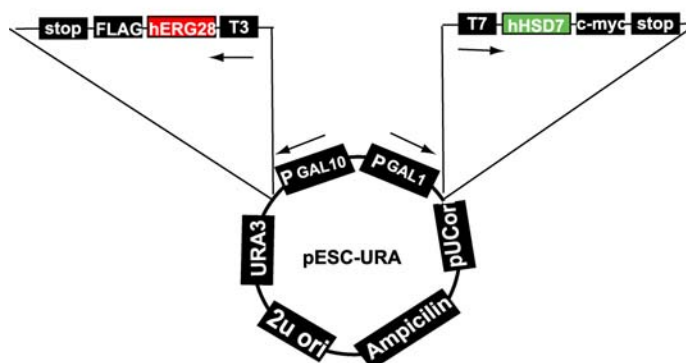


Figure 5.2a. Constructs used in yeast complementation assay. Figure A represents constructs made by cloning of PCR products into pYES2.1/V5-His-TOPO vector: yERG25 (pYES2.1/yERG25); yERG27 (pYES2.1/yERG27); h17 β -HSD7 (pYES2.1/hHSD7; C-terminus is marked in yellow); h17 β -HSD7tr. (pYES2.1/hHSD7tr.; note that C-terminus is missing); m17 β -HSD7 (pYES2.1/mHSD7); 17 β -HSD1 (pYES2.1/hHSD1); 17 β -HSD5 (pYES2.1/hHSD5). The proteins were expressed only when galactose was added and GAL1 promoter was turned on. Figure B represents double construct carrying both h17 β -HSD7 (here hHSD7) and C14orf1 (here hERG28) cloned in pESC-URA vector (pESC/hHSD7/hERG28).

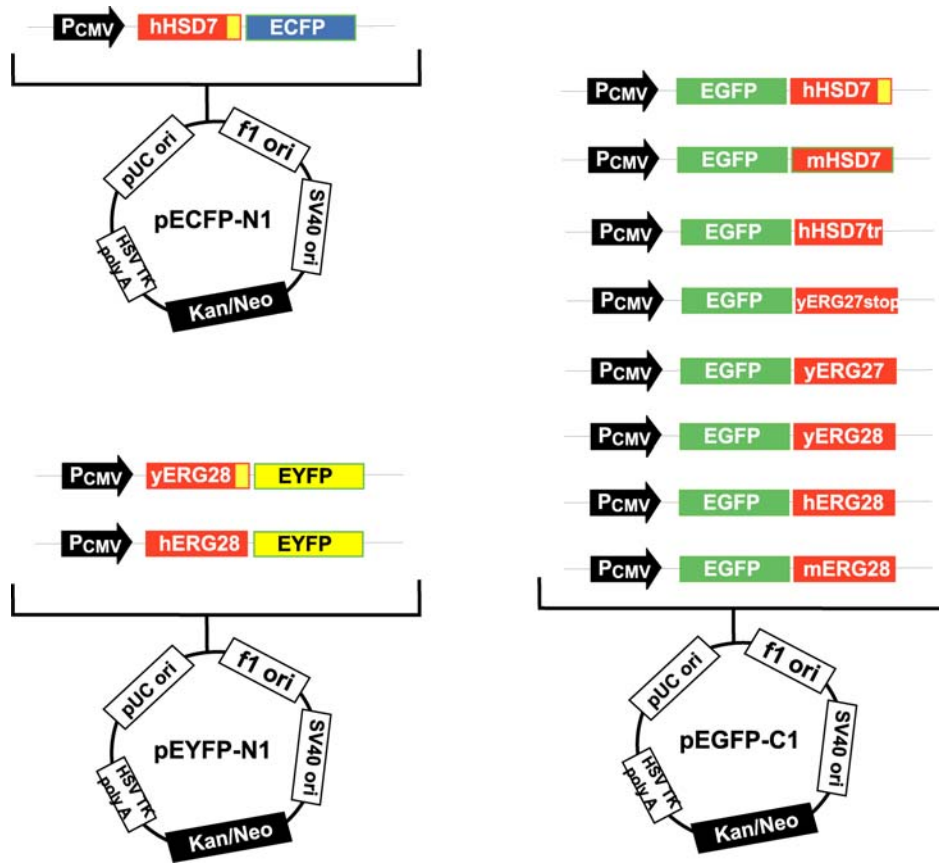


Figure 5.2b. Constructs used for localization experiments. EGFP was fused in all cases to the N-termini of the proteins. ECFP and EYFP were fused to the C-termini of the proteins. The proteins were constitutively expressed from cytomegalovirus promoter (PCMV). Note that hHSD7tr. is missing the C-terminus (yellow box). yERG27 stop was generated by a spontaneous mutation during PCR reaction. Constructs were named as follows (from left to right and up to down): hHSD7/CFP; yERG28/YFP; hERG28/YFP; pEGFP/hHSD7; pEGFP/mHSD7; pEGFP/hHSD7tr.; pEGFP/yERG27stop; pEGFP/yERG27; pEGFP/yERG28; pEGFP/hERG28; pEGFP/mERG28.

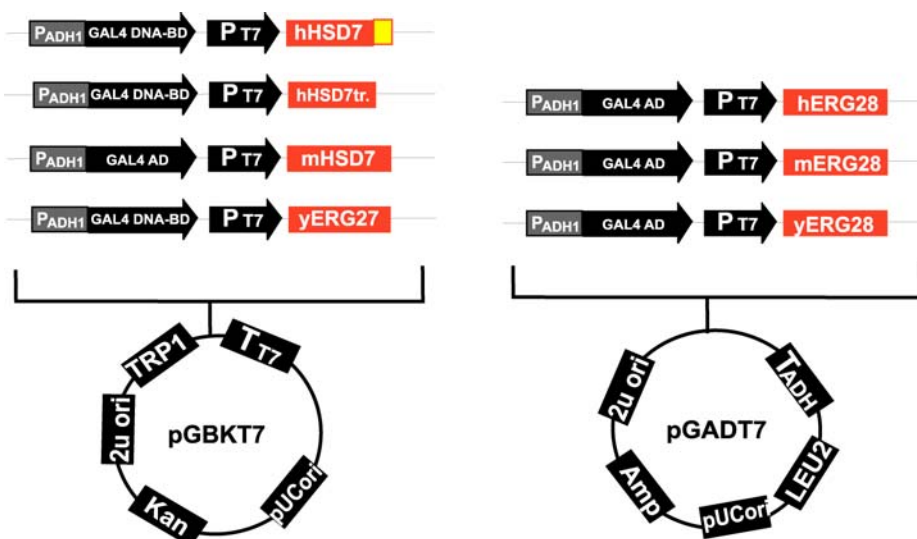


Figure 5.2c. Constructs used for Two-hybrid experiments. h17 β -HSD7 (hHSD7), h17 β -HSD7tr. (hHSD7tr.), m17 β -HSD7 (mHSD7) and yERG27 were fused to the GAL4 DNA binding domain (GAL4 DNA-BD) and are expressed from the constitutive ADH1 promoter. hERG28, mERG28 and yERG28 were fused to the GAL4 activation domain (GAL4 AD). The constructs were named as follows (from left to right and up to down): pGBKT7/hHSD7; pGBKT7/hHSD7tr.; pGBKT7/mHSD7; pGBKT7/yERG27; pGADT7/hERG28; pGADT7/mERG28; pGADT7/yERG28.

5.3. GC/MS spectra measured from media

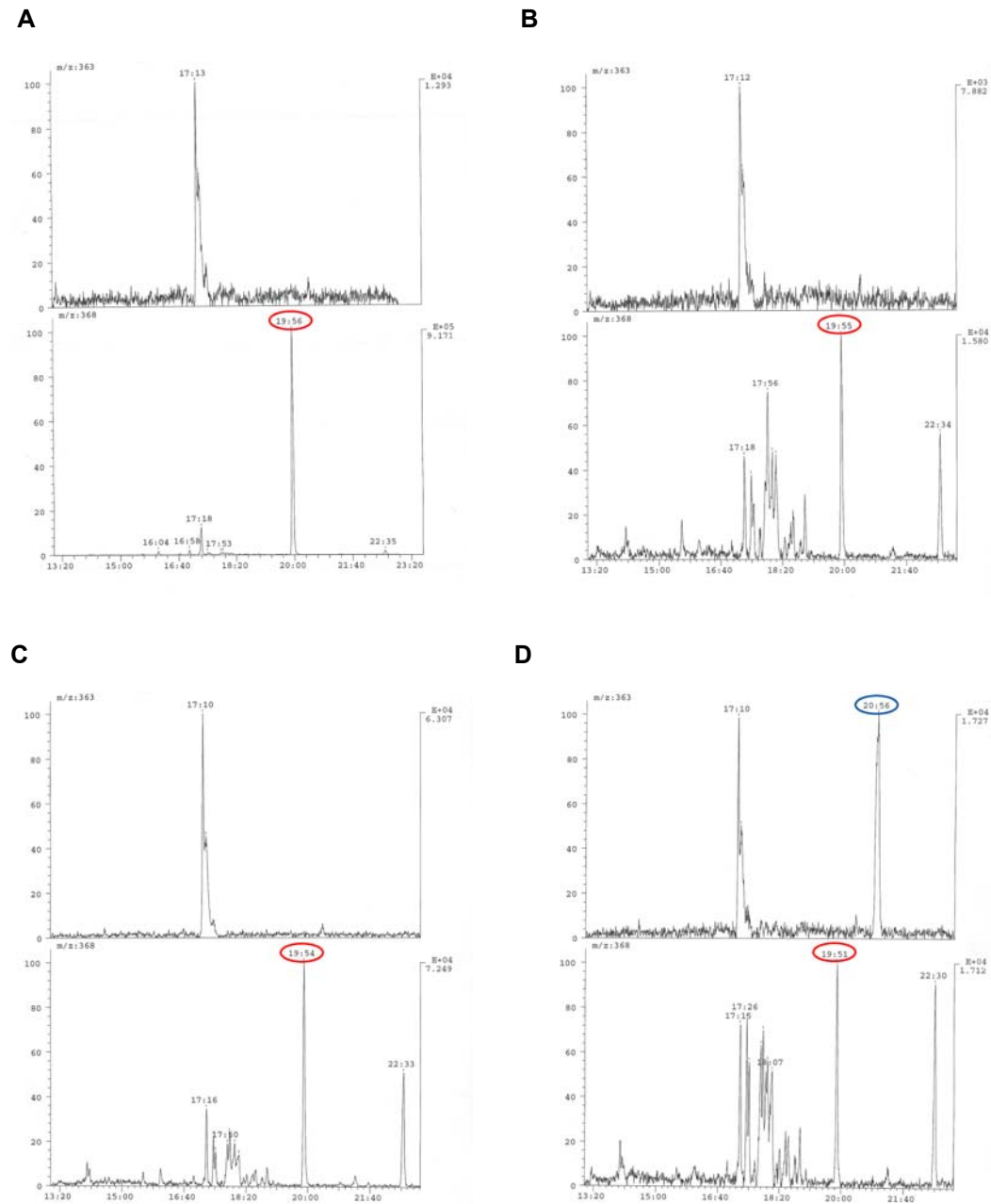


Figure 5.3a. Initial values of free cholesterol and ergosterol level measured in media. Figure A, B and C represent amount of free cholesterol measured from RPMI+10% FBS, RPMI+0,1% FBS and RPMI+0,1% FBS+cholesterol respectively. Figure D represents amount of free cholesterol and ergosterol measured from RPMI+0,1% FBS+ergosterol. Retention time for cholesterol peak is marked with red circle and for ergosterol peak with blue circle.

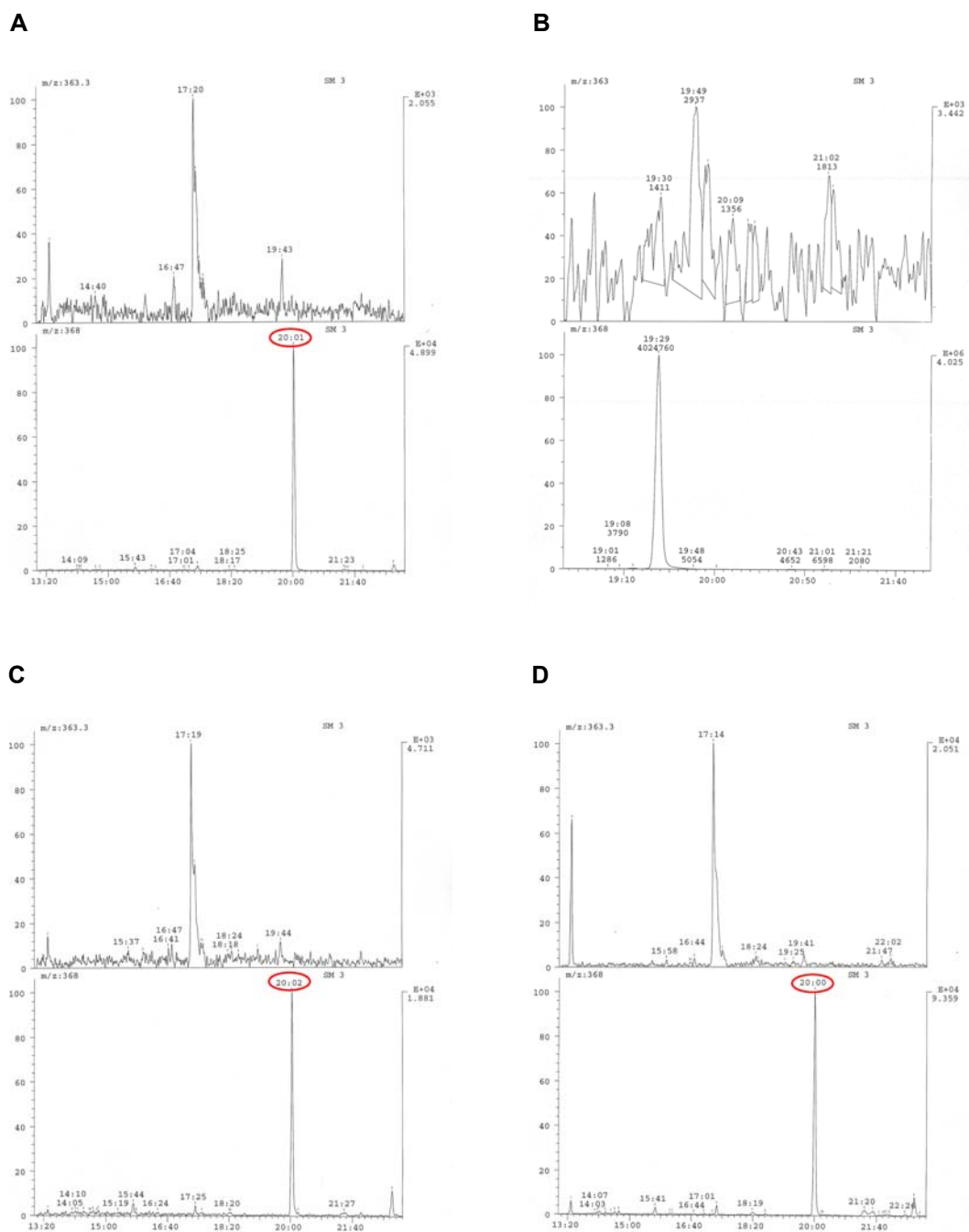


Figure 5.3b. Free cholesterol level measured from RPMI+10% FBS taken from U-937 cells in different time points after plating. Figure A, B, C and D represent free cholesterol amount measured from media taken 6 h, 24 h, 48 h and 72 h after U-937 cells were plated. Retention time for free cholesterol is marked by red circle. In case of medium taken 24 h after plating no free cholesterol could be detected. The values were normalized according to cell number and presented as a percentage of initial values in Results.

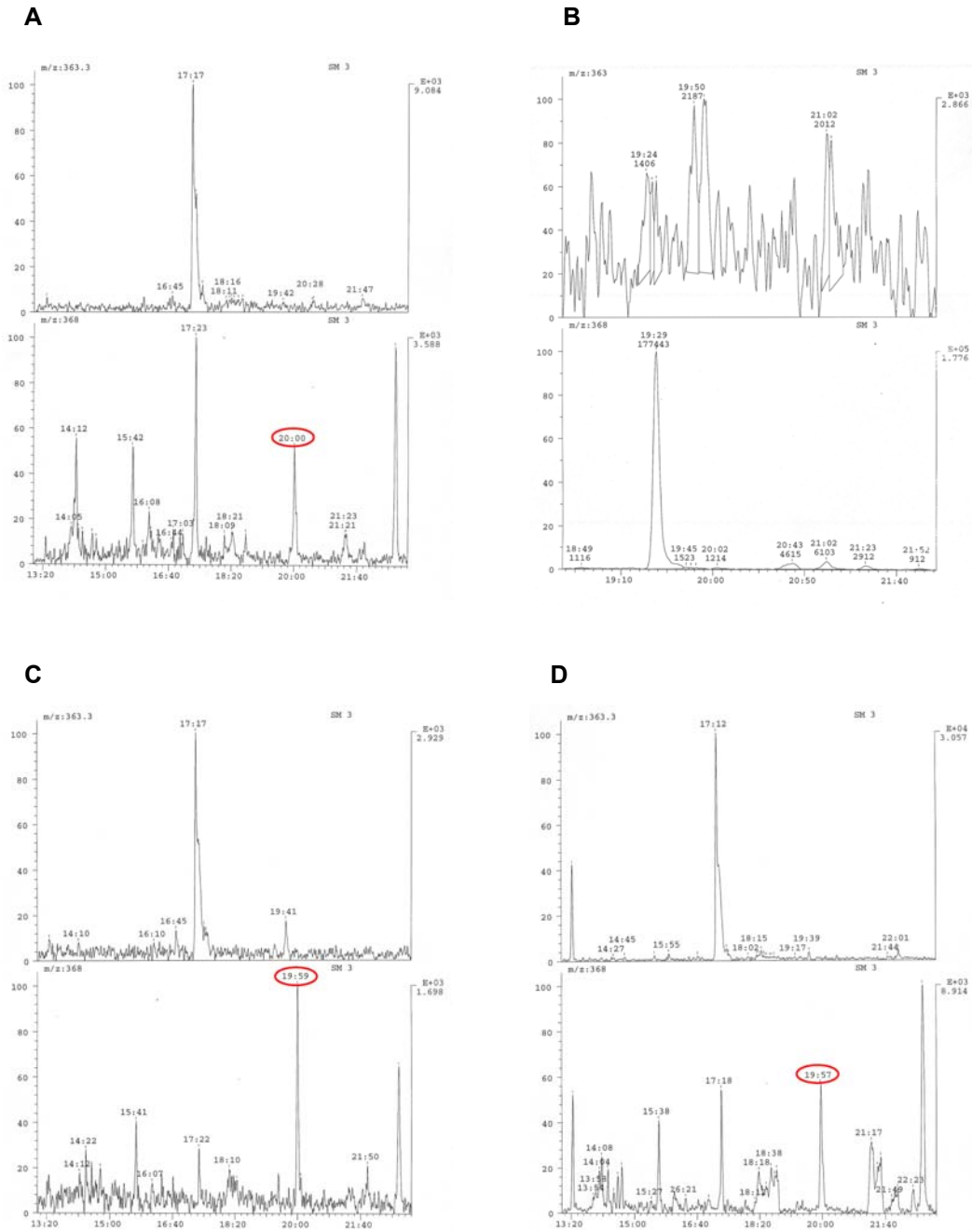


Figure 5.3c. Free cholesterol level measured from RPMI+0,1% FBS taken from U-937 cells in different time points after plating. Figure A, B, C and D represent free cholesterol amount measured from media taken 6 h, 24 h, 48 h and 72 h after U-937 cells were plated. Retention time for free cholesterol is marked by red circle. In case of medium taken 24 h after plating no free cholesterol could be detected. The values were normalized according to cell number and presented as a percentage of initial values in Results.

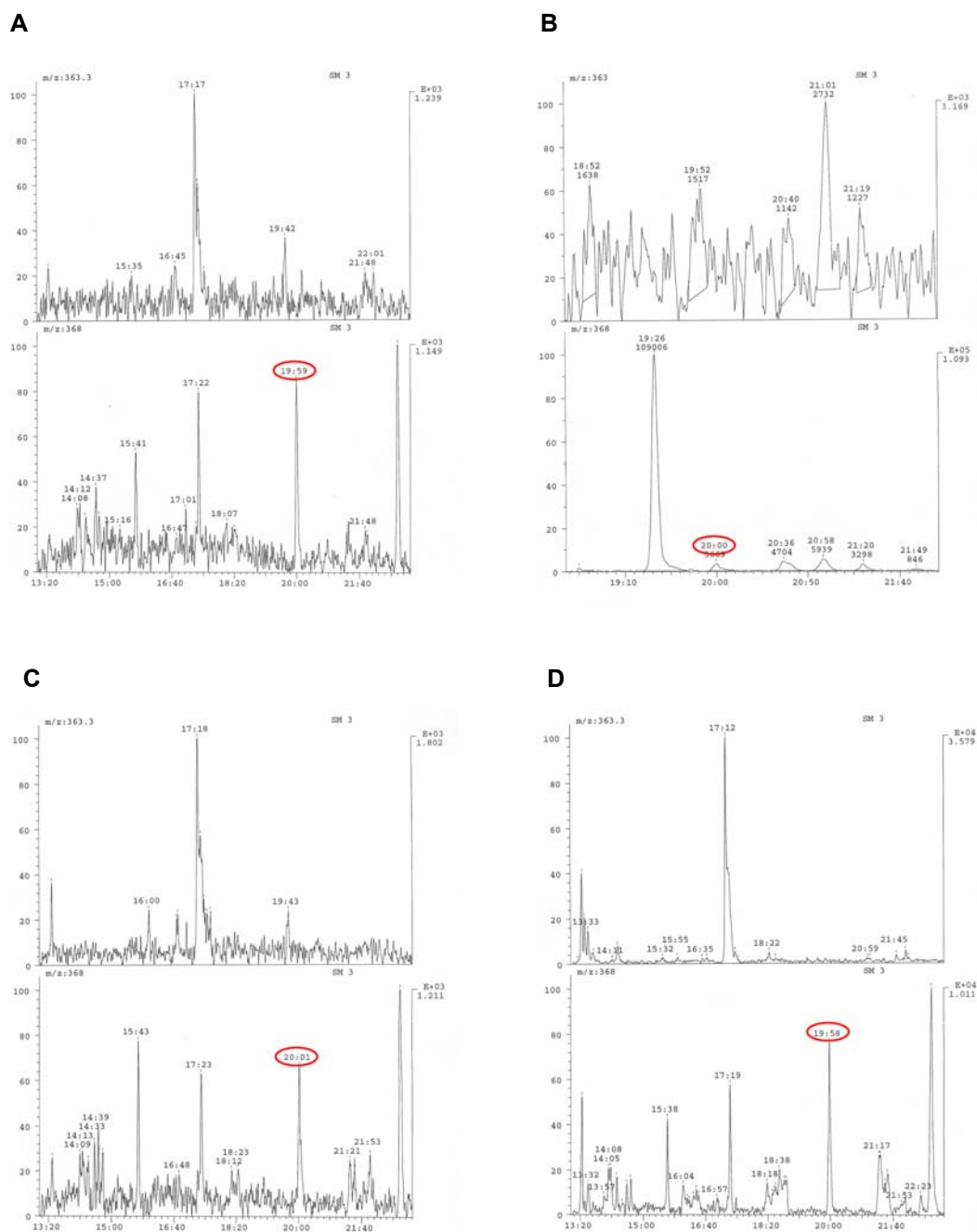


Figure 5.3d. Free cholesterol level measured from RPMI+0,1% FBS+cholesterol taken from U-937 cells in different time points after plating. Figure A, B, C and D represent free cholesterol amount measured from media taken 6 h, 24 h, 48 h and 72 h after U-937 cells were plated. Retention time for free cholesterol is marked by red circle. The values were normalized according to cell number and presented as a percentage of initial values in Results.

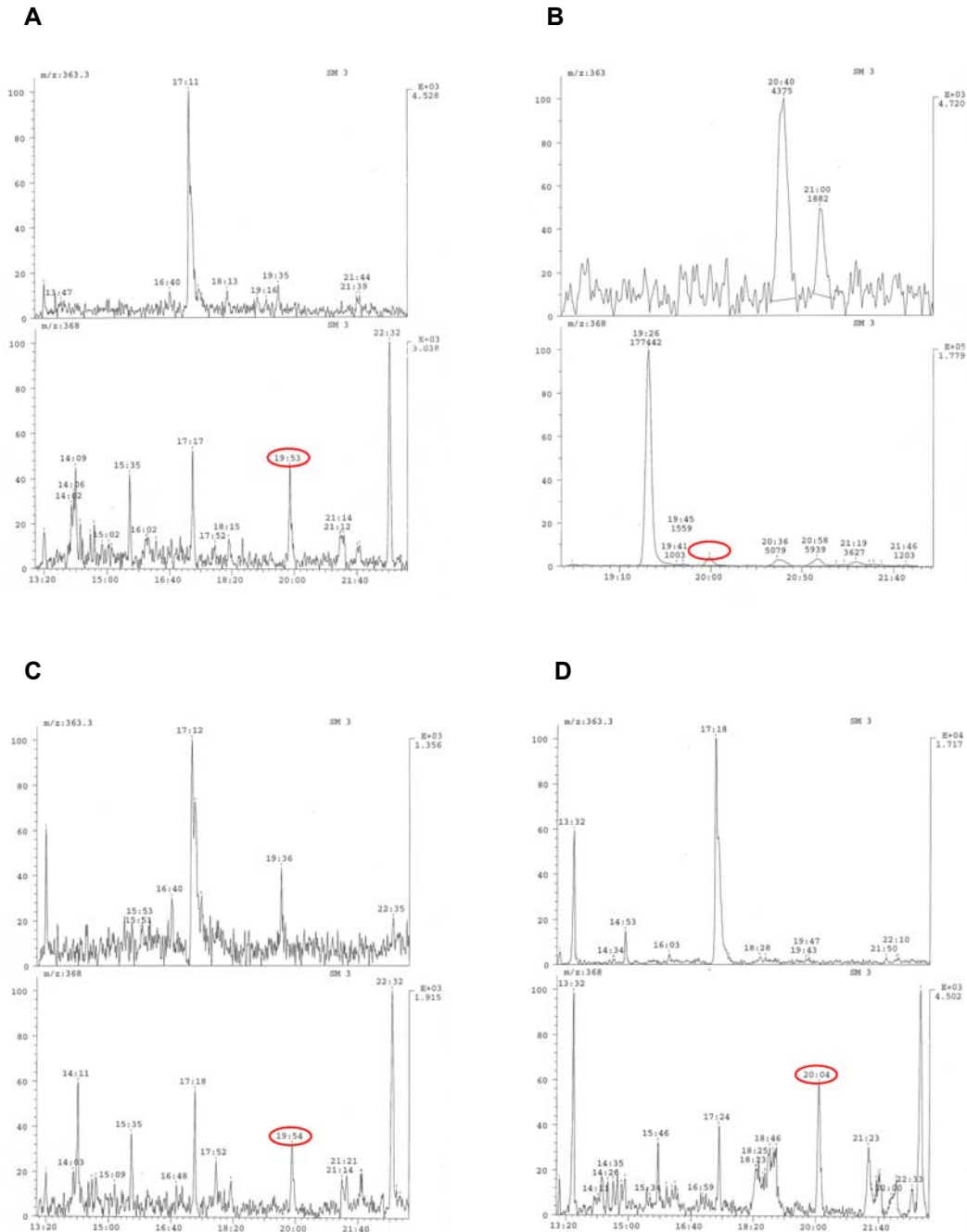


Figure 5.3e. Free cholesterol and ergosterol levels measured from RPMI+0,1% FBS+ergosterol taken from U-937 cells in different time points after plating. Figure A, B, C and D represent free cholesterol level measured from media taken 6 h, 24 h, 48 h and 72 h after U-937 cells were plated. Retention time for free cholesterol is marked by red circle. The values were normalized according to cell number and presented as a percentage of initial values in Results. Note that no free ergosterol could be detected in the media during the entire time course.

5.4. GC/MS spectra measured from cell lysates

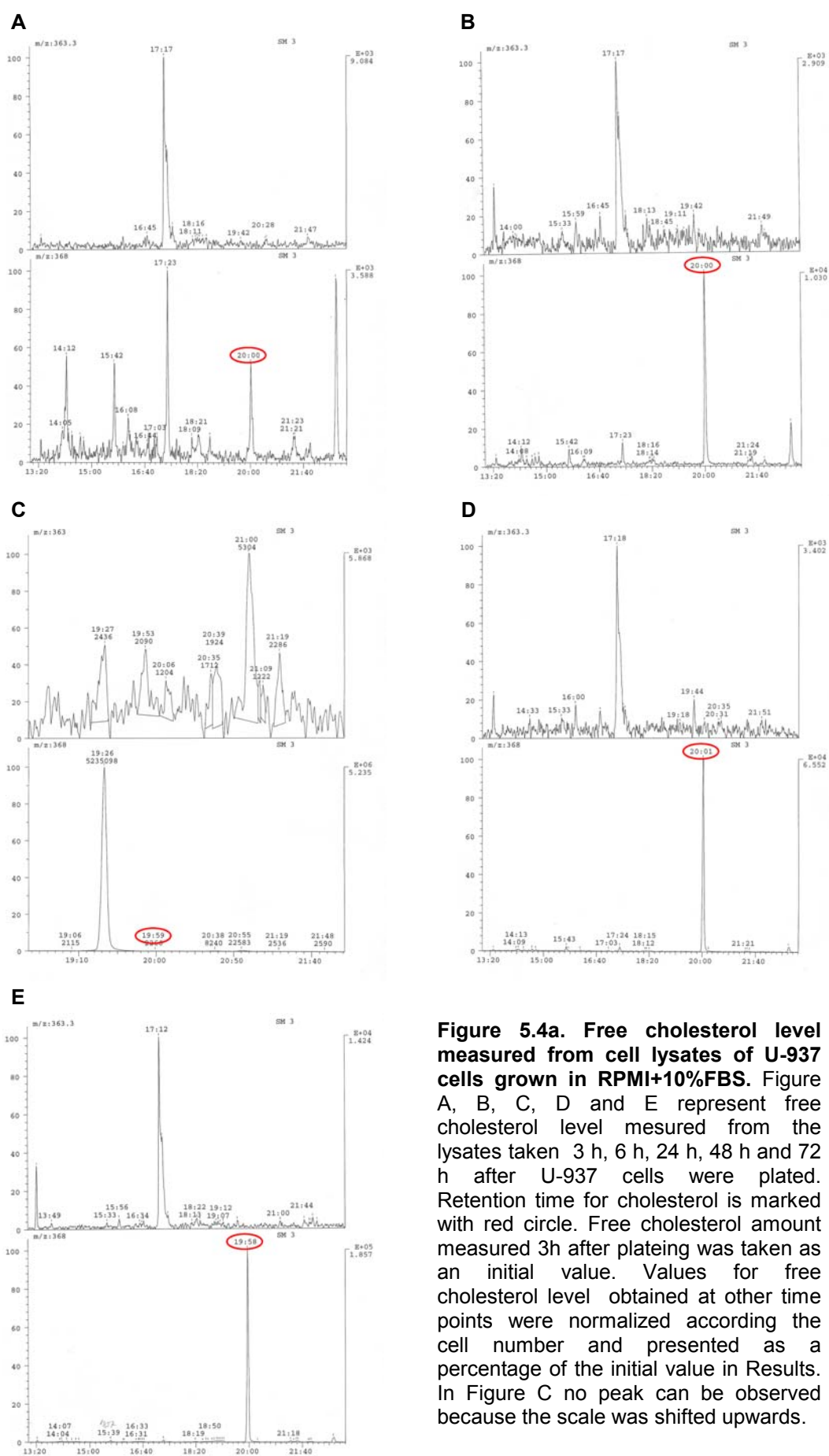


Figure 5.4a. Free cholesterol level measured from cell lysates of U-937 cells grown in RPMI+10%FBS. Figure A, B, C, D and E represent free cholesterol level measured from the lysates taken 3 h, 6 h, 24 h, 48 h and 72 h after U-937 cells were plated. Retention time for cholesterol is marked with red circle. Free cholesterol amount measured 3h after plating was taken as an initial value. Values for free cholesterol level obtained at other time points were normalized according the cell number and presented as a percentage of the initial value in Results. In Figure C no peak can be observed because the scale was shifted upwards.

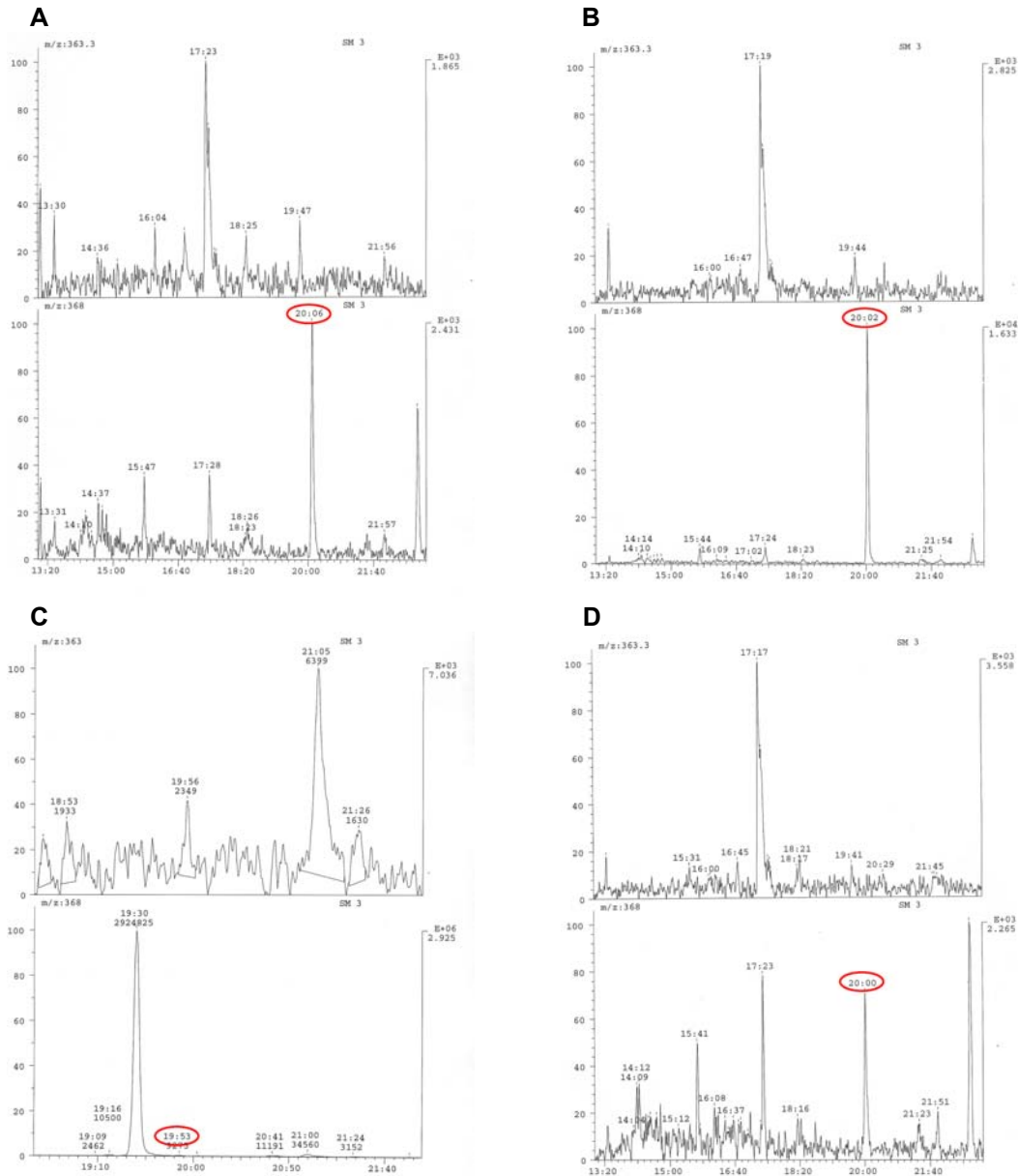


Figure 5.4b. Free cholesterol level measured from cell lysates of U-937 cells grown in RPMI+0,1%FBS. Figure A, B, C and D represent free cholesterol level measured from the lysates taken 3 h, 6 h, 24 h and 48 h after U-937 cells were plated. 72h time point is missing in this case because cells died already 48 h after plating and no pellet could be collected after 72 h. Retention time for cholesterol is marked with red circle. Free cholesterol amount measured 3h after plating was taken as an initial value. Values for free cholesterol level obtained at other time points were normalized according the cell number and presented as a percentage of the initial value in Results. In Figure C no peak can be observed because the scale was shifted upwards.

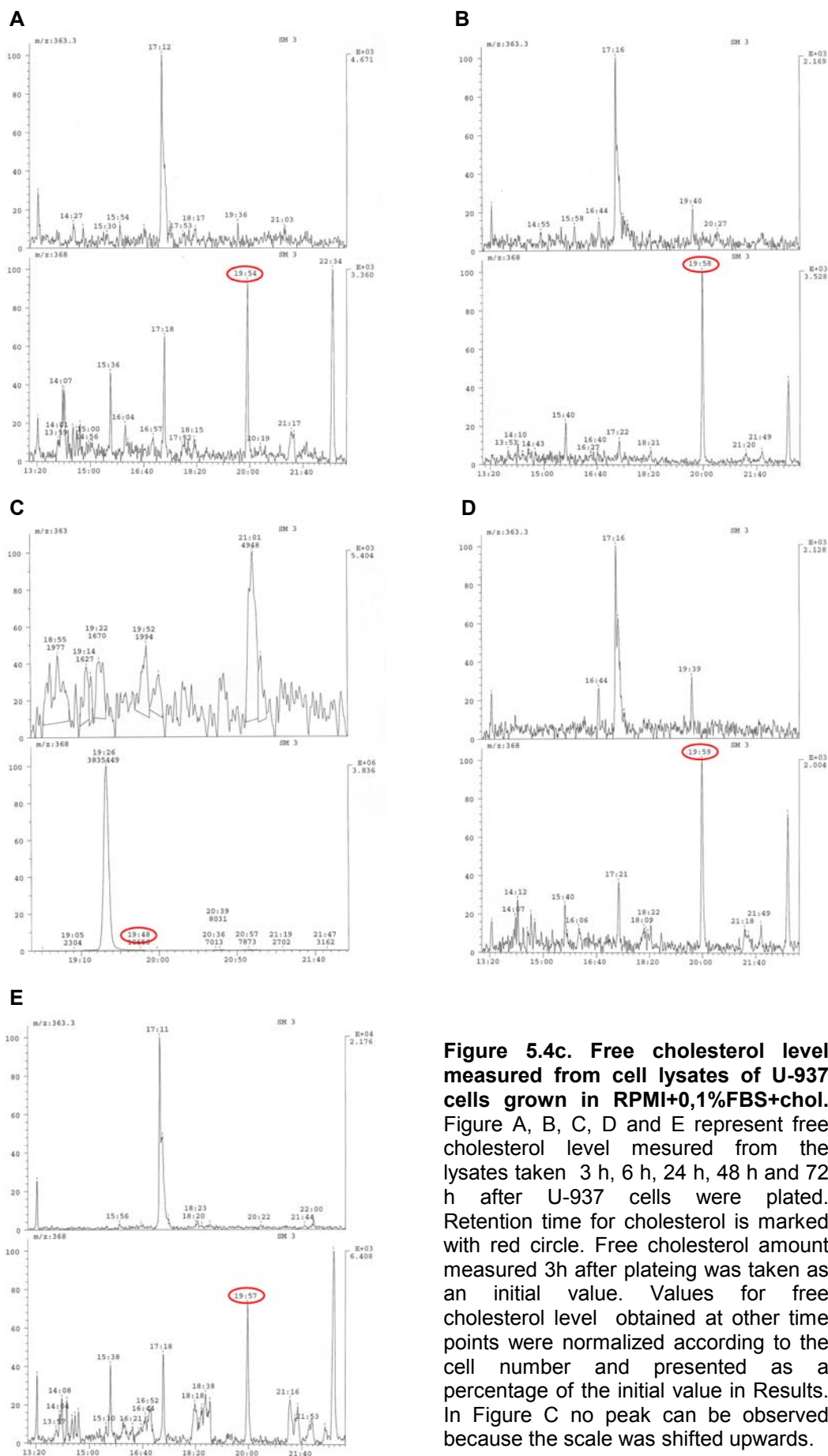


Figure 5.4c. Free cholesterol level measured from cell lysates of U-937 cells grown in RPMI+0,1%FBS+chol. Figure A, B, C, D and E represent free cholesterol level measured from the lysates taken 3 h, 6 h, 24 h, 48 h and 72 h after U-937 cells were plated. Retention time for cholesterol is marked with red circle. Free cholesterol amount measured 3h after plating was taken as an initial value. Values for free cholesterol level obtained at other time points were normalized according to the cell number and presented as a percentage of the initial value in Results. In Figure C no peak can be observed because the scale was shifted upwards.

APPENDIX

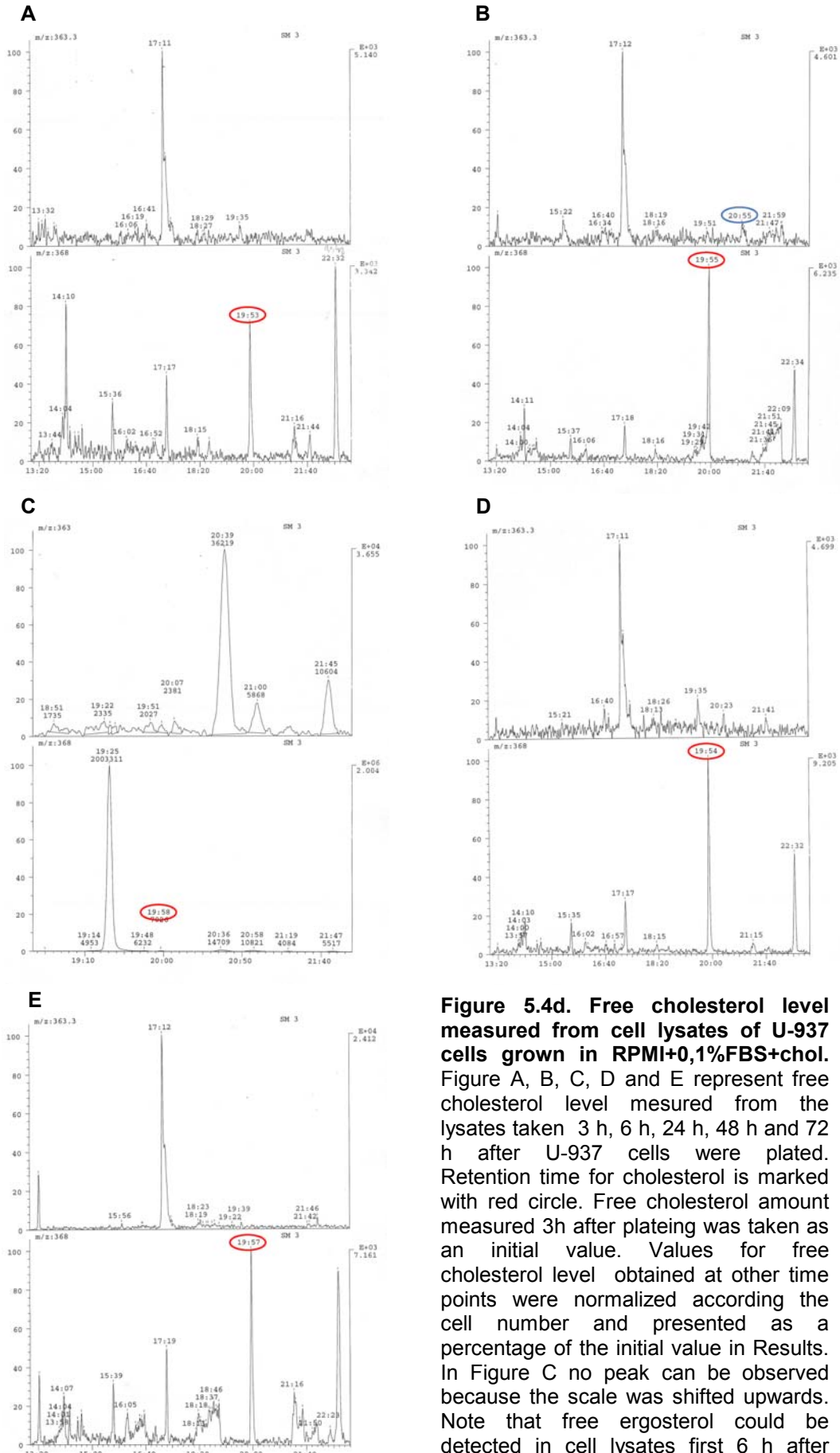


Figure 5.4d. Free cholesterol level measured from cell lysates of U-937 cells grown in RPMI+0,1%FBS+chol. Figure A, B, C, D and E represent free cholesterol level measured from the lysates taken 3 h, 6 h, 24 h, 48 h and 72 h after U-937 cells were plated. Retention time for cholesterol is marked with red circle. Free cholesterol amount measured 3h after plating was taken as an initial value. Values for free cholesterol level obtained at other time points were normalized according the cell number and presented as a percentage of the initial value in Results. In Figure C no peak can be observed because the scale was shifted upwards. Note that free ergosterol could be detected in cell lysates first 6 h after plating and was absent afterwards.

ACKNOWLEDGEMENTS

My special thanks goes to:

PD Dr. Jerzy Adamski, my supervisor, for giving me the chance to do my Ph.D. work in Germany and for all support during the time I've spent in his lab,

Dr. Rainer Breitling for having enough confidence in me to give part of his projects in my hands, for all support and critical observations that helped me to evolve as a scientist and finally, for being a friend.

I would like to thank,

- Dr. Peter Hutzler and Ulrike Buchholz for their kind help with the confocal microscopy technique,
- Dr. Andrea Völkl for help with HPLC,
- Dr. Susanne Schüren, Andre Enseleit and Bernhard Henkelmann for help with GC/MC,
- Prof.Dr. Friederike Eckardt-Schupp for the nice introduction in yeast genetics,
- Dr. Josef-Karl Gerber for suggestions considering yeast Two-Hybrid system and for providing me with some of his constructs for control experiments.

I would also like to thank all my colleagues for a nice working atmosphere and scientific support but the most of all:

- Dr. Daniela Laubner for her friendship, nice ideas and good discussions that helped me to make this work better
- Dr. Gabriele Möller for taking care of me from the beginning of my work, for going through all complicated bureaucratic things together with me and for all given support.

At the end my very special thanks goes to my friend, flatmate and working colleague Daniela Perovic for somehow finding the way to get along with me during all this time, for all her support and help in professional as well as in privat life, to my family and friends for their interest in my work and for helping me to cope more easily with the distance.

